

Doctoral Thesis

**The purification of industrial wastewater to
remove heavy metals and investigation into the
use of zeolite as a remediation tool**

Ali Mohammed Salih



2017

**The purification of industrial wastewater to remove heavy metals
and investigation into the use of zeolite as a remediation tool**

Ali Mohammed Salih

BSc Geology, MSc Environmental Technology

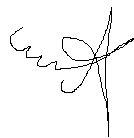
**A thesis submitted in partial fulfilment of the requirements of the University
of Wolverhampton for the degree of Doctor of Philosophy**

**This research programme was carried out in collaboration with the School of
Architecture and Built Environment**

March 2017

This work or any part thereof has not previously been presented in any form to the University or to any other body whether for the purposes of assessment, publication or for any other purpose (unless otherwise indicated). Save for any express acknowledgments, references and/or bibliographies cited in the work, I confirm that the intellectual content of the work is the result of my own efforts and of no other person.

The right of Ali Salih to be identified as author of this work is asserted in accordance with ss.77 and 78 of the Copyright, Designs and Patents Act 1988. At this date copyright is owned by the author.



Signature.....

Date.....26/06/2017.....

ABSTRACT

Zeolites are well-known aluminosilicate minerals that have been widely used as adsorbents in separation, purification processes and environmental pollution control. Zeolites are used in various industrial applications due to their high cation-exchange ability, molecular sieve and catalytic properties. In order to reduce the costs of acquisition and minimise the disposal of adsorbents, both modified natural zeolite and synthetic zeolite (derived from kaolinite) were used for the purification of wastewater. The characteristic properties and applications of adsorbents are also discussed including the advantages and disadvantages of each technique.

The present work involves the study of the removal of Cu^{2+} , Fe^{3+} , Pb^{2+} and Zn^{2+} from synthetic metal solutions using natural zeolite. Laboratory experiments were used to investigate the efficiency of adsorbents in the uptake of heavy metals from industrial wastewater. These include equilibrium tests, kinetic studies and regeneration studies.

The physical and chemical characterization of the zeolites was carried out using different analytical techniques such as Scanning Electron Microscopy (SEM), Energy Dispersive Spectroscopy (EDS), X – Ray Diffraction (XRD), X – Ray Fluorescence (XRF), Thermogravimetric Analysis (TGA), Fourier Transform Infrared (FT-IR) Spectroscopy and Inductively Coupled Plasma-Optical Emission Spectrometer (ICP-OES).

The kinetic study indicated the suitability of the natural zeolite for the removal of Cu^{2+} , Fe^{3+} , Pb^{2+} and Zn^{2+} ions from synthetic wastewater. Batch experiments were used to identify the effect of parameters that affect the rate of adsorption such as the effect of adsorbent mass, effect of adsorbent particle size, effect of initial solution pH, effect of initial solution concentration, effect of agitation speed and effect of pre-treatment of adsorbent and evaluated their impact on the efficiency of the zeolite in the removal of heavy metals from industrial wastewater.

The kinetic studies showed that the capacity of the adsorbents for the removal of heavy metals increased with a greater mass of adsorbent, increased initial solution pH, increased agitation speed, higher solution concentration as well as the application of a pre-treatment.

The results from the equilibrium studies positively demonstrated that natural zeolite can be used as an excellent adsorbent for removing heavy metals from multi-component solutions. The equilibrium experiments indicated that the capacities of natural zeolite for the uptake of heavy metals increased when the initial solution pH increased. The results indicated that the maximum removal capacities Q were 22.83, 14.92, 14.49 and 17.54 mg/g natural zeolite for copper, iron, zinc, and lead respectively.

Both the Langmuir and Freundlich isotherm models were used to characterize the experimental data and to assess the adsorption behaviour of natural zeolite for copper, iron, lead and zinc. The experimental data were slightly better suited to the Langmuir isotherm than the Freundlich isotherm. The value of the correlation coefficients r^2 ranged from 0.93 to 0.99 for the Langmuir isotherm and from 0.90 to 0.99 for the Freundlich isotherm.

The present work also involved the study of synthetic zeolite A, which was derived from natural kaolinite. The conversion of the raw materials into zeolitic materials was carried out in two ways: first, conventional hydrothermal synthesis and second, alkaline fusion prior to hydrothermal synthesis. The results from both routes show that zeolite A was synthesised successfully.

Finally, the experiments show that both natural and synthetic zeolites can be available in commercial quantities. Synthetic zeolites are more attractive for some specific applications, while the cheapness of natural zeolite may favour its use.

TABLE OF CONTENTS

ABSTRACT.....	II
TABLE OF CONTENTS.....	IV
ACKNOWLEDGEMENTS	IX
CHAPTER 1	1
1. INTRODUCTION	1
1.1. Background and motivation	1
1.2. Justification	3
1.3. Problem statement	3
1.4. Objectives and aims of thesis	5
1.5. Thesis structure	6
CHAPTER 2	9
2. LITERATURE REVIEW	9
2.1. Introduction	9
2.2. Wastewater Treatment Processes	10
2.2.1. Preliminary Treatment	11
2.2.2. Primary (mechanical) treatment	11
2.2.3. Secondary (biological) treatment.....	11
2.2.4. Tertiary treatment	12
2.3. Existing wastewater treatment technologies for heavy metal removal	12
2.4. Adsorption and ion exchange processes.....	12
2.4.1. Ion exchange.....	12
2.4.2. Adsorption	13
2.4.2.1. Types of adsorbents	15
2.4.2.2. Low cost alternative adsorbents	15
2.4.2.3. Characteristics of adsorbents	15
2.4.2.4. Examples of adsorbents used for wastewater treatment	15

CHAPTER 3	19
3. CASE STUDY	19
3.1. Historical remarks	19
3.2. Zeolite framework structure	20
3.3. Geographical distribution and occurrence of natural zeolites	26
3.4. Synthetic zeolites using kaolinite as a base material	27
3.5. Properties of zeolites	28
3.6. Application of zeolites	28
CHAPTER 4	30
4. Materials and Methods	30
4.1. Introduction	30
4.2. Materials and sample preparation	30
4.2.1. Synthetic solutions and other chemicals	30
4.2.2. Characterisation of natural zeolite and raw materials	31
4.2.2.1. Scanning Electron Microscopy (SEM)	31
4.2.2.2. Energy Dispersive Spectroscopy (EDS)	31
4.2.2.3. X-Ray Diffraction (XRD)	31
4.2.2.4. X – Ray Fluorescence (XRF)	31
4.2.2.5. Thermogravimetric Analysis (TGA)	31
4.2.2.6. Fourier Transform Infrared (FT-IR) Spectroscopy	31
4.2.2.7. Inductively Coupled Plasma-Optical Emission Spectrometers (ICP-OES) analysis	31
4.3. Experimental procedure	34
4.3.1. Equilibrium studies	34
4.3.2. Regeneration in batch studies	34
4.3.3. Kinetic studies	35
4.3.3.1. Effect of adsorbent particle size	35
4.3.3.2. Effect of adsorbent mass	35
4.3.3.3. Effect of initial solution pH	35
4.3.3.4. Effect of initial metal concentration	35
4.3.3.5. Effect of agitation speed	35
4.3.3.6. Thermal pre-treatment of adsorbent	35
4.3.3.7. Chemical pre-treatment of adsorbent	35

4.4. Synthetic zeolite procedure	37
4.4.1. Conventional hydrothermal synthesis	37
4.4.2. Alkaline fusion followed by hydrothermal reaction.....	38
4.5. Synthetic zeolite experimental procedure	39
 CHAPTER 5	40
5. CHARACTERISATION OF NATURAL ZEOLITE	40
5.1. Introduction	40
5.2. Analytical techniques	40
5.2.1. Scanning Electron Microscopy (SEM).....	40
5.2.2. Energy Dispersive Spectroscopy (EDS)	44
5.2.3. X – Ray Diffraction (XRD)	45
5.2.4. X – Ray Fluorescence (XRF)	46
5.2.5. Thermogravimetric Analysis (TGA)	47
5.2.6. Fourier Transform Infrared (FT-IR) Spectroscopy.....	48
5.2.7. Inductively Coupled Plasma-Optical Emission Spectrometers (ICP-OES) analysis	49
5.3. Conclusion:.....	50
 CHAPTER 6	51
6. EQUILIBRIUM STUDIES	51
6.1. Introduction	51
6.2. Adsorption isotherms	51
6.2.1. Langmuir adsorption isotherm.....	52
6.2.2. Freundlich adsorption isotherm	58
6.3. Regeneration studies	62
6.4. Selectivity of natural zeolite.....	66
6.5. Conclusion.....	68

CHAPTER 7	69
7. KINETIC STUDIES.....	69
7.1. Introduction.....	69
7.2. Kinetic study results	70
7.3. Factors that affect the rate of adsorption.....	71
7.3.1. Effect of adsorbent mass.....	71
7.3.2. Effect of adsorbent particle size.....	73
7.3.3. Effect of initial solution pH	75
7.3.4. Effect of initial solution concentration	78
7.3.5. Effect of agitation speed	79
7.3.6. Effect of pre-treatment.....	82
7.3.6.1. Thermal treatment of natural zeolite	82
7.3.6.2. Modification of zeolite with solution of inorganic salts.....	82
7.4. Conclusion.....	87
CHAPTER 8	88
8. SYNTHESIS AND CHARACTERIZATION OF ZEOLITE A BY HYDROTHERMAL TRANSFORMATION OF NATURAL KAOLINITE	88
8.1. Introduction.....	88
8.2. Kaolinite framework structure	88
8.3. Kaolinite structural transformations.....	91
8.3.1. Drying phase.....	91
8.3.2. Metakaolinite phase	91
8.3.3. Spinel phase	92
8.3.4. Platelet mullite phase.....	92
8.3.5. Needle mullite phase.....	92
8.4. Characterization of the untreated and thermally treated kaolinite	93
8.4.1. Scanning Electron Microscopy (SEM).....	93
8.4.2. Energy Dispersive Spectroscopy (EDS).....	97
8.4.3. X-ray diffraction (XRD)	98
8.4.4. X – Ray Fluorescence (XRF)	100
8.4.5. Thermogravimetric analysis (TGA).....	101
8.4.6. Fourier Transform Infrared (FT-IR) Spectroscopy.....	104

8.5. The synthesis of zeolite A from kaolinite materials.....	106
8.5.1. Synthetic zeolite procedure.....	106
8.5.2. Synthetic zeolite experimental Procedure.....	107
8.6. Conclusions	109
 CHAPTER 9	 110
9. GENERAL CONCLUSIONS AND RECOMMENDATION FOR FUTURE WORK.	110
9.1. Critical overview	110
9.1.1. Characterisation of natural zeolite	110
9.1.2. Equilibrium studies	111
9.1.3. Kinetic studies	112
9.1.4. Characterisation of synthetic zeolite.....	113
9.2. Future work and recommendation.....	115
 BIBLIOGRAPHY	 115
APPENDIX.....	118
APPENDIX A	140
APPENDIX B	144
APPENDIX C	145

ACKNOWLEDGEMENTS

First of all, I would like to give my immensely thanks to God for blessing me with success during my study and also for granting me with strength, power and good health to reach my ambition.

I would also like to thank my supervisor Prof. Dr. Craig Williams who took part in this study for generously sharing his time, dedicated, guidance and ideas. I would also like to thank co-supervisor Prof. Dr. Jamal Khatab for his valuable assistance, advice and encouragement throughout the research.

Finally, I would like to gratefully acknowledge the valuable support and encouragement that I have received during my work project from my wife and for giving me a push to get started. I would like also to express my profound gratitude to my mother, father for their moral, love and encouragement.

LIST OF FIGURES

Figure 2.1: Shows the adsorption process in which atoms, ions or molecules are adhering to the surface of the adsorbent.	14
Figure 2.2: Shows the absorption process, in which atoms, ions or molecules entering the volume of the absorbing substance.	14
Figure 2.3: Shows selected and possible classifications of low-cost adsorbents.....	16
Figure 2.4: Shows zeolite sieve separation process of a straight-chain hydrocarbon (octane) from a branching-chain hydrocarbon (isooctane).	18
Figure 3.1: Diagrammatic sketch of the zeolite structure and representation of $[\text{SiO}_4]^{4-}$ or $[\text{AlO}_4]^{5-}$ tetrahedral (Dyer, 1988).	21
Figure 3.2: Shows the SBUs in zeolites, the second structural classification as described by Meier (1968).	23
Figure 3.3: Shows the structural units, which may be used to assemble the zeolite frameworks (Breck, 1974; Gottardi and Galli, 1985).	25
Figure 4.1: Flowchart showing the conversion of the raw materials into zeolitic materials conducted by conventional hydrothermal synthesis.	38
Figure 4.2: showing the conversion of the raw materials into zeolitic materials conducted by alkaline fusion followed by hydrothermal reaction	39
Figure 5.1: Showing the SEM micrograph of as-received natural zeolite (Clinoptilolite) at a magnification of: (a) 5000x and (b) 1000x.	41
Figure 5.2: Showing the randomly oriented crystallites and in particular indicating the crystalline nature of natural zeolite, at a magnification of 5000x.....	41
Figure 5.3 : Showing the randomly oriented crystallites and in particular indicating the crystalline nature of natural zeolite at a magnification of 1000x.....	42
Figure 5.4: SEM micrographs of chemical pre-treatment of natural zeolite (Clinoptilolite) at different magnifications: (a) 10000x and (b) 5000x.	42
Figure 5.5: SEM microstructure of natural zeolite thermally pre-treated in a muffle furnace at (a) 200 °C (b) 400 °C, at a magnification of 5000x.	43
Figure 5.6: SEM microstructure of natural zeolite shows the collapse of the structure of natural zeolite due to thermal run away at 600 °C, at a magnification of 3000x.	44

Figure 5.7: EDS analysis showing the elemental composition and the scanning method for natural zeolite.....	45
Figure 5.8: XRD analysis showing the mineralogical analysis of natural zeolite.	46
Figure 5.9: Thermogravimetric analysis (TGA/DTG) of clinoptilolite showing curves between 20-900°C.....	47
Figure 5.10: Shows the FT-IR spectra analysis of the as received clinoptilolite.....	49
Figure 6.1: Showing the kinetic experimente for the removal of copper, iron, lead and zinc ions from solution at different pH values	56
Figure 6.2: Equilibrium adsorption using Langmuir isotherm constants for the removal of copper, iron, lead and zinc ions from solution.....	57
Figure 6.3: Equilibrium adsorption using Freundlich isotherm constants for the removal of copper, iron, lead and zinc ions from solution.....	61
Figure 6.4: The amount of recovery of heavy metals from natural zeolite by regeneration....	64
Figure 6.5: The percentage of recovery of heavy metals from natural zeolite by regeneration.	65
Figure 7.1: Diffusion processes in the system of zeolite/aqueous solution (Margeta <i>at el.</i> , 2013).	69
Figure 7.2: Shows the effect of the mass of natural zeolite on the adsorption of copper, iron, lead and zinc from solution.....	73
Figure 7.3: Shows the effect of particle size on the adsorption of iron, copper, lead and zinc from solution.....	75
Figure 7.4 : Shows the effect of initial solution pH on the adsorption of copper, iron, lead and zinc from solution.	77
Figure 7.5: Shows the effect of initial solution concentration and the amount of heavy metals adsorbed q_e (mg/g) by natural zeolite.....	79
Figure 7.6: Shows the effect of agitation speed on the adsorption of heavy metals by natural zeolite.....	81
Figure 7.7: Show loss of mass of clinoptilolite by thermogravimetric analysis (TGA) which show curves between 20-900°C.....	83

Figure 7.8: Shows the comparison of natural and thermally treated natural zeolite.....	84
Figure 8.1: Diagrammatic sketch of the kaolinite structure and representation of (SiO ₄) tetrahedral or Al(O,OH) ₆ octahedral (Grim, 1968).	89
Figure 8.2: SEM micrograph of the as-received kaolinite at a magnification of 20000x.....	93
Figure 8.3: The SEM micrograph of kaolinite showing the crystalline nature of kaolinite at a magnification of 2000x.....	94
Figure 8.4: SEM micrograph showing the crystalline nature of metakaolinite at a magnification of (a) 20000x and (b) 10000x.	94
Figure 8.5: SEM microstructure showing the oriented crystallites conducted by conventional hydrothermal synthesis reaction at a magnification of 5000x.	95
Figure 8.6: SEM microstructure showing the oriented crystallites conducted by conventional hydrothermal synthesis reaction at a magnification of 10000x.	95
Figure 8.7 (a,b): SEM microstructure showing the oriented crystallites synthesised by alkaline fusion followed by hydrothermal reaction.	96
Figure 8.8: SEM microstructure showing the oriented cubic shaped crystals of zeolite A with rounded edges at a magnification of x 10000.	96
Figure 8.9: EDS analysis showing the elemental composition and the scanning method for kaolinite.....	97
Figure 8.10: Shows the XRD pattern of kaolinite. Kaolinite (K); illite(Ili); muscovite(Ms); quartz(Q); halloysite (Hal).	98
Figure 8.11: XRD patterns of uncalcined and calcined kaolinite at different temperatures. Ili (illite), K (kaolinite), Ms (muscovite), Mul (mullite).	99
Figure 8.12: XRD analysis showing the mineralogical analysis of zeolite A (conventional hydrothermal synthesis).	99
Figure 8.13: XRD analysis showing the mineralogical analysis of zeolite A (alkaline fusion prior to hydrothermal synthesis).	100
Figure 8.14: Thermogravimetric analysis (TGA/DTG) of Iraqi kaolinite showing curves between 30-1000°C.....	102
Figure 8.15: Thermogravimetric analysis (TGA/DTG) of zeolite A prepared by conventional hydrothermal synthesis routes, showing curves between 20-900°C.....	103

Figure 8.16: Thermogravimetric analysis (TGA/DTG) of zeolite A prepared by alkaline fusion prior to hydrothermal synthesis routes, showing curves between 30-900°C.....	103
Figure 8.17: Shows the FT-IR spectra analysis of as received kaolinite before calcination.	104
Figure 8.18: FT-IR spectra of kaolinite and metakaolinite obtained after calcination of kaolinite at 600, 950 and 1000 °C.....	105
Figure 8.19: show the FT-IR spectra of zeolite A obtained from kaolinite after treatment. .	107
Figure 8.20: Shows the adsorption of copper, iron, lead and zinc from solution by zeolite A.	108
Figure 8.21: Shows the adsorption of copper, iron, lead and zinc from solution by natural zeolite.....	108

LIST OF TABLES

Table 3.1: The variations in the Si/Al ratio of zeolite (Ribero <i>et al.</i> , 1984).....	22
Table 3.2: Classification of zeolite structures (Breck, 1974).....	24
Table 5.1: EDS analysis showing the elemental composition and the scanning method for natural zeolite.....	45
Table 5.2: Chemical composition (wt.%) of the natural zeolite.	46
Table 6.1: Calculated equilibrium adsorption Langmuir isotherm constants for the removal of copper, iron lead and zinc ions from solution.....	54
Table 6.2: Calculated equilibrium adsorption Freundlich isotherm constants for the removal of copper, iron, lead and zinc ions from solution.	59
Table 6.3: Shows the selectivity series of natural zeolite towards Cu^{2+} , Fe^{3+} , Pb^{2+} and Zn^{2+} cations in solutions with a different initial pH.	67
Table 7.1: Shows the effect of natural zeolite mass on the removal of heavy metals from solution.....	71
Table 7.2: Shows the effect of initial solution concentration on the adsorption capacity of natural zeolite.....	78
Table 7.3: Shows the structural stability of some natural zeolites (Breck, 1974).	82
Table 8.1: EDS analysis showing the elemental composition and the scanning method for the “as received” kaolinite.	97
Table 8.2: The chemical composition (wt.%) of the Iraqi kaolinite used in the preparation of zeolite type A.	100
Table 8.3: The chemical composition (wt.%) of zeolite A using the conventional hydrothermal synthesis route.	101
Table 8.4 : The chemical composition (wt.%) of zeolite A using alkaline fusion prior to the hydrothermal synthesis route.	101

List of Abbreviations and Nomenclatures

Å	Angstrom
b	Langmuir constant related to adsorption energy (l/mg).
BET	Brunauer Emmett and Teller analysis
CAN	Cancrinite
C_e	Residual liquid phase concentration at equilibrium (mg/l)
CHA	Chabazite
cm	Centimetre
C°	Celsius
C_o	initial concentration of adsorbate (mg/l)
D4R	Double four ring
D6R	Double six ring
DTG	First derivative of thermogravimetry
DTA	DTA Differential thermal analysis
DTG	DTG Differential thermal gravimetry
DSD	Division for Sustainable Development
EDS	Energy Dispersive Spectroscopy
FT-IR	Fourier transform infrared spectroscopy
g	Gram
Hal	Halloysite
Hem	Hematite
hr	Hour
ICDD	International Centre for Diffraction Data
ICP-OES	Inductively Coupled Plasma-Optical Emission Spectrometers
Ili	Illite
IZA	International Zeolite Association
IMA	International Mineralogical Association,
IMF	The International Monetary Fund
k	Freundlich constant for adsorption capacity (mg/g).
kV	Kilovolt
l	Litre

m	Metre
M	Molarity
<i>m</i>	mass of adsorbent (g)
mA	Milliampere
mg	Milligram
mg l ⁻¹	Milligram per litre
min	Minute
ml	Millilitre
mm	Millimetre
μm	Micrometre
Ms	Muscovite
MDGs	Millennium Development Goals
Mul	Mullite
mV	Millivolt
<i>n</i>	Freundlich constant for adsorption intensity (l/mg).
OECD	Organisation for Economic Co-operation and Development
pH	Negative log of hydrogen ions in solution.
ppm	Parts per million
<i>Q</i>	Langmuir constant related to maximum sorption capacity(mg/g)
<i>q_e</i>	the amount of solute adsorbed per unit mass of adsorbent at equilibrium (mg/g)
Qtz	Quartz
<i>R</i> ²	correlation coefficient
S4R	Single four ring
S6R	Single six ring
S8R	Single eight ring
SBU	Secondary building unit
SDA	Structure directing agent
SDGs	Sustainable Development Goals
SE1	Forward-scattered primary electron
SEM	Scanning electron microscopy
SOD	Sodalite
TG	Thermogravimetry

TGA	Thermogravimetric analysis
UN	United Nations
V	Volume of solution (l).
WBG	World Bank Group
XRD	X-ray diffraction analysis
XRF	X – Ray Fluorescence analysis

CHAPTER 1

1. INTRODUCTION

1.1. Background and motivation

The accumulation of a huge quantity of hazardous waste in the environment has become a worldwide concern. This problem includes wastewater pollution. Fresh water is important in order for life to be continued on our planet, but nowadays, the world is facing a water crisis due to less availability of clean fresh water. Concerns on freshwater are rising every day this is due to the expanding needs of food production, agriculture and energy consumption as well as the weaknesses of water management (Pandey *et al.*, 2009). Globally, millions of tonnes of various waste materials and pollutants are dumped in the environment annually; this is sourced from household, industrial, transports, mining and agricultural wastes (Misaelides, 2011; Tchobanoglous and Burton, 1991; Pandey *et al.*, 2009). Wastes are generated regularly without a proper sustainable and suitable treatment. An increase in such activities has resulted in the discharge of huge quantities of hazardous inorganic and organic pollutants into aqueous systems (Misaelides, 2011). Therefore these accumulated pollutants in water may become a potential hazard to our health and ecological environments (Alvarez-Ayuso *et al.*, 2003).

According to the Division for Sustainable Development (DSD), the management of quality drinking water and maintaining pollutant-free water has become a crucial task in order to prevent any sort of diseases and avoid further the destruction of the environment (Polat *et al.*, 2004). All over the world, there are general consensuses about challenges concerning the handling of wastewater for a sustainable future. Research by Mulligan, Yong and Gibbs (2001) showed that wastewater may produce both short term and long term harmful impacts on human health and ecological systems.

To prevent this problem, there are some international polices and regulations such as International Kyoto protocol (United Nations Framework Convention on Climate Change, 2007). Towards the end of the last century, terms such as ‘waste water’, ‘air pollution’, ‘protection of the environment’ and ‘ecology’ became household words (Deunert *et al.*, 2007; Ramalho, 1997). Since then, developing and developed countries have started to take some

steps towards reducing the risk of water systems becoming contaminated. Research by Peng *et al.* (2009) showed that, when the concentration of pollutants exceeds certain limits immediate remediation actions are necessary.

The international agreement framework took place by the United Nations and established 17 goals. Each goal has specific targets to be achieved over the next 15 years. On September 25th 2015, countries adopted a set of goals to end poverty, protect the planet, and ensure prosperity for all as part of a new sustainable development agenda (sustainable development goals, 2016). This agreement was complemented by many technical indicators from the United Nations, IMF, OECD and the World Bank in order to evaluate progress towards the Millennium Development Goals (MDGs). In The United Nations Sustainable Development Goals (SDGs); goal 6, incorporates the principles of sustainable development into country strategies and policies to protect the natural resources to give every human being a right to get access to safe drinking water and improved hygiene conditions (SUSTAINABLE DEVELOPMENT GOALS, 2016).

As a part of sustainable development and waste management programs we should attempt to reduce waste materials and convert them into useful products by recycling or reusing procedures (Crini, 2006). This can be useful for reducing the amount of raw materials used and operating costs, reducing the volume of waste materials and reducing their environmental impact.

Currently, purification of wastewater via an adsorption process is believed to be a simple, cheap and effective technique for removal of dissolved heavy metals from wastewater. According to Babel and Kurniawan (2003) the achievement of the technique mainly depends on characterises and properties of an efficient adsorbent. Although a number of materials and techniques have been utilized for these purposes, the use of natural zeolites and their modified forms offer as advantages the low-cost and the availability in large quantities in many parts of the world (Misaelides, 2011; Peng *et al.*, 2009; Crini, 2005; Inglezakis *et al.*, 2004). Thus, zeolites have been widely used as adsorbents for the removal of ions in wastewater treatment (Misaelides, 2011; Pandey *et al.*, 2009; Babel and Kurniawan, 2003).

1.2. Justification

As discussed above, the adsorption and ion exchange process are the most widely used techniques that have attracted increasing interest in different companies. Furthermore, synthetic zeolites were developed due to their excellent adsorption capacities and higher performances, compared to natural zeolites, but they are usually very expensive. Various zeolites from kaolinite or other ashes and have made great progress in synthesis of 4A, mordenite, X, Y zeolites, etc. (Inglezakis *et al.*, 2004; Pandey *et al.*, 2009). Meanwhile, many modified zeolites have been developed that can be rated as having a median adsorption capacity, while they do not cost as much as synthetic zeolite and have a better adsorption capacity than natural zeolite (Colella, 2007). Many studies have shown that zeolites have high adsorption capacities for removal of pollutants from solutions and can reach adsorption equilibrium level in short periods of time (Blanchard *et al.*, 1984; Erdem *et al.*, 2004; Inglezakis *et al.*, 2004).

There are many types of natural zeolite that have been identified in the world; there are very common forms such as clinoptilolite, mordenite, stilbite, analcime, phillipsite, chabazite, and laumontite, whereas paulingite, offretite, mazzite and barrerite are much rarer forms (Blanchard *et al.*, 1984). Galli (1983) argues that clinoptilolite is the most abundant of the natural zeolites. Its characteristic tabular morphology shows an open reticular structure of easy access, formed by open channels of 8- to 10-membered rings. Argun (2008) has also suggested that clinoptilolite has good adsorption capacities and is widely used in the world. However, different types of zeolite have different adsorption capacities based on their physicochemical properties (Inglezakis, 2007).

1.3. Problem statement

The reduction of heavy metal contamination in aquatic systems is a global problem (Peng *et al.*, 2009). In the meantime, the treatment of industrial wastewater contaminated by heavy metals has become a major challenge. According to Bish and Ming (2001) the wastewater collected from municipalities, communities and industry needs to be treated then returned back to aquatic systems or to the land. Patterson (1987) argues that in developed countries, polluting industries have to conform to more and more rigid environmental regulations (Patterson, 1987). Research by Salam *et al.* (2011) showed that the main sources of heavy metal pollution occurs in wastewater from various sources such as metal plating facilities,

battery manufacturing processes, mining operations, nuclear power generation, use of pesticides, vehicle emissions, the ceramic and glass industries, paints, and treated timber and microplastics. Andras *et al.* (2012) proved that over limit heavy metals are recognized as toxic elements and their discharge into the water system affects both human health and the natural ecosystem. Since they are not biodegradable, and cause numerous diseases and disorders (Pandey *et al.*, 2009; Tchobanoglous and Burton, 1991). Pb^{2+} , Cu^{2+} , Fe^{3+} , Zn^{2+} and Cr^{3+} are especially common metals that tend to accumulate in organisms, causing numerous diseases and disorders (Inglezakis *et al.*, 2003). Wastewater containing heavy metals should be treated before being discharged into the natural environment (Kesraoui *et al.*, 1994).

In order to achieve the above goal, Wang (2008) suggested many processes such as precipitation, adsorption, ion exchange, reverse osmosis, foam flotation techniques and cementation that can be used to remove or reduce heavy metals from wastewaters (Wang, 2008). Many of these techniques require high energy that cost a lot and advanced operational requirements. They may also result in large amounts of sludge that requires treatment and is difficult to treat. Furthermore, some approaches do not enable the recovery of the metals or materials (Popuri *et al.*, 2009). According to Panayotova and Velikov (2003) the advantage of using clinoptilolite is relatively cheap, abundant in supply, sustainability and it is environmentally friendly. It exhibits improved adsorption capacities when it is modified (Panayotova and Velikov, 2003; Gunay *et al.*, 2007; Gedik and Imamoglu, 2008). The application of natural zeolites to the environmental remediation is mainly based on their ion-exchange properties (Colella, 1999).

Heavy metals can attach to the surface of microorganisms and may even penetrate to the inside of the cell. Inside the microorganism, the heavy metals can be chemically changed as the microorganism uses chemical reactions to digest food. A well-known example is the ability of some bacteria to change mercury to a modified form called methylmercury. Methylmercury can be absorbed much more easily than mercury into the bodies of insects and other small organisms. When these small organisms are eaten by bigger living organisms such as fish, the heavy metals enter the fish and can remain in the fish for extended periods. As bigger organisms eat the smaller organisms (making up the food chain), the heavy metals build-up in concentration in the larger living things. This increase in concentration of substances over time and in bigger living organisms is called bioaccumulation (In Depth Tutorials and Information, 2017).

1.4. Objectives and aims of thesis

The aim of this investigation is to develop an effective, low cost, flexible, sustainable and environmentally friendly adsorbent as an alternative method for removing heavy metals from industrial wastewaters. The efficiency of clinoptilolite for the removal of four heavy metal ions from a solution was considered; these were Fe^{3+} , Cu^{2+} , Pb^{2+} and Zn^{2+} . These were chosen as abundance pollutants that are contained in industrial wastewaters.

The effectiveness of clinoptilolite as an adsorbent in industrial wastewater treatment was further investigated by studying further characteristics of the USA clinoptilolite. The main parameters that influence clinoptilolite's adsorption abilities are considered with regard to heavy metals from industrial wastewaters, thus, the main aims of the thesis can be discussed as follows:

- ❖ To analyse clinoptilolite in both its natural and modified forms, by determining whether pre-treating clinoptilolite improves its selectivity properties or adsorption capacity.
- ❖ To determine the factors that impact on the performance of clinoptilolite and affect the rate of adsorption.
- ❖ To examine clinoptilolite's capacity after regeneration and investigate its life span in the case of repeated loading and regeneration.
- ❖ To determine the applicability of both the Langmuir and Freundlich isotherms and estimate the parameters characterising the performance of the batch process.
- ❖ To investigate the transformation of kaolinite clay to prepare synthetic zeolite via conventional hydrothermal treatment with alkaline solutions and alkaline fusion prior to hydrothermal reaction methods.

1.5. Thesis structure

This thesis is formed from a number of chapters, each chapter studies different aspects of the investigation followed by data analysis and summarises the results as given below:

Chapter 1:

This chapter describes a brief background and motivation of the waste water problems in general and industrial heavy metals pollution. Then this chapter concludes with different wastewater treatment techniques to solve the problem. An outline of the justification, objectives and aims of thesis are also briefly discussed followed by thesis structure.

Chapter 2:

This chapter presents a detailed literature review of the prevention and different wastewater technologies used in the world; especially it describes the wastewater treatment technologies available for removal of heavy metals. Then an outline of the wastewater treatment processes, ion exchange and adsorption process, different available adsorbents used for wastewater treatment and the characteristics of the adsorbents are also discussed.

Chapter 3:

This is an introduction to natural zeolites, generally it consists of a discussion on the historical remarks, the geographical distribution, framework structure, properties and applications of natural zeolite.

Chapter 4:

This chapter discusses the experimental materials and methods used for the adsorption of heavy metals from synthetic wastewaters. The experiments included are the most widely used techniques for the batch system. The conversion of the raw materials into zeolitic materials method is also discussed in this chapter, using both conventional hydrothermal synthesis technique and alkaline fusion prior to hydrothermal synthesis technique.

Chapter 5:

In this chapter different methods of characterising natural zeolites are described. The results obtained from analytical techniques such as Scanning Electron Microscopy (SEM), Energy Dispersive Spectroscopy (EDS), X – Ray Diffraction (XRD) and X – Ray Fluorescent Spectroscopy (XRF), Thermogravimetric Analysis (TGA), Fourier Transform Infrared (FT-IR) Spectroscopy are analysed.

Chapter 6:

In this chapter equilibrium studies are described for the removal of iron, copper, lead and zinc from multi-component solutions under different initial solution pH, initial solution concentration. The experimental data were also analysed using Freundlich and Langmuir adsorption isotherms models. Other studies such as maximum effective capacity of natural zeolites, the regeneration of adsorbent with selectivity of natural zeolites for the heavy metals cations under investigation were determined.

Chapter 7:

This chapter describes the kinetic studies in order to investigate the behaviour of adsorbents and understand the removal mechanisms involved in the adsorption process. In this chapter, a number of these factors that effect the efficiency of natural zeolite in removing of Fe^{3+} , Cu^{2+} , Pb^{2+} and Zn^{2+} from solution are investigated in detail.

Chapter 8:

This chapter briefly provides background information on the kaolinite structural transformations phases and characterising of kaolinite is described. The results obtained from analytical techniques are analysed. This chapter also describes the conversion of kaolinite as a starting material into synthetic zeolite using hydrothermal transformation methods. Other studies such as kinetic studies in order to investigate the behaviour of synthetic zeolites are presented.

Chapter 9:

In this chapter the specific aims of this study are reviewed to present an overview of the conclusions of this study and to make a critical evaluation. This chapter also discusses the recommendations for further work.

CHAPTER 2

2. LITERATURE REVIEW

2.1. Introduction

This introductory section describes general aspects of the major wastewater treatment technologies used to remove heavy metals and different types of adsorbents and their characteristics.

For the purpose of the removal of contaminants from wastewater, a variety of techniques were developed such as adsorption, chromatography, ion exchange, electrodialysis and membrane technologies (Macingova and Luptakova, 2012). As suggested by many researchers, adsorption processes are assumed to be an effective technique to purify wastewater and the success of the technique primary depends on the improvement of an efficient adsorbent. Activated carbon (Pollard *et al.*, 1992), zeolites (Babel and Kurniawan, 2003; Dyer, 1988; Gottardi and Galli, 1985) clay minerals (Crini, 2006), biomaterials (Crini, 2005) and some industrial solid wastes (Wang, *et al.*, 2008; Wang and Wu, 2006) have been widely used as adsorbents for the adsorption of ions in wastewater treatment.

Different methods and techniques have been utilised for the purpose of removing heavy metal ions from wastewater. Some of these processes are relatively cheap in operational costs, abundant in supply, ease of use and flexibility to quickly switch to different applications such as adsorption and ion exchange technique. Other techniques, are expensive in operational costs and incur the problem of residual disposal (Ramalho, 1997). Therefore, many companies have experienced economic pressures due to the costs of operation and remediation (Popuri *et al.*, 2008). Previous studies established the findings of the successful modification of zeolite and the good achievement while using zeolites as adsorbents for the purpose of removing heavy metal ions from wastewater. Zeolites have advantages over other adsorbents due to their special characteristics as mentioned in section 2.4.2.3 (Inglezakis *et al.*, 2004; Gedik and Imamoglu, 2008; Misaelides *et al.*, 1994; Dyer, 1988; Gottardi and Galli, 1985; Erdem *et al.*, 2004; Peric *et al.*, 2004).

Ion exchange and adsorption are common operations used for wastewater treatment. Over the last few years, the use of ion exchange and adsorption processes in treating wastewater, with the potential use of natural zeolite (clinoptilolite), have become more credible and have been the focus of intensive studies by researchers (Oztas *et al.*, 2008; Blanchard *et al.*, 1984; Panayotova and Velikov, 2003; Argun, 2008; Inglezakis *et al.*, 2007; Polat *et al.*, 2004; Gunay *et al.*, 2007).

The multiple uses of natural zeolite, including the removal of heavy metal ions in wastewater treatment, are based on its physical and chemical properties. These properties explain their wide range of agricultural and industrial applications (Rivera *et al.*, 2000). As reported by Colella (1999) the application of natural zeolites for wastewater treatment is mainly based on their ion-exchange and adsorption properties. It is also well established that ion-exchange in the case of zeolites takes place among cations and only their modification can provide them with anion sorption properties (Colella, and Wise, 2014). The uptake of metal cations from solutions by the zeolites is affected by a numerous of factors such as the temperature, the initial solution pH, the presence of competing ions, the particle size, the dimensions of the hydrated dissolved species compared to the opening of their channels and the external surface activity (Colella, 2007).

Zeolites are stable solid and can resist high temperatures since they have high melting points over 1000°C. They also resist high pressures and do not oxidize in air and dissolve in water or other inorganic solvents (Dyer, 1988; Gottardi and Galli, 1985; Guinier, 1963).

This thesis has focused on the efficiency of natural clinoptilolite in the removal of heavy metals cations (Fe^{3+} , Cu^{2+} , Co^{2+} and Zn^{2+}) from synthetic industrial wastewater, to achieve allowable limits. The adsorption behaviour of natural clinoptilolite and a number of factors which can affect the efficiency of natural clinoptilolite were also investigated.

2.2. Wastewater Treatment Processes

Wastewater treatment is the final step against water pollution, which is closely related to the regulations, standards and principles set out regarding effluent quality (World Bank Group, 2016). The aim of the processes is to improve the quality of the wastewater. There are various wastewater treatment processes including primary, secondary, and tertiary treatment. Below is a brief description of each process.

2.2.1. Preliminary Treatment

The preliminary treatment is the first stage of the treatment process. The main aim of this process is to remove coarse solids and other large materials that are often found in raw wastewater such as paper and plastics (World Bank Group, 2016). The removal of these materials is necessary to protect the operation system from blockages or any damage to the equipment. Generally, the preliminary stage does not treat any pollutants in the water but prevents the wastewater operation system being blocked (Harrison, 1993).

2.2.2. Primary (mechanical) treatment

Following the first stage of treatment, the wastewater goes through a primary sedimentation process (screening stage), which involves the separation of organic and inorganic solids by sedimentation, such as sand, grease, grit and other materials that have passed through the preliminary stage (Imhoff *et al.*, 1971). The removal of these materials is necessary to protect pipe work from any damage and also to prevent abrasion to the pumps. Thus during the primary treatment process the total suspended solids (SS), biochemical oxygen demand (BOD₅), oil and grease as well as some of the nitrate, phosphate and heavy metals are also removed (World Bank Group, 2016).

2.2.3. Secondary (biological) treatment

This next treatment stage involves the removal of the any remaining organics and inorganics which have escaped the primary treatment process. Secondary treatment is a biological process which involves removal of dissolved and suspended organic compounds using naturally occurring microorganisms (Masters, 1998). It is called the activated sludge process (secondary treated wastewater).

At each stage, the level of oxygen in the wastewater is changed to generate aerobic and anaerobic environments. Different bacterial communities can thrive in each of these two environments and each community removes different pollution components from the water (World Bank Group, 2016).

2.2.4. Tertiary treatment

Tertiary treatment is the last stage of the water cleaning process then after this the treated water can be returned back to the aquatic system or discharged into agriculture (World Bank Group, 2016). This stage is an advanced treatment stage that is used to remove the remaining suspended solids, dissolved solids, refractory organics, heavy metals and odour, as well as metals and nutrients that pose a risk to human health (Imhoff *et al.*, 1971).

2.3. Existing wastewater treatment technologies for heavy metal removal

It can be observed from prior sections that efforts have been directed towards developing technologies to remove heavy metals and hence there is a need for an economic technology capable of achieving the desired results. It has recently been mentioned that there are various processes and technologies that are available for the purpose of removing heavy metals from wastewaters. These processes include membranes, ultrafiltration precipitation, reverse osmosis, electrodialysis, adsorption and ion exchange (Richardson and Harker, 2002; Hamdaoui, 2009; Peric *et al.*, 2004; Rengaraj *et al.*, 2001; Macingova and Luptakova, 2012).

Adsorption is effective, available in large quantities and an economic method with great potential for the removal of metals from wastewater, compared to other wastewater treatment techniques that have expensive operational costs. They also incur the problem of residual disposal (Ramalho, 1997; Bailey *et al.*, 1999) below is a brief description of both adsorption and ion exchange processes.

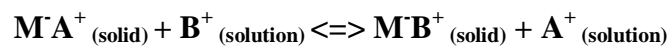
2.4. Adsorption and ion exchange processes

2.4.1. Ion exchange

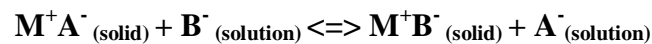
Ion exchange is a chemical process, whereas adsorption may be a physical or chemical process. The ion exchange process is the reversible interchange of ions between a solid phase and a solution phase in which no structure change appears in the solid phase. The solid phase is usually insoluble in the solution medium in which the exchange process is carried out (Grimshaw and Harland, 1975). Ion exchange can be used in different treatment processes such as purification, separation and decontamination processes. As reported by Ramalho

(1997) the ion exchange process is widely used in wastewater treatment since it is able to achieve complete demineralization through simultaneous cation and anion exchange. The clinoptilolite structure contains some exchangeable cations, which are readily exchanged for other types of cations from solution. This property of zeolite has been exploited in a major way in water softening, where alkali metals such as sodium or potassium prefer to exchange out of the zeolite, being replaced by the "hard" calcium and magnesium ions from the water (Alvarez-Ayuso *et al.*, 2003). According to Mumpton (1999) ion exchangers can be cations that exchange positively charged ions or anions that exchange negatively charged ions as shown in the following equation below:

Cationic Exchanger;



Anionic Exchanger;



In trying to find out whether adsorption and ion exchange are identical to each other, Hamdaoui (2009) stated that both adsorption processes and ion exchange are related to each other, but in the meantime each process has their own special areas of concern. Schroeder (1977) provided that adsorption is the accumulation of materials at a boundary, and this boundary may be liquid - liquid, solid - liquid, gas - solid or gas - liquid.

In this thesis the term of “adsorption” and “ion exchange” are used interchangeably as the removal of heavy metals from the solution are associated with both processes of ion exchange and adsorption (Curkovic *et al.*, 1997).

2.4.2. Adsorption

The term adsorption was first used by Heinrich Kayser in the year 1881. Adsorption is a removal process of a substance (atoms, ions, or molecules) called an “adsorbate” from a gas, liquid, or dissolved solid phase by a solid material called an “adsorbent” (Bansal and Goyal, 2005). Hence many studies have been carried out on adsorption techniques as important processes in separation technology (Gupta *et al.*, 2009; Erdem *et al.*, 2004; Freitas *et al.*, 2008; Hameed, 2009). Adsorption processes differ from absorption processes; adsorption is a

surface-based process in which atoms, ions or molecules from a substance adhere to the surface of the adsorbent as shown in figure 2.1. Absorption is the process which involves the entire volume of the absorbing substance into the solid material body as shown in figure 2.2 (Erdem *et al.*, 2004).

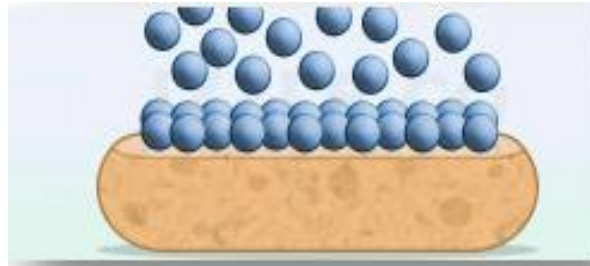


Figure 2.1: Shows the adsorption process in which atoms, ions or molecules are adhering to the surface of the adsorbent.

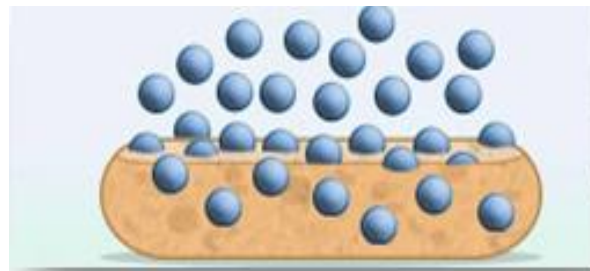


Figure 2.2: Shows the absorption process, in which atoms, ions or molecules entering the volume of the absorbing substance.

The removal efficiency of any adsorption process depends on selectivity and affinity. According to the type of adsorbent and adsorbate bonds formed, adsorption can be classified into:

- i. **Physical adsorption:** occurs when the adsorbate sticks to the surface of the adsorbent only through Van der Waals (weak intermolecular) interactions (Somorjai, 1993). Physical adsorption is usually fast and reversible this is because the physical adsorptions process involves the formation of week bonds between the adsorbate and adsorbent, thus the adsorption bonds are easily formed and broken (Somorjai, 1993).

- ii. **Chemical adsorption:** occurs as a result of a chemical interaction between the adsorbate molecules and the adsorbent surface. A chemisorption process is usually slow and irreversible this is because the chemisorptions process involves the formation of strong bonds between the adsorbate and adsorbent and can change both the surface and adsorbate chemical character (Somorjai, 1993).

2.4.2.1. Types of adsorbents

According to the source, generally adsorbents can be classified into:

- i. **Natural adsorbents:** These types of adsorbents occur naturally such as zeolites, clay minerals, charcoal, red mud, sediment and soil, ore minerals etc. They are low cost in acquisition and abundant in supply. They can be easily modified and increase their adsorption capabilities (Nageeb, 2013).
- ii. **Synthetic adsorbents:** These adsorbents are prepared from raw materials such as household waste, industrial wastes, agricultural waste, sewage sludge and polymeric adsorbents etc. They are expensive compared to natural adsorbents (Nageeb, 2013).

Each adsorbent type has its own characteristics and specific properties. There are many types of adsorbent that have been identified in the world such as activated carbon, activated alumina, activated clay, and molecular sieves are very common forms (Nageeb, 2013).

2.4.2.2. Low cost alternative adsorbents

Typically, an adsorbent can be assumed to be low cost and they are generally available in large quantities, as stated by Pollard (1992) the cost factor plays a major role in selecting an adsorbent. Therefore, efforts have been directed towards developing low cost alternative adsorbents and a wide variety of materials have been investigated for this purpose. They can be classified in two ways: either (i) on basis of their availability, i.e., (a) natural material (b) agricultural waste or by-products or (c) industrial waste or by-products; or (ii) depending on their nature, i.e., (a) inorganic or (b) organic material (Gupta *et al.*, 2009; Ahmaruzzaman, 2008; Wan and Hanafiah, 2008).

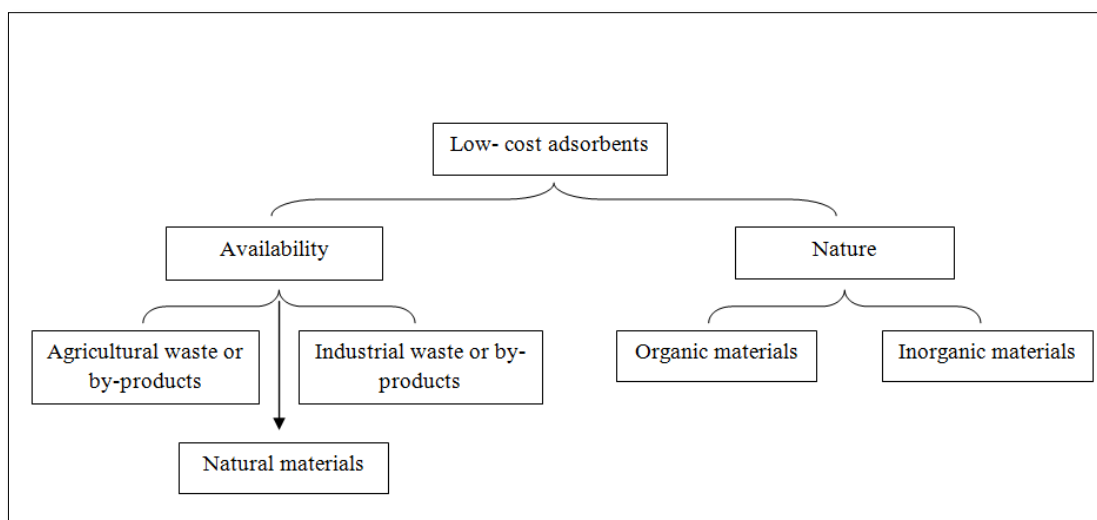


Figure 2.3: Shows selected and possible classifications of low-cost adsorbents.

2.4.2.3. Characteristics of adsorbents

The most important attributes for any adsorbent are: capacity, selectivity, regenerability, kinetics, compatibility and cost. Adsorbents can be based on inorganic materials such as zeolites or they can be based on organic material sources such as activated carbon.

The good adsorbents have to have the following important characterises: (Ruthven, 1984; Richardson *et al.*, 2002; Gedik and Imamoglu, 2008; Inglezakis *et al.*, 2004; Peric *et al.*, 2004; Erdem *et al.*, 2004; Misaelides *et al.*, 1994):

- High porosity, uniform molecular-sized channels and large specific surface area.
- High adsorption capacity in a wide range of adsorbate concentrations.
- High ion exchange capacities.
- High catalytic properties and accessibility through pores to allow certain molecules passage during adsorption and to break down others.
- Simplicity and low cost in operation and effective technique.
- Easy to regenerate and reuse for many times.
- High melting point, thermal stability and structural stability toward dehydration.
- Low cost of acquisition and does not introduce additional pollution into the environment, minimal waste generation.

2.4.2.4. Examples of adsorbents used for wastewater treatment

A variety of adsorbents are used for adsorption purposes in industry such as activated alumina, activated carbon, activated clays and molecular sieves (Richardson *et al.*, 2002; Ruthven, 1984). These adsorbents can be natural or modified ones or those that are synthetically prepared (Ruthven, 1984; Richardson *et al.*, 2002).

i. Activated Carbon

Activated carbon is well known to be very effective in wastewater treatment. The raw material used for activated carbon needs to be organic material with high carbon content such as hard wood, black carbon, rice husks, bagasse ash, saw dust or lignin (Crittenden and Thomas, 1998). Most coal is not porous and hence it needs to be activated in order to generate a system of fine pores. The carbon-based material can be converted to activated carbon by thermal treatment using heat between 700 – 1100 °C. The activated carbon contains carbon, which accounts up to 95% of the mass weight and other hetero atoms such as hydrogen, nitrogen, sulphur and oxygen. It has a large surface area ranging between 500 and 1500 m²/g (Yin *et al.*, 2007). Activated carbon is used in different applications such as water, gas and metal purification (Panday *et al.*, 1985).

ii. Activated Alumina

Activated alumina is made of aluminium oxide (Al₂O₃). Activated alumina has a high porosity and large specific surface area, significantly over 200 m²/g. It is prepared through calcinations of bauxite (Al₂O₃.3H₂O) under specific temperature conditions. Activated alumina is most commonly used in a wide range of adsorption and catalyst applications for example it is used as a desiccant for drying gases and as a filter of selenium, arsenic and fluoride in drinking water (Richardson *et al.*, 2002).

iii. Activated clays

Activated clay is a naturally occurring porous mineral that has no adsorption ability unless it is activated by acid treatment. Mantell (1951) stated that activated clays are limited in use to the contact process and are not regenerated. However, they are about four times as powerful as natural clays. Activated clay can be used in different industry applications, including diagnostics, pharmaceuticals, medical, nutraceuticals, food, confectionary and electronics (Mantell, 1951).

iv. Molecular sieves

Molecular sieves are crystalline metal aluminosilicates naturally occurring as adsorbents with high uniform size pores and large specific surface area. The adsorbent lets small molecules pass through their pores and are adsorbed while not letting any larger molecules pass through their pores as shown in figure 2.4. As described by Anne (2014) the molecular sieves are used as adsorbents for a wide range of applications for gases and liquids purification. In this study, natural zeolites were used as adsorbents to remove natural heavy metals from the industrial wastewater. The next chapter describes the general aspects of zeolites in detail.

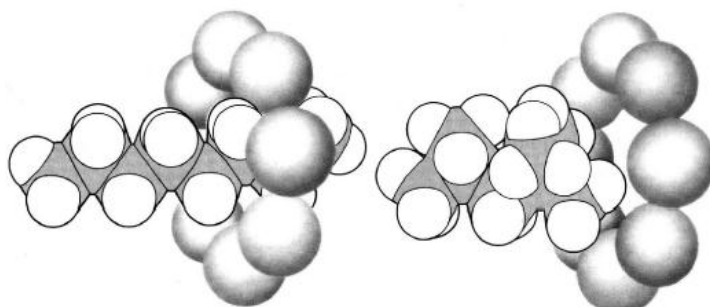


Figure 2.4: Shows zeolite sieve separation process of a straight-chain hydrocarbon (octane) from a branching-chain hydrocarbon (isooctane).

CHAPTER 3

3. OVERVIEW OF ZEOLITES

This introductory section describes the general aspects of zeolite, its history, the geographical distribution and occurrence of zeolites. It also reviews zeolite science by focusing on structures, properties, industrial applications of zeolites and its role in solving environmental problems.

3.1. Historical remarks

Zeolites have been well-known for more than 200 years and since the 1950s they have attracted the attention of many scientists and their industrial and commercial potential has been recognized (Ribero, *et al.*, 1984; Barrer, 1982; Mumpton, 1978; Ouki *et al.*, 1994). The term ‘zeolite’ was coined by the Swedish mineralogist Baron Cronstedt in 1756. Zeolite was created from two Greek words meaning “to boil” and “stone”, which refers to certain silicate minerals that force out water when heated (Dyer, 1988; Gottardi and Galli, 1985; Newsam, 1986; Polat *et al.*, 2004). The mineralogist Tobern Olof Bergman (1735–1784) developed some of the techniques of wet quantitative analysis and analysed some zeolite specimens, and Anton von Swab (1702–1768) added new discoveries to the number of known zeolites a few months after the publication of Cronstedt’s paper (Carminie and William, 2014). Since then, zeolites have been known as a different group of minerals, one of the most plentiful on earth. St Claire-Deville in 1862 was the first to attempt to synthesize zeolitic materials (Barrer, 1982; Breck, 1974) when he prepared levynite through the hydrothermal treatment of potassium silicate and sodium aluminate in a sealed glass tube (Breck, 1974).

Barrer and co-workers made the breakthrough in the 1940s when they successfully synthesized analcime (Barrer, 1982). Barrer in 1948 reported that a wide range of zeolites can be synthesized from aluminosilicate gels and he attempted to synthesize mordenite at high temperatures and pressures (Barrer, 1982). Milton and Breck in 1950 discovered zeolites A, X and Y at the Union Carbide Corporation (UCC). The real success achieved by Breck and his colleagues was utilizing mild hydrothermal conditions using a temperature of 100°C and self-generated pressure to synthesize the first non-natural zeolites (Dyer, 1988; Chiang, 2001). Thus, by late 1950s zeolites had found significant commercial use. In 1953, zeolite A

was used to remove oxygen pollution from argon at a Union Carbide plant (Milton, 1968). However, in 1954, Union Carbide introduced the use of synthetic zeolites as a new class of industrial adsorbents and later in 1959 they introduced the use of synthetic zeolites as hydrocarbon-conversion catalysts (Dyer, 1988; Gottardi and Galli, 1985; Flanigen, 1991).

In 1961, a commercially significant synthetic zeolite was discovered by Barrer and Denny when they investigated the synthesis of high silica zeolite using an organic alkylammonium as a template. Mobil Oil used zeolite X as a cracking catalyst in 1962, followed by the synthesis of ZSM-5 as well as the high silica beta zeolite. Throughout the 1960s, new zeolites were discovered and new applications appeared steadily (Dyer, 1988; Gottardi and Galli, 1985).

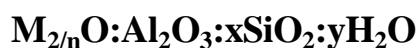
Then in the 1970s the synthesis of zeolite A from kaolinite material sources started using hydrothermal reaction of dehydroxylated kaolinite with sodium hydroxide solution (Breck, 1974; Szoztak, 1998). Thus far 40 different types of natural zeolites have been found and more than 200 types of zeolites were synthesized. Synthesized zeolites are designated by a letter A, X, Y, and ZSM-5, as adopted by the International Zeolite Association (IZA) (Yang, 2003; Colella and Wise, 2014). In 2016, there were 232 framework type codes and the database were updated and modernized once again by (IZA). 176 of these appear in the 6th edition of the Atlas of Zeolite Framework Types 56 additional codes have since been approved.

3.2. Zeolite framework structure

The crystal structure of zeolite was analysed for the first time by Taylor in 1930. Since then, their unique physicochemical properties have attracted the attention of many researchers and additional investigations into the framework structures of zeolite have continued. Hey (1930) concluded that natural zeolite is a class of crystalline, porous, hydrated aluminosilicates frameworks with loosely bonded alkaline or alkaline earth metals with important physicochemical characteristics, and can be used in many applications as a cation exchange, molecular sieving or catalysis (Dyer, 1988).

In general zeolite can be defined as a microporous crystalline solid substance that is inorganic and contains silicon, aluminium and oxygen in its framework and cations and water

molecules within it spores (Mortier, 1982; Dyer, 1988). The general chemical formula of zeolites would be:



M represents the charge-balance cation (Na, K, Li) and/or (Ca, Mg, Ba, Sr), **n** is the cation charge, **x** is generally ≥ 2 , and **y** is the water contained in the natural zeolite.

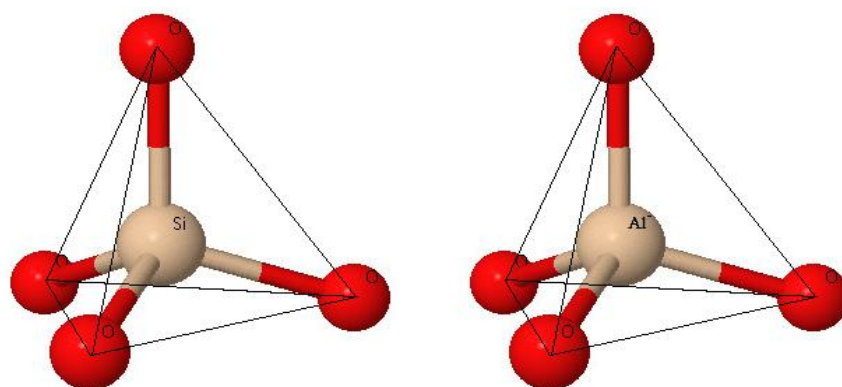


Figure 3.1: Diagrammatic sketch of the zeolite structure and representation of $[\text{SiO}_4]^{4-}$ or $[\text{AlO}_4]^{5-}$ tetrahedral (Dyer, 1988).

The above figure shows that the tetrahedron structure unit of the zeolite in which the centre is occupied by a silicon or aluminium atom connected to four oxygen atoms at the corners. The positive charge deficiency caused by the substitution of Al^{3+} by Si^{4+} is compensated by cations located together with water molecules in the channels (Mortier, 1982). The framework contains open cavities in the form of channels and cages. Channels and cages are occupied by water molecules and extra-framework cations (Na, K, Li, Ca, Mg, Ba, Sr) that are commonly exchangeable (Gottardi and Galli, 1985; Ribero *et al.*, 1984).

Zeolites can be widely classified in to three schemes. Two of these are based upon specifically defined aspects of the crystal structure, while the third has a more historical basis, placing zeolites with similar properties (e.g., morphology) into the same group. This third method also related to its crystal structure, but not as directly as the first two, which are based upon the crystal structure (Armbruster and Gunter, 2001). In the zeolite structure, three relatively independent components are found: the alumina-silicate framework, exchangeable cations and zeolitic water (Dyer, 1988; Gottardi and Galli 1985).

The alumina-silicate framework is the most conserved and stable component of zeolite. The topology of the framework, and the numbers and distribution of the charges (Al^{3+} sites) are basically formed at the crystal growth stage and they define a series of technologically important properties of zeolites (Dyer, 1988; Gottardi and Galli 1985). The water content clearly depends on the distribution of cations because the cations in the channels and cavities are surrounded by both water molecules and oxygen atoms. All water molecules are associated with non-skeletal cations and each hydrogen is bound to a tetrahedral oxygen atom. All of the oxygen in the framework participates in a cation or hydrogen bond. Cations are bound more strongly by water oxygen than by framework oxygen atoms (Dyer, 1988; Gottardi and Galli, 1985; Breck, 1974). The water molecules can be present in the voids of large cavities and bonded between framework ions and exchangeable ions via aqueous bridges. The most significant feature of the zeolite structure is the presence of voids and channels, which define the specific properties of these minerals (Gottardi and Galli, 1985). These structural cavities and channels are occupied by alkaline and alkaline-earth cations and water molecules and they constitute 20%-50% of the total volume (Gottardi and Galli, 1985).

As described by Bekkum (1991) both the Si/Al ratio and the cation content determine the properties of most zeolites. Based on the correlation Si/Al ratio zeolites are divided into high, middle, and low silica, which determines their stability at different pH values (Ribero *et al.*, 1984). Low, intermediate and high silica zeolites are listed in table 3.1.

Table 3.1: The variations in the Si/Al ratio of zeolite (Ribero *et al.*, 1984).

“Low” Si/Al Zeolites (1 to 1.5): A,X
“Intermediate” Si/Al Zeolites (2 to 5):
Natural Zeolite: mordenite, erionite, chabazite,clinoptilolite
Synthetic Zeolites: Y, L, large pore mordenite, omega
“High” Si/Al Zeolites (10 to 100):
By thermochemical framework modification: high siliceous variants of Y, mordenite, erionite
By directed synthesis:ZMS-5

The first structural classification scheme is described by Meier *et al.* (1996) which are based upon the framework topology of the crystal structure, with separate frameworks receiving a three letter code. The frameworks for zeolites with the same code are identical (e.g. heulandite and clinoptilolite). A framework type code of three letters has been assigned to zeolites and the priority in the naming of zeolites depends on the first mineral discovered in the group (Armbruster and Gunter, 2001).

The second structural classification is described by Meier (1968). It is based on a concept termed the ‘secondary building unit’ (SBU), as shown in Figure 3.2. The primary building unit for zeolites is the tetrahedron. SBUs are geometric arrangements of the tetrahedra (Dyer, 1988; Breck, 1974; Armbruster and Gunter, 2001). Frequently, these SBUs tend to control the zeolite’s morphology. This classification is useful in silicate minerals when tetrahedra can be arranged into groups such as rings, chains, sheets, or frameworks.

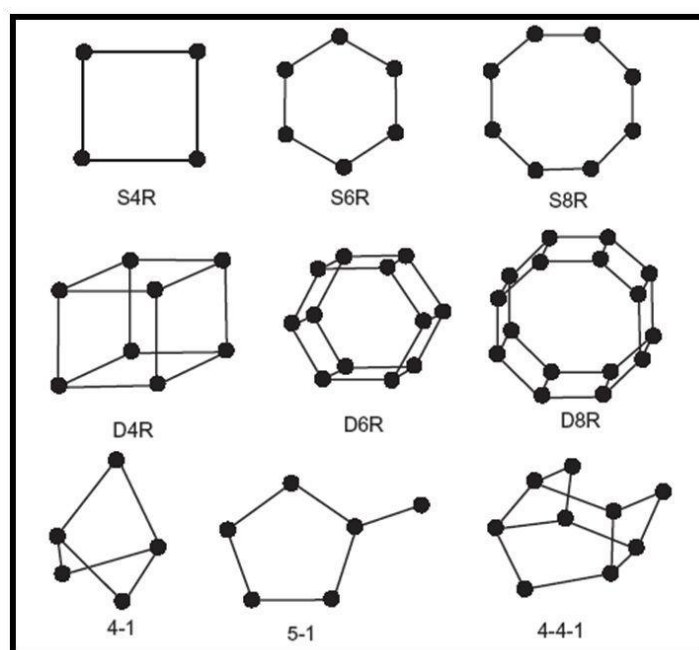


Figure 3.2: Shows the SBUs in zeolites, the second structural classification as described by Meier (1968).

In these SBUs only the position of tetrahedral (T) Si and Al are shown. Oxygen atoms lie near the connecting solid lines, which are not intended to mean bonds. Breck (1974) lists seven major groups of zeolites based upon the geometry of the SBU (Dyer, 1988; Gottardi and Galli 1985). This classification is based on the framework topology of the zeolites for which the structures are known (Table 3.2), within which zeolites have a common subunit of

structure that is a specific array of (Al, Si)O₄ tetrahedra. In the classification, the Si-Al distribution is neglected. These subunits have been called SBUs by Meier (1968). The primary building unit for zeolites is the tetrahedron. These secondary building units (SBU's) - (the primary building units being the TO₄ tetrahedra) - can contain up to 16 T atoms. It can be noted that SBU's are non-chiral (neither left nor right "*handed*"). A unit cell always contains the same number of SBU's, and although rare, some materials can have different combinations of SBU's within the zeolite framework.

The framework may be considered in terms of large polyhedral building blocks forming characteristic cages. For example, sodalite, zeolite A and zeolite X/Y (Faujasite) can all be generated by the truncated octahedron known as the b-cage. One interesting problem in zeolite chemistry is the distribution of silicon and aluminium atoms among the T sites. According to Lowenstein's rule, Al-O-Al linkages in zeolitic frameworks are forbidden. As a result, all aluminate tetrahedra must be linked to four silicate tetrahedra, and in general this is proved to be the case, but recent investigations into zeolites synthesised at high temperatures have shown non-Lowenstein distributions in sodalite materials.

Table 3.2: Classification of zeolite structures (Breck, 1974).

Group	Secondary Building Unit (SBU)
1	Single 4-ring, S4R
2	Single 6-ring, S6R
3	Double 4-ring, D4R
4	Double 6-ring, D6R
5	Complex 4-1, T ₅ O ₁₀ unit
6	Complex 5-1, T ₈ O ₁₆ unit
7	Complex 4-4-1, T ₁₀ O ₂₀ unit

The third broad classification scheme proposed by Gottardi and Galli (1985) is quite similar to the SBU classification described by Breck (1974). Moreover the third classification scheme includes some historical background of how the zeolites were discovered and named (Figure 3.2). This scheme is widely used by geologists (Dyer, 1988; Gottardi and Galli 1985). They use a combination of zeolite group names that have specific SBUs and consist of some complex structural units of tetrahedra, whether finite or infinite, as shown in figure 3.3. The grouping of zeolites by some zeolite species name was also used by Meier (1968).

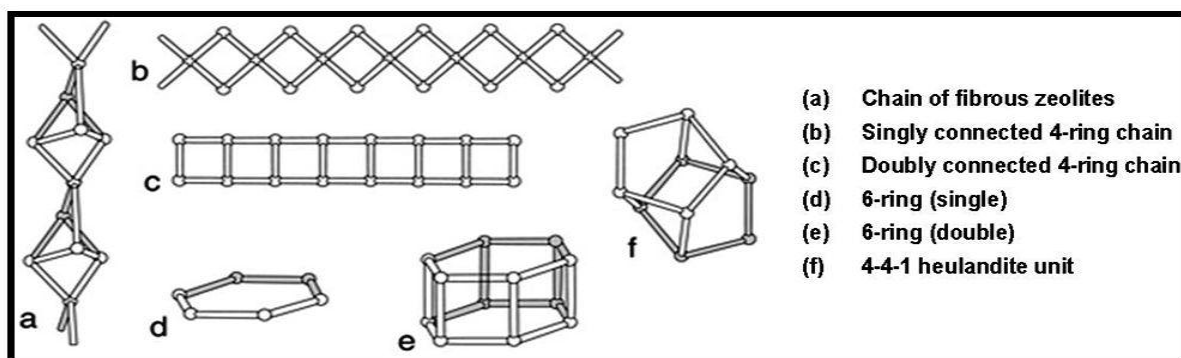


Figure 3.3: Shows the structural units, which may be used to assemble the zeolite frameworks (Breck, 1974; Gottardi and Galli, 1985).

Researchers may find these multiple classification schemes very confusing and complex. Each scheme is used by a group of researchers; for example both crystallographers and mineralogists are more used to the structure codes and SBUs, while the third classification scheme are more useful to geologists and descriptive mineralogists.

Zeolite pores consist of 6, 8, 10, 12 and 14 member oxygen ring systems that form a tube-like structure and pores that are consistent to each other (Bahruji, 2005). On the other hand, other factors such as the size, location, and coordination of the extra-framework cations can also influence the pore size (Gualtieri, 2006). Zeolites can be used in various industrial processes due to their high attractive properties such as cation-exchange ability, and molecular sieve and catalysis properties. The uses of zeolites essentially depend on their unique structural characteristics such as the interconnected regular three-dimensional network of micropores, the Si/Al ratio and the nature and content of the extra-framework cations. Thus the well-defined micropores give the zeolites molecular sieving properties while the Si/Al ratio affects the surface when the ratio decreases surface becomes more hydrophilic. As well as more cations are needed to compensate for the negative charges introduced by aluminium (Gualtieri, 2006).

The crystal structure of clinoptilolite has 3-dimensional aluminosilicate framework, which specific structure causes the developed system of micropores and channels occupied by water molecules and exchangeable cations. Unit cell parameters of clinoptilolite crystals are as follows: $a = 17.66 \text{ \AA}$, $b = 17.963 \text{ \AA}$, $c = 7.400 \text{ \AA}$ and $\beta = 116^\circ 47'$ (Koyama and Takeuchi, 1977). Two-dimensional channel system is formed in the clinoptilolite minerals (parallel to a and c axes) row based on the features of alumino-silicate framework structure. There are two

channels running parallel to each other and to the c axis: a channel consisting of a 10-member (tetrahedron) ring of the size of 4.4–7.2 Å and a channel consisting of an 8-member ring with the size of 4.1–4.7 Å and a channel run parallel to a axis consisting of an 8-member ring with the size of 4.0–5.5 Å (Breck, 1974).

3.3. Geographical distribution and occurrence of natural zeolites

Many types of zeolite have been found in different places of the world since the first discovery of zeolite. In 1988 it was estimated that the world's natural zeolite consumption was 3.98Mt and that it would reach 5.5Mt by 2010 (Dyer, 1988). According to the U.S. Geological Survey in 2016 the world's annual production of natural zeolite approximates 3 million tonnes. Major producers in 2010 included China (2 million tonnes), South Korea (210,000 t), Japan (150,000 t), Jordan (140,000 t), Turkey (100,000 t) Slovakia (85,000 t) and the United States (59,000 t).

Zeolites are found in many types of rocks, of different ages and in a variety of geological environments (Barrer, 1982; Dyer, 1988). Zeolites are formed by the reaction of pore water with solid material. Natural zeolites can be found in altered mafic volcanic rocks as cavity fillings, probably as a primary phase in some under saturated volcanic rocks as a result of deposition by weathering. Zeolite can be found in sedimentary rocks too as alteration products of volcanic glass and in chemical sedimentary rocks of marine origin. Metamorphic rocks also contain a sequence of zeolite minerals, which were formed due to their depth of burial by subsequent layers of geologic formations under significant geothermal condition (Barrer, 1982; Sand and Mumpton, 1978). The chemical, physical and mineralogical properties of natural zeolite depend upon their geological features. The nature of the rock minerals involved determines the composition and pore size of the zeolite (Barrer, 1982; Sand and Mumpton, 1978; Barrer, 1982).

Clinoptilolite is the most abundant natural zeolite and it is widely used throughout the world (Barrer, 1945; Colella and Wise, 2014; Gottardi and Galli, 1985). Clinoptilolite is common as a major constituent of submarine volcanic sediments of tuffites and it can be found principally as microcrystalline sedimentary masses (Erdem *et al.*, 2004; Gottardi and Galli, 1985).

3.4. Synthetic zeolites using kaolinite as a base material

A base material that contains a high level of silica and alumina can be used for the preparation of synthetic zeolites, such as clay minerals, volcanic glasses, diatomite, natural zeolites, high silica bauxite or oil shale.

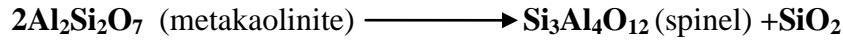
Many researchers have converted clay minerals to synthetic zeolite, such as kaolinite, bentonite (montmorillonite), halloysite, illite, smectite, interstratified illite-smectite, mordenite, bauxite, diatomite and have made great progress in synthesis of 4A, X, Y zeolites (Breck, 1974; Boukadir *et al.*, 2002; Barrer, 1982; Cañizares *et al.*, 2000; Klimkiewicz and Drag, 2004; Baccouche *et al.*, 1998; Ruiz *et al.*, 1997; Boukadir *et al.*, 2002).

With regard to the use of kaolinite as a precursor for zeolite production, previous studies have shown that an improvement in the properties of the kaolinite using chemical methods, which is necessary for zeolite formation, but is difficult due to its low reactivity. Kaolinite does not show significant change by acid or alkaline treatments (Murat *et al.*, 1992; Lussier, 1991; Akolekar *et al.*, 1997). Therefore, kaolinite needs to be decomposed by calcination at temperatures between 550-950°C to obtain a metakaolineite phase after loss of structural water and reorganization of the structure (Lambert, 1989; Mackenzie, 1971). The transition of kaolinite, when heated in a furnace in which air is circulating, has been reported and found that metakaolinisation achieved by calcining the kaolinite in open air at around 550-900°C with different exposure times (Breck, 1974, Madani *et al.*, 1989; Brindley and Nakahira, 1959). Previous experiments reported that the best heating values for obtaining a reactive metakaolinite can be between 600-800 °C (Lussier, 1991; Akolekar *et al.*, 1997). Mackenzie (1971) showed in his investigation that calcinations of kaolinite at very high temperatures resulted in formation of mullite and cristobalite.

Previous studies have reported the production of different zeolites from different kaolinite deposits around the world using specific synthesis conditions. Different researches have successfully synthesised zeolite using different temperatures for metakaolinization and different exposure times (Huang, 1993; Bauer and Berger, 1998; Bauer *et al.*, 1998; Cama *et al.*, 2000, Mousa and Buhl, 2014; Ayele *et al.*, 2015; Jamil, *et al.*, 2011; Salem and Sene, 2011; Ibrahim *et al.*, 201, Rios *et al.*, 2007). This reaction series includes the formation of highly disordered metakolinite formed at around 550-900°C when kaolinite is air calcined as shown below:



On further heating, a new phase is obtained at around 925°C called spinel, which is a defect alumina-silica structure:



More stable materials called mullite and cristobalite are formed at a temperature of 1050°C



A variety of investigations have been carried out on the optimization of the hydrothermal synthesis including the stability of kaolinite under different pH conditions (Huang, 1993; Bauer and Berger, 1998; Bauer *et al.*, 1998; Cama *et al.*, 2000) and with various NaOH concentrations and different reaction times (Mousa and Buhl, 2014; Lijalem *et al.*, 2015; Jamil *et al.*, 2011; Salem and Sene, 2011; Ibrahim *et al.*, 2010).

Synthetic zeolite production from kaolinite material was performed in this study because kaolinite as good aluminosilicate source and can be used in zeolite synthesis. Kaolinite as natural clay, relatively cheap, abundant in supply and kaolinite does not introduce additional pollution into the environment (Georgiev *et al.*, 2009; Rios *et al.*, 2007; Basaldella *et al.*, 1993; Basaldella and Tara, 1995).

3.5. Properties of zeolites

As discussed in the previous chapter, the most important attributes for any adsorbent application are: capacity, selectivity, regenerability, kinetics, compatibility and cost. Most researchers have observed that synthesized zeolites have a higher ion exchange capacity than natural zeolites, while the pre-treatment improves the efficiency of natural zeolite in the removal of heavy metals from the industrial wastewater (Inglezakis *et al.*, 2004; Gunay *et al.*, 2007; Han *et al.*, 2006).

3.6. Application of zeolites

Clinoptilolite have been utilized for many applications in several fields such as pollution control. The applications of clinoptilolites are depening on three special properties:

Ion exchange: zeolite has high ion exchange ability since they can interact with phases and replace existing ions.

Molecular sieves: zeolite can selectively absorb or release ions and molecules depending on their cavities in their structures.

Catalytic cracking: zeolite can also react with large molecules and break in them down into smaller pieces.

The potential environmental applications of clinoptilolite can be given as:

- Nuclear effluents containing radioactive isotopes in the take-up of Cs and Sr from nuclear waste and fallout (Abusafa and Yücel, 2002; Dyer and Zubair, 1998; Faghihian *et al.*, 1999; Gennaro *et al.*, 2003; Shahwan *et al.*, 2005; Um and Papelis, 2004).
- Ammonia removal from municipal wastewaters (Langella *et al.*, 2000; Cincotti *et al.*, 2001, Watanabe *et al.*, 2003; Sarioglu, 2005; Duff *et al.*, 2005; Ramos *et al.*, 2004).
- Heavy metal removal from industrial and agricultural effluents for example remediation of acid mine drainage (Ouki and Kavannagh, 1999; Halimoon and Yin 2010; Mier *et al.*, 2001; Langella *et al.*, 2000; Cincotti *et al.*, 2001; Curkovic *et al.*, 1997; Blanchard *et al.*, 1984; Šiška, 2005; Peric *et al.*, 2004).
- The ion exchange property of clinoptilolites is also used in controlling soil pH and nutrient levels (soil conditioning), and also as an animal feed supplement (Alvarez *et al.*, 2003; Sand and Mumpton, 1978).
- Air pollution control (Khulbe *et al.*, 1994; Axente *et al.*, 1983; Ackley *et al.*, 2003).
- More recently in several emerging field such as health and medicine (Payra and Dutta 2003).

CHAPTER 4

4. MATERIALS AND METHODS

4.1. Introduction

This chapter is split into two parts; the first part generally describes the methods and materials used in the investigation of natural zeolite as a potential adsorbent in synthesised industrial wastewaters. The second part describes methods and materials of kaolinite clay which is used as a source of aluminosilicate to prepare synthetic zeolite. Batch methods used in this thesis includes both kinetic studies and equilibrium studies. Both studies are very important in order to obtain a realistic result in determining the efficiency of the zeolite in removing heavy metal ions from solution.

The efficiency of clinoptilolite for the removal of four heavy metal ions from a solution was considered; these were Fe^{3+} , Cu^{2+} , Pb^{2+} and Zn^{2+} . These four ions were chosen as abundance more pollutants that are contained in industrial wastewaters. These metals are very common in water and sediment pollutants in harbours surrounded by industrial facilities.

There are some factors that affect the capacity of the adsorption process, including the adsorbent particle size, the mass of adsorbent, the initial solution pH and concentration, the agitation speed and the effect of chemical and thermal pre-treatment of the adsorbent. The preparation and analysis of the synthetic solutions used in this research is also discussed.

4.2. Materials and sample preparation

4.2.1. Synthetic solutions and other chemicals

The experiments have focused on the efficiency of natural zeolite and synthetic zeolite for the removal or reduction of Fe^{3+} , Cu^{2+} , Pb^{2+} and Zn^{2+} ions from synthetic industrial wastewater, to achieve allowable limits.

Synthetic multi-component solutions of Fe^{3+} , Cu^{2+} , Pb^{2+} and Zn^{2+} ions were prepared from analytical grade iron (III) chloride hexahydrate ($\text{H}_{12}\text{Cl}_3\text{FeO}_6$), Copper (II) chloride dehydrate ($\text{H}_4\text{Cl}_2\text{CuO}_2$), Lead(II) acetate trihydrate ($\text{C}_4\text{H}_{12}\text{O}_7\text{Pb}$) and Zinc acetate dehydrate ($\text{C}_4\text{H}_{10}\text{O}_6\text{Zn}$).

The initial concentration of the heavy metals in the synthetic industrial wastewater was in the range of 40, 141, 335 and 87 mg/l of Fe^{3+} , Cu^{2+} , Pb^{2+} and Zn^{2+} ions respectively. In all the experiment stages deionised water was used, which had almost all of its mineral ions removed. The pH of the starting solution was pH 4 due to get the best adsorption rate. The pH values were monitored and adjusted using a pH meter (Microprocessor pH Meter – pH 211-HANNA instruments). The pH was adjusted to 2, 4, and 6 ± 0.1 by adding hydrochloric acid (HCl) or bases sodium hydroxide (NaOH). To observe the effect of agitation speed; agitation in a beaker was obtained by using a magnetic stirrer (stuart-SB162) at a speed of 100 rpm, 150 rpm and 200 rpm.

Samples were ground manually in a porcelain mortar and sieved using laboratory soil sieves. The mesh sizes of the zeolite particle used in this study was $125 \mu\text{m} < \text{dp} < 250 \mu\text{m}$, unless stated. A Carbolite BWF 11/13 high temperature furnace was used for calcination and sintering. A Memmert model UM200 stainless steel universal oven was used to dry and heat the samples.

4.2.2. Characterisation of natural zeolite and raw materials

In this study natural zeolite (clinoptilolite) was used. The natural clinoptilolite was mined in Anaconda and supplied by the Anaconda mining company, Denver Colorado, USA it is 97% pure. The kaolinite clay used in the present investigation collected from the site in the western part of Iraq and supplied by Kurdistan Institution for Strategic Studies and Scientific Research (KISSR). The natural zeolite and raw material samples were used as received without any modification from their natural state, unless stated. The raw and zeolitic material samples were washed with deionised water to remove unwanted dust from their surfaces before use and then dried at room temperature for about 24 hrs.

Each analysis technique typically investigated only a particular aspect of the material and, therefore, a combination of methods was necessary to obtain a complete description of the raw materials as well as the different zeolitic products. This is very important to use and improve a zeolitic material for a specific application. Generally, the characterization of a zeolite has to provide information on: (1) its structure and morphology; (2) its chemical composition; (3) its ability to sorb and retain molecules; and (4) its ability to chemically convert those molecules.

4.2.2.1. Scanning Electron Microscopy (SEM)

The surface morphology, topography of the raw and zeolitic materials was investigated using a ZEISS EVO50 scanning electron microscope. The samples were prepared by spreading dried raw material or zeolite powder onto 12mm aluminium stubs using double-sided sticky carbon discs and then placing them in a vacuum sample chamber. The samples were coated with gold using an Emscope SC500 sputter coater. Images were taken under high vacuum condition using the secondary electron detector.

4.2.2.2. Energy Dispersive Spectroscopy (EDS)

The Energy Dispersive Spectroscopy analytical technique was used in this study for the elemental analysis or chemical characterization of the samples. EDS is a chemical microanalysis technique can be used together with SEM. For the EDS analysis the samples were prepared in a similar way to the SEM. However, instead of using aluminium stud a carbon sample holder was used to avoid errors in the aluminium content, and the samples were not coated with gold.

4.2.2.3. X-Ray Diffraction (XRD)

X-ray diffraction (XRD) was the analytical technique used for phase identification of the natural zeolite samples, raw materials and synthesis products of crystalline materials. The samples were ground to a powder and pressed firmly into the sampler holder before analysis using the Empyrean, PANalytical X-ray diffractometer with Cu-K α radiation at 40 mA and 40 kV and secondary monochromation. All data collection database was presented in the 2 θ range at start position 5 and end Position 50 or 80 degree, with a scanning step of $^{\circ}2\ \Theta$. The raw materials and zeolitic products were crushed with an agate mortar and pestle, ground to powder form (<15 μm) and mounted in aluminium plate sample holders with a volume of 0.1 cm^3 . The results of crystalline patterns were compared with the standard line patterns database supplied by the International Centre for Diffraction Data (ICDD).

4.2.2.4. X – Ray Fluorescence (XRF)

XRF analysis technique was used in this study to determine the chemical composition of the zeolite, raw materials and synthesis products. The XRF technique depends on fundamental principles involving interactions between electron beams and X-rays with samples. Mostly, the samples were prepared in a similar way to the XRD sample preparation technique. The samples were prepared by grinding to a powder then pressed firmly into the sampler holder. All samples were analysed using the Empyrean, PANalytical XRF spectrometer with 60Kv energy of the X-ray tube.

4.2.2.5. Thermogravimetric Analysis (TGA)

The thermogravimetric analysis technique was used for the measurement of changes in the physical and chemical properties whilst increasing the temperature constantly. The raw materials were analysed using thermogravimetry on a Perkin Elmer TGA7 thermobalance between 30-1000 °C. The heating rate of 20 °C min⁻¹ was used and the atmosphere in the TGA was nitrogen. The amount 10-15 mg of ground sample was placed directly into the crucible for TGA testing. The TGA crucible was cleaned properly before test and after each run. The results of TGA patterns were analysed and interpreted at each stage. This analytical technique was very useful in estimating the thermal stability of the thermally treated zeolite and synthetic zeolite products.

4.2.2.6. Fourier Transform Infrared (FT-IR) Spectroscopy

The ALPHA make FTIR Platinum ATR single reflection diamond module was used for materials analysis in this study. An infrared spectrum represents a finger print of the sample.

The sample platform and the stub were cleaned properly before sample analysis and after each run using acetone. The amount 10-15 mg of ground samples were placed onto the diamond ATR crystal surface. Finally, a force was applied to the sample for spectrum collection. OPUS software was used. The sample was then removed from the crystal surface and cleaned again in order to prepare the accessory to collect additional spectra.

4.2.2.7. Inductively Coupled Plasma-Optical Emission Spectrometers (ICP-OES) analysis

The heavy metal ion concentrations in the solution were determined using Agilent 5100 ICP-OES. The standard solutions for metal analysis using the ICP-OES were prepared from standard metal solutions to determine the amount of Cu^{2+} , Fe^{3+} , Pb^{2+} and Zn^{2+} ion concentrations which present in the solutions before and after the exchange.

Samples were filtered before being analysed to remove any contained solids using Whatman filter papers. 2% nitric acid was used to dilute all samples, standards and prepare a blank solution. Samples were diluted to a concentration of acid into the specified range of less than 5%. The sample volume was 10ml in a 15ml centrifuge vial then analysed.

4.3. Experimental procedure

4.3.1. Equilibrium studies

Equilibrium studies were carried out when 4g of natural zeolite was mixed with 100 ml of multi-component solutions. The level of initial heavy metal concentrations was (40, 141, 335 and 87) mg/l of Cu^{2+} , Fe^{3+} , Pb^{2+} and Zn^{2+} respectively. Three different pH values of initial solution were preferred 2, 4 and 6 ± 0.1 . The particle size of the adsorbent used was $>250 \mu\text{m}$. The mixtures were agitated for 360 minutes at 150 rpm, until equilibrium was achieved then the solution samples were filtered to remove solids and analysed using the ICP-OES.

4.3.2. Regeneration in batch studies

Regeneration of the natural zeolite was carried out using 0.5M NaCl. After each run, the zeolite sample was agitated in the stripping solution using a magnetic stirrer at 150 rpm for 45 minutes. The samples were rinsed twice in deionised water for 15 minutes and dried at room temperature. They were then re-used for the next experiment run and the regeneration was repeated 4 times in order to observe the adsorption efficiencies with time. The adsorption/ desorption cycle was performed to determine the reversibility of the reactions and reusability of natural zeolite.

4.3.3. Kinetic studies

Zeolite samples with masses 2g, 4g and 8g were contacted with constant volume (100 ml) of multi - component synthetic solutions containing Cu^{2+} , Fe^{3+} , Co^{2+} and Zn^{2+} ions. They were agitated at agitation speeds of 100,150 and 200 rpm for agitation times of 60, 120, 180, 240, 300 and 360 minutes in a magnetic stirrer at room temperature. Every hour 15 ml of the samples were filtered and taken for metal ion concentration analysis using the ICP-OES. The pH values were monitored and adjusted regularly.

The experiments were duplicated three times in order to examine the reproducibility of the results, while the mean value was used for all taken data. The deviation between the duplicate samples in analysing the cations was $\pm 6.4\%$, 6.3% , 5.6% and 6.4% for Cu^{2+} , Fe^{3+} , Co^{2+} and Zn^{2+} ions respectively.

4.3.3.1. Effect of adsorbent particle size

The effect of adsorbent particle size on adsorption process was investigated. Two different sizes of zeolite particles were selected $<125\ \mu\text{m}$ and $<250\ \mu\text{m}$. The adsorbent was mixed with 100 ml solutions of the appropriate multi - component solutions. Hence, 4g natural zeolite was used at an agitation speed of 150 rpm for 360 minutes and samples were collected every hour, then filtered to remove solids and analysed using the ICP-OES. The pH of the solution was adjusted to 4 ± 0.1 .

4.3.3.2. Effect of adsorbent mass

The effect of adsorbent mass on the adsorption capacities from solutions was also investigated. Three different masses were used in this study, 2g, 4g and 8g of natural zeolite in 100 ml solutions. The mixture was agitated at 150 rpm for 360 minutes and samples were collected every hour and analysed using the ICP-OES. The particle size of zeolite used was $250\ \mu\text{m}$. The agitation speed was 150 rpm at room temperature. The pH of the solution was adjusted to 4.

4.3.3.3. Effect of initial solution pH

Three different pH values of initial solution were preferred 2, 4 and 6 ± 0.1 for the multi-component solutions. The solution pH was adjusted using sodium hydroxide (NaOH) solution and hydrochloric acid (HCl) solution. Thus 100ml of the multi- component solution samples were in contact with 4g of natural zeolite for 360 minutes. Samples were collected every hour and analysed using the ICP-OES. The particle size of zeolite used was 250 μm . The agitation speed was 150 rpm at room temperature.

4.3.3.4 Effect of initial metal concentration

The effect of the initial metal concentration on the efficiency of natural zeolite in the removal of heavy metals from the solution was determined using multi-component solution concentrations in the range of (50, 100, 200 and 400) mg/l. Thus 100ml of the multi-component solution samples were in contact with 4g of zeolite at an agitation speed of 150 rpm for 360 minutes. The pH of the solution was adjusted to 4 ± 0.1 .

4.3.3.5. Effect of agitation speed

The effect of agitation speed on the removal of the heavy metal cations from the solution by natural zeolite was determined using a magnetic stirrer at a speed of 100, 150 and 200 rpm. Thus 100ml of the multi- component solution samples were in contact with 4g of zeolite for 360 minutes and samples were collected every hour and analysed using the ICP-OES. The pH of the solution was adjusted to 4 ± 0.1 .

4.3.3.6. Thermal pre-treatment of adsorbent

The thermal pre-treatment process of natural zeolite was performed by heating natural zeolite samples in a furnace for 30 minutes under a slow heating rate of 200, 400 and 600°C to avoid desroy the zeolite structuer. Then 4g of the thermally modified natural zeolite samples were were in contact with 100 ml of multi- component solutions. Agitation was carried out in a beaker using a stirrer at a speed of 150 rpm for 360 minutes at room temperature. The pH of the solution was adjusted to 4 ± 0.1 .

4.3.3.7. Chemical pre-treatment of adsorbent

The chemical pre-treatment of the natural zeolite were carried out by placing natural zeolite sample with 200 ml of 0.5M NaCl. The zeolite sample was agitated in a beaker using a stirrer at a speed of 150 rpm for 24 hours at room temperature. Thereafter the sample was rinsed three times in ample deionised water for a total period of 15 minutes and put in an oven to be dried at 100°C. Then 4g of chemically modified natural zeolite samples were in contact with 100 ml of multi- component solutions for 360 minutes. The agitation speed applied was 150 rpm at room temperature. The pH of the solution was adjusted to 4 ± 0.1 .

4.4. Synthetic zeolite procedure

Kaolinite as an aluminosilicate source was prepared prior to the synthesis process. Samples were ground manually to powder form in a porcelain mortar and sieved using laboratory soil sieves. The mesh sizes of the kaolinite particle selected in this study was $75 \mu\text{m} < dp < 125 \mu\text{m}$.

The synthesis of zeolite A from kaolinite involves two basic steps: metakaolinization, which is thermal treatment of the raw kaolinite at high temperature. The second step is chemical treatment of the obtained metakaolinite with NaOH. The conversion of the raw materials into zeolitic materials method was conducted using the conventional hydrothermal synthesis technique and alkaline fusion prior to hydrothermal synthesis technique. Both procedures were described as the following:

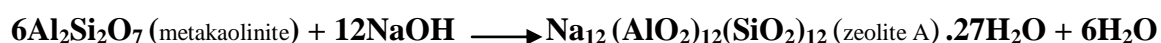
4.4.1. Conventional hydrothermal synthesis

The conventional hydrothermal synthesis technique was used, when 50gm of kaolinite clay powder ($< 125 \mu\text{m}$) was calcined at 600°C for 3 hours to convert kaolinite to metakaolinite (scheme 4.1.). Kaolinite structure was destroyed and any undesired volatile matter is removed and converted to a metakaolinite, as shown in the following equation:



The above produced metakaolinite was treated with NaOH solution with a ratio of 1:5 and using stainless steel autoclaves with a teflon liner heated to 200 °C in a oven for 24 hr in

order to insert the sodium ion into the metakaolinite structure where the following reaction occurs:



The acid treated kaolinite clay was washed with deionised water three times to remove the excess unreacted NaOH. It was then filtered and dried in an oven at 100 °C overnight as shown in figure 4.1.

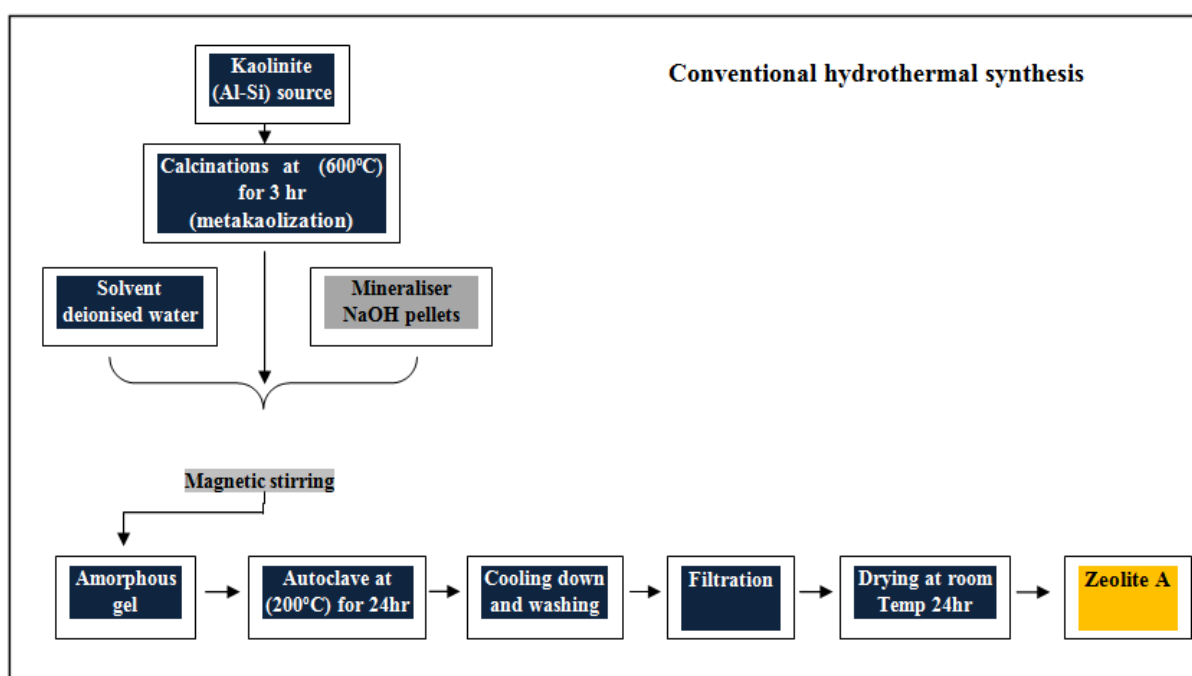


Figure 4.1: Flowchart showing the conversion of the raw materials into zeolitic materials conducted by conventional hydrothermal synthesis.

4.4.2. Alkaline fusion followed by hydrothermal reaction

In the second method, an alkaline fusion step was introduced prior to the hydrothermal treatment as shown in scheme 4.2. While 6.20 g of clay powder (< 125 µm) was mixed manually with 7.44 g of NaOH (ratio = 1/1.2 in weight) in a porcelain mortar and left for 40 min at room temperature. Then the mixture was calcined at 600 °C for 1 h to convert kaolinite to metakaolinite. The fused solid product obtained had to be ground manually again to powder form in a porcelain mortar.

Then 5 g of the produced metakaolinite was contacted with 25ml of distilled water (ratio = 1/5) for 15 minutes at room temperature. The hydrothermal reaction was carried out using stainless steel autoclaves with a teflon liner heated to 200 °C in an oven in order to insert the sodium ion into the metakaolinite. The reactors were removed from the oven after 24 hr and cooled with water to stop the reaction.

The acid treated kaolinite clay was washed with deionised water three times to remove the excess unreacted NaOH. It was then filtered and dried in an oven at 100 °C overnight.

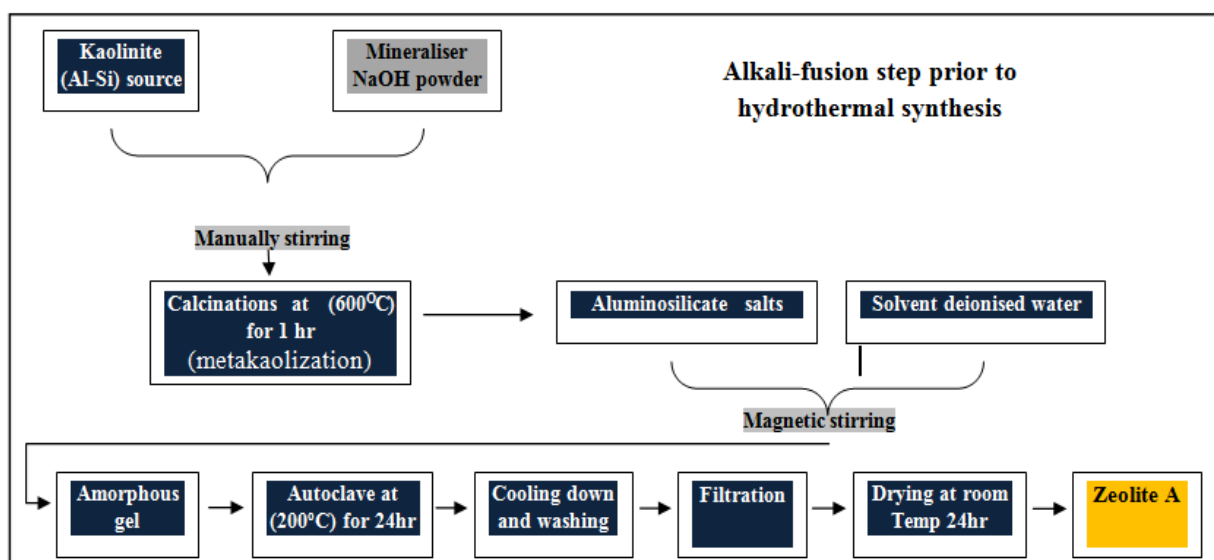


Figure 4.2: Flowchart showing the conversion of the raw materials into zeolitic materials conducted by alkaline fusion followed by hydrothermal reaction

4.5. Synthetic zeolite experimental procedure

Batch adsorption tests were carried out to determine the efficiency of synthetic zeolite type A in the removal of heavy metals from the solution. Thus 4g of synthetic zeolite A mixed with 100 ml multi - component synthetic solutions containing Cu^{2+} , Fe^{3+} , Co^{2+} and Zn^{2+} metal ions. They were agitated at agitation speed of 150 rpm for agitation times of 60, 120, 180, 240, 300 and 360 minutes in a magnetic stirrer at room temperature. The pH of the solution was adjusted to 4 ± 0.1 and the particle size of the dry synthetic zeolite samples used was $>125 \mu\text{m}$.

CHAPTER 5

5.CHARACTERISATION OF NATURAL ZEOLITE

5.1 . Introduction

Knowledge of the characteristics of natural zeolite, raw materials used in synthesis are very important. The technological properties of zeolite products depend on the physical, chemical and mineralogical characteristics of the starting materials; this also controls the overall processing treatment of polluted effluents.

Particle characterisation discloses information on the physical, chemical and mineralogical nature of zeolite product particles, which is related to removal efficiency of heavy metals ions from solution. This chapter describes the characterisation of the natural zeolite to provide information on: (a) its structure and morphology; (b) its chemical composition; (c) its ability to sorb and retain molecules; and (d) its ability to chemically convert those molecules.

In this study different analytical techniques were used to study natural zeolite (discussed in this chapter) and kaolinite and synthesis product samples (discussed in detail in chapter 8). This used analytical techniques including: Scanning Electron Microscopy (SEM), Energy Dispersive Spectroscopy (EDS), X – Ray Diffraction (XRD), X – Ray Fluorescence (XRF), Thermogravimetric Analysis (TGA), Fourier Transform Infrared (FT-IR) and Inductively Coupled Plasma-Optical Emission Spectrometers (ICP-OES).

5.2. Analytical techniques

5.2.1. Scanning Electron Microscopy (SEM)

The surface morphology of the different natural zeolite samples was determined using SEM under the following analytical conditions: EHT = 10.00 kV and 20.00 kV, Signal A = SE1 and VPSE, WD = 6.0, 6.5, 7.0 and 8.5mm at different magnifications.

Scanning Electron Microscopy (SEM) results

The surface morphologies of the different natural zeolite samples before and after modification were analysed. Figure 5.1 show the micrographs of the “as received” natural zeolite samples. The images were taken under the following SEM analytical conditions: EHT =10.00 kV and Signal A = SE1, WD 6.5mm at a magnification of 1000x, 5000x. The micrographs clearly show that the natural zeolite structure contains a number of different diameter size macro-pores ($1\text{ }\mu\text{m} \leq d \leq 3\text{ }\mu\text{m}$).

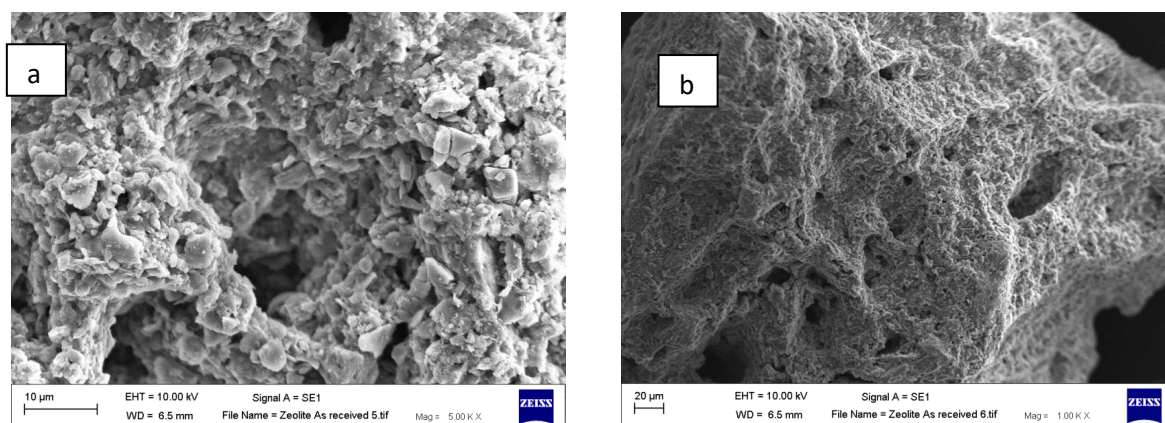


Figure 5.1: Showing the SEM micrograph of as-received natural zeolite (Clinoptilolite) at a magnification of: (a) 5000x and (b) 1000x.

Figure 5.2 and 5.3 shows the natural zeolite under the following SEM analytical conditions: EHT = 20.00 kV, Signal A = VPSE, WD 8.5mm at a magnification of 5000x, 1000x. The micrographs mostly show well defined crystals of natural zeolite (SBU is 6-6).

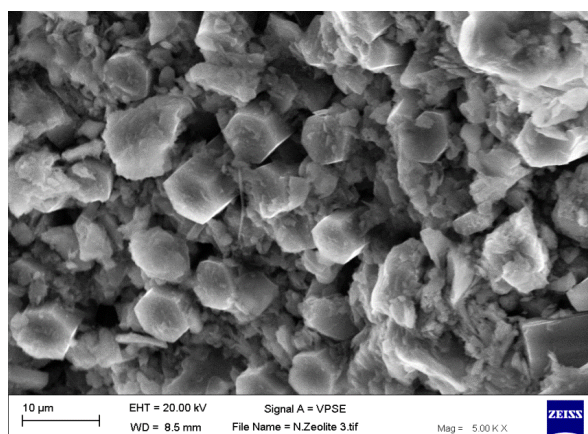


Figure 5.2: Showing the randomly oriented crystallites and in particular indicating the crystalline nature of natural zeolite, at a magnification of 5000x.

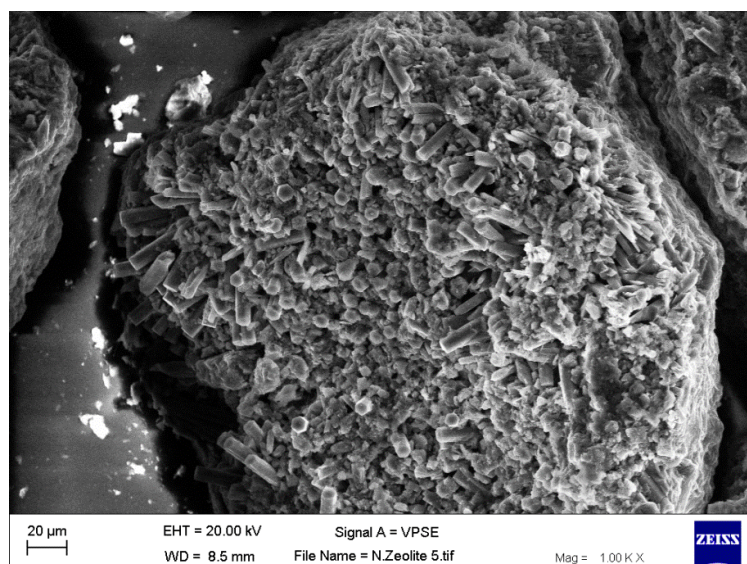


Figure 5.3 : Showing the randomly oriented crystallites and in particular indicating the crystalline nature of natural zeolite at a magnification of 1000x.

The effect of chemical pre-treatment was analysed when 0.5M of NaCl acidic solution was used for the chemical pre-treatment of zeolite to remove all of the undesired volatile matter (unwanted waste material) and obtain a clean surface, as shown in figure 5.4 under the following SEM analytical conditions: EHT =10.00 kV, Signal A = SE1, WD 6.5mm at a magnification of 1000x and 5000x. The micrographs below show a clean surface and well defined crystal structures of clinoptilolite.

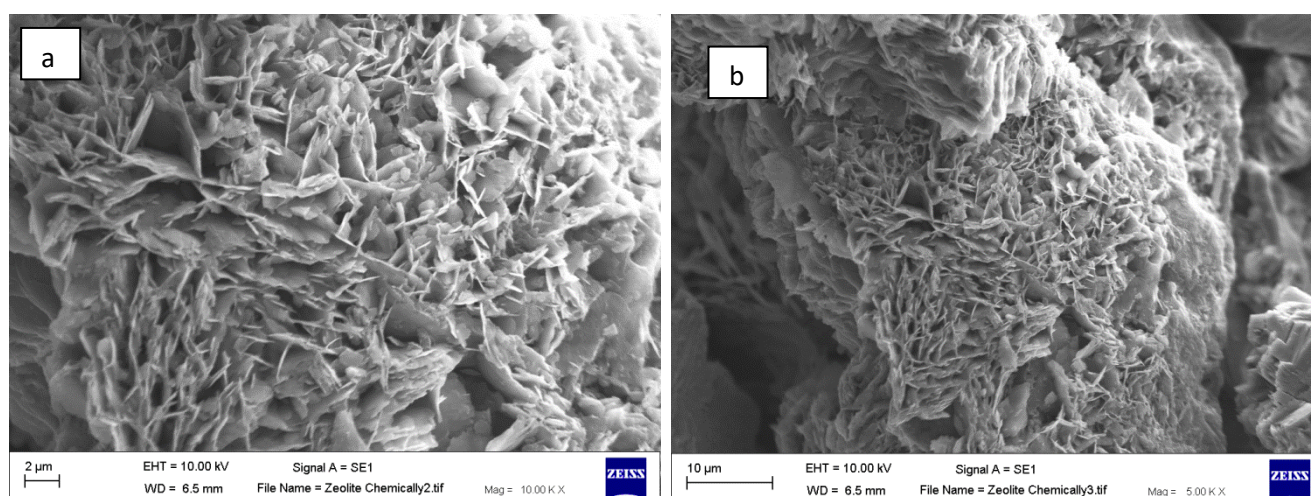


Figure 5.4: SEM micrographs of chemical pre-treatment of natural zeolite (Clinoptilolite) at different magnifications: (a) 10000x and (b) 5000x.

The thermal pre-treatment process of natural zeolite was performed by heating natural zeolite samples in a furnace for 30 minutes at 200, 400 and 600°C. Thermal pre-treatment of zeolite was applied to remove all of the undesired volatile matter but at some point its structure was destroyed. Figure 5.5 (a) shows that there is not significant change in the microstructure of natural zeolite that is thermally treated at 200 °C. The images were taken under the following SEM analytical conditions: EHT =10.00 kV, Signal A = SE1, WD 6.5mm at a magnification of 5000x. The SEM figures show some well-defined zeolite crystals but the surface of the crystals seem to have considerably decomposed due to direct heating at 400 °C; this can be noticed in figure 5.5 (b). The macro-pores on the clinoptilolite structure also seem to have slightly collapsed and the distinct crystal structures of clinoptilolite have disappeared. This was lead to appearance more solid less porous surface on the natural zeolite structure.

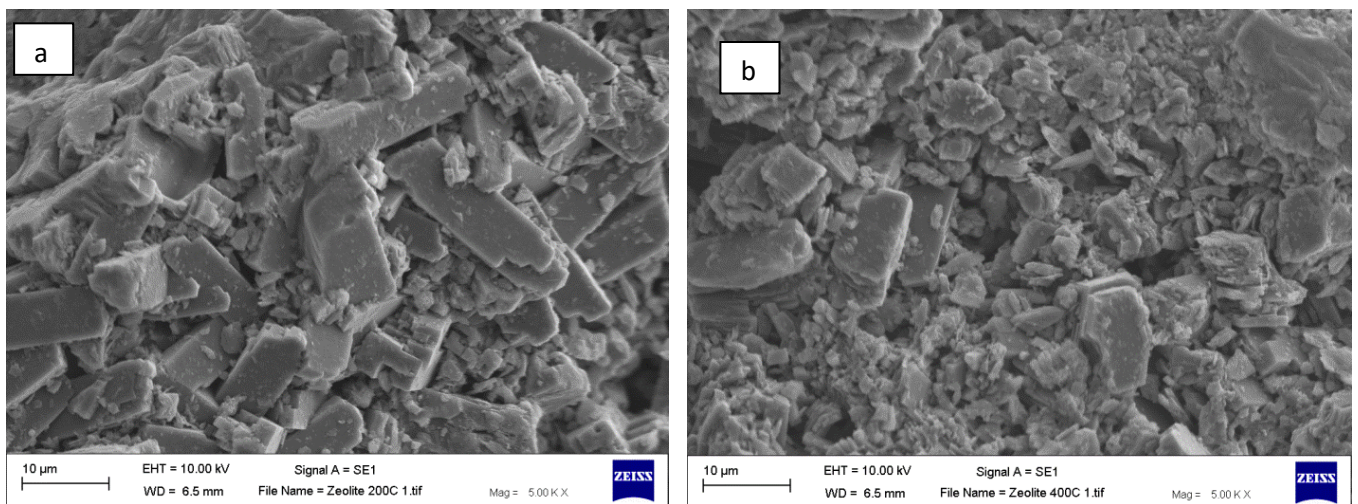


Figure 5.5: SEM microstructure of natural zeolite thermally pre-treated in a muffle furnace at (a) 200 °C (b) 400 °C, at a magnification of 5000x.

Figure 5.6 shows the natural zeolite sample that was exposed to extreme thermal conditions. The images were taken under the following SEM analytical conditions: EHT =10.00 kV, Signal A = SE1, WD 6.0 mm at a magnification of 3000x. The sample heated to 600 °C shows how thermal radiation has had a negative impact on the structure of natural zeolite. As the heating rate increased, the structure became more distorted and the macro-pores on the natural zeolite structure have collapsed.

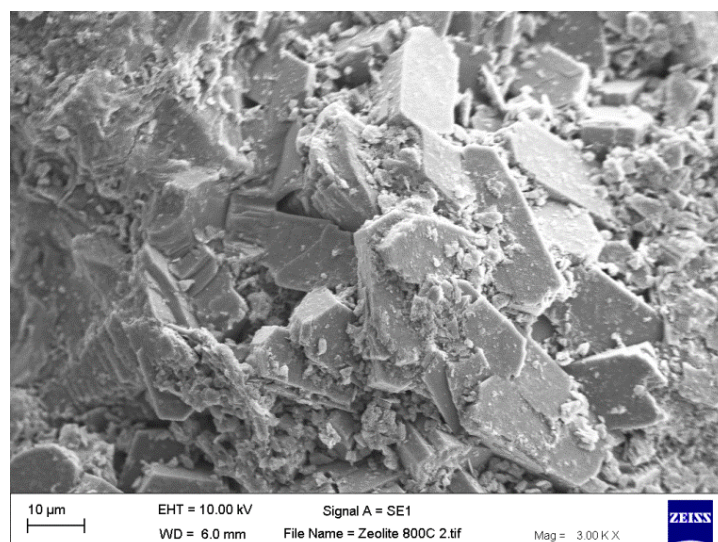


Figure 5.6: SEM microstructure of natural zeolite showing the collapse of the structure of natural zeolite due to thermal damage at 600 °C, at a magnification of 3000x.

5.2.2. Energy Dispersive Spectroscopy (EDS)

EDS is an analytical technique that was used to identify the elemental composition and chemical characterization of different natural zeolite samples as presented below:

Energy dispersive spectroscopy (EDS) results

An electron beam was randomly directed onto different parts of the natural zeolite samples in order to get a more accurate analysis. As shown in figure 5.7 it is noticeable how the different parts of the sample were analysed. In the meantime the elemental composition for all natural zeolite samples were indicated rapidly. The main elements and their corresponding oxides were determined by EDS. The localisation of four analysed sites designated by numbers and a typical EDS spectra are shown in appendix A.

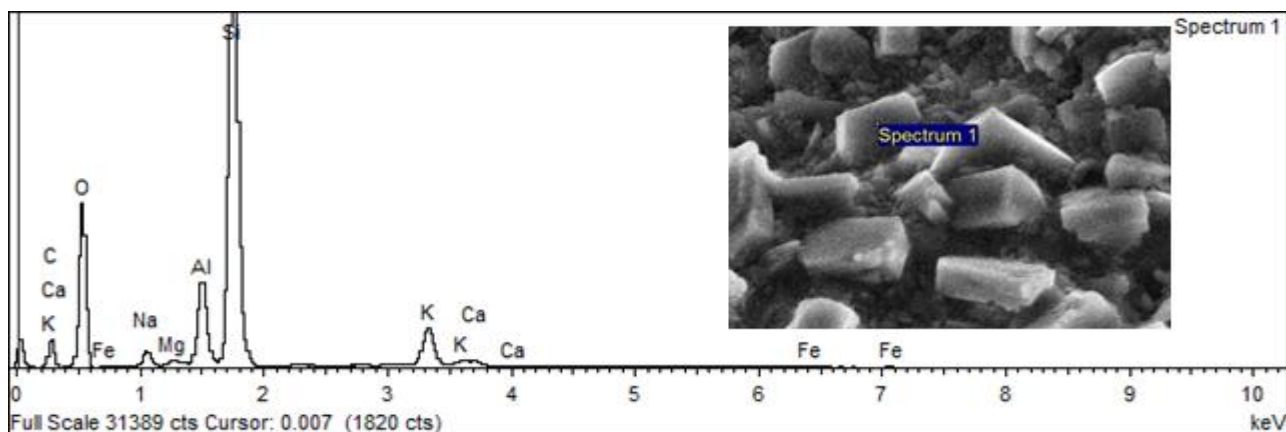


Figure 5.7: EDS analysis showing the elemental composition and the scanned image for natural zeolite.

The results of the EDS analysis also shows that the predominant exchangeable cations in the natural zeolite structure were found to be Na^+ , Mg^{2+} , K^+ and Ca^{2+} .

Table 5.1: EDS analysis showing the elemental composition and the scanning method for natural zeolite.

Element	Na_2O %	MgO %	Al_2O_3 %	SiO_2 %	K_2O %	CaO %	TiO_2 %	Fe_2O_3 %
wt.%	1.33	0.29	3.93	21.22	2.39	0.31	0.06	0.34

5.2.3. X – Ray Diffraction (XRD)

X-ray diffraction (XRD) analytical technique was used for phase identification of the natural zeolite samples and characterisation of the heterogeneous solid mixtures to determine the relative abundance of crystalline compounds and obtain information on the unit cell dimensions.

X – Ray Diffraction (XRD) results

The procedure was carried out and data were collected in the range 0-50 degrees, with a scanning step of $2^\circ \Theta$. The crystalline patterns were compared with the standard line patterns from the powder diffraction file database supplied by the International Centre for Diffraction

Data (ICDD). Thus the XRD result showed that the sample contained clinoptilolite in the majority (Figure 5.8).

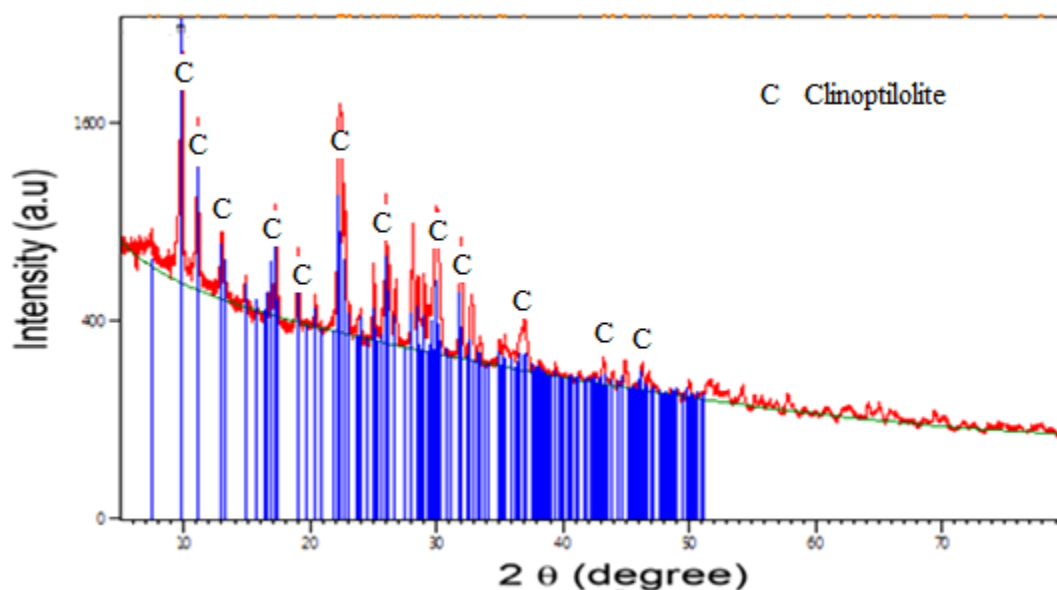


Figure 5.8: XRD analysis showing the mineralogical analysis of Clinoptilolite (Natural Zeolite).

5.2.4. X – Ray Fluorescence (XRF)

XRF analytical analysis of the natural zeolite samples was carried out to determine the elemental composition of the samples.

X-Ray Fluorescence (XRF) result

The results of the XRF analysis are presented in Table 5.2. The result shows that SiO_2 , Al_2O_3 , Na_2O and K_2O are main components of natural zeolite with higher rate compared to EDS analysis result. The results of the EDS analysis also showed that the predominant exchangeable cations in the natural zeolite structure were Na^+ , Mg^{2+} , K^+ and Ca^{2+} . The result of six analysed samples designated by numbers and a typical table are shown in appendix B.

Table 5.2: Chemical composition (wt.%) of the natural zeolite.

Element	Na_2O %	MgO %	Al_2O_3 %	SiO_2 %	K_2O %	CaO %	TiO_2 %	Fe_2O_3 %
wt. %	4.12	0.89	4.53	37.97	2.12	0.96	0.06	0.74

5.2.5. Thermogravimetric Analysis (TGA)

The thermal stability of the clinoptilolite was obtained from thermogravimetric analysis (TGA) this is to measure changes in the physical and chemical properties whilst increasing temperature constantly and to obtain information about the mass loss during the thermal treatment process.

Thermogravimetric Analysis (TGA) result

Results obtained from TGA/DTG show that, clinoptilolite samples were continually losing weight after heating up to 1000 °C (Figure 5.9). The main reasons of this are due to dehydration and dehydroxylation processes. The DTA curve shows an endothermic peak at 50–150 °C (Sprynskyy, 2010). According to Perraki and Orfanoudaki (2004) weight losses at 20–100 °C and 100–200 °C are due to hygroscopic water and loosely bonded water, respectively (Dyer, 1988; Gottardi and Galli, 1985).

In the first step, when the clinoptilolite was heated, the intact water was eliminated at below 200 °C. In the hydrated phases, dehydration occurs at temperatures mostly below about 400 °C and is largely reversible, whereas in the second step hydroxyl groups were removed at temperature above 400 °C (Colella and Wise, 2014). Then dehydroxylation took place in the range 400-600 °C (Ribero *et al.*, 1984). Kurkuna *et al.* (2006) reported two forms of water molecules and hydroxyl groups existing in the structure of silicate minerals such as clinoptilolite.

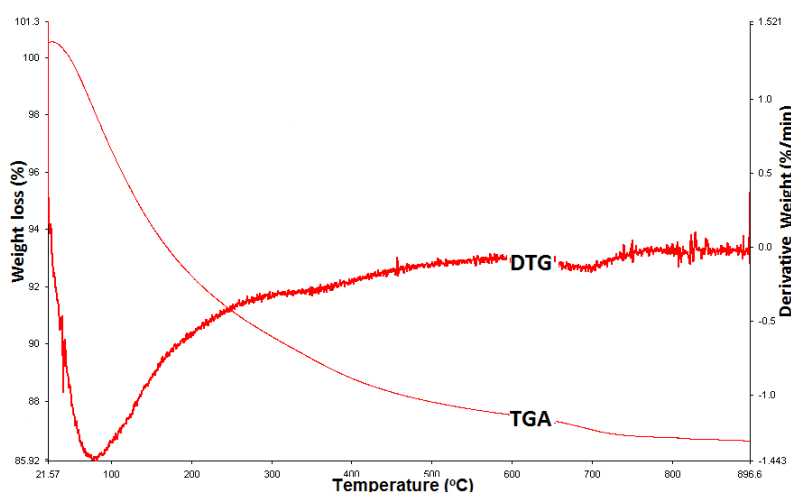


Figure 5.9: Thermogravimetric analysis (TGA/DTG) of clinoptilolite between 20-900°C.

The results indicated that any loss below 400°C was corresponding to the zeolitic materials water. The total loss calculated from the thermogravimetric analysis was 13 wt. %. Similar values were obtained by other authors (Korkuna *et al.*, 2006; Al-Dwairi, 2009; Ugal *et al.*, 2010; Perraki and Orfanoudaki, 2004). The DTG pattern of clinoptilolite displays a new peak at 750-800°C, which could be attributed to the formation of sodalite.

5.2.6 . Fourier Transform Infrared (FT-IR) Spectroscopy

FT-IR spectra of the natural zeolite were carried out for materials analysis in this study. FT-IR spectroscopy is used to probe the structure of zeolites and monitor reactions in zeolite pores. Initially the data were collected in the range of 4000-400 cm^{-1} .

Fourier Transform Infrared (FT-IR) Spectroscopy results

In this study the characterization of zeolites with transmission Fourier transform infrared spectroscopy (FT-IR) is described. Only the 1200-400 cm^{-1} region was investigated; this is where the all spectra showed remarkable changes. A broad band between 3500 and 3700 cm^{-1} in all the adsorbents is indicative of the presence of both free and hydrogen bonded OH groups on the adsorbent surface. In the OH stretching region, infrared spectra of zeolites provide a wealth of information on hydroxyl groups attached to zeolite structures (Li, 2005). FT-IR results demonstrate (Figure 5.10) that zeolites are significantly hydrated. These bands, which were centered at 3444 (OH group) and 1637 cm^{-1} refer to water molecules associated with Na and Ca in the channels and cages in the of the zeolite structure (Wilson, 1994). The 1015 cm^{-1} band corresponds to asymmetric stretching vibration modes of internal Si-O-Si or Si-O-Al bonds. The 796 and 448 cm^{-1} bands are assigned to the stretching vibration modes of Si-O-Si or Si-O-Al bonds groups and the bending vibrations of Si-O bonds, respectively (Tanaka *et al.*, 2003). These results are similar as those obtained by other authors (Olad and Naseri, 2010; Perraki and Orfanoudaki, 2004).

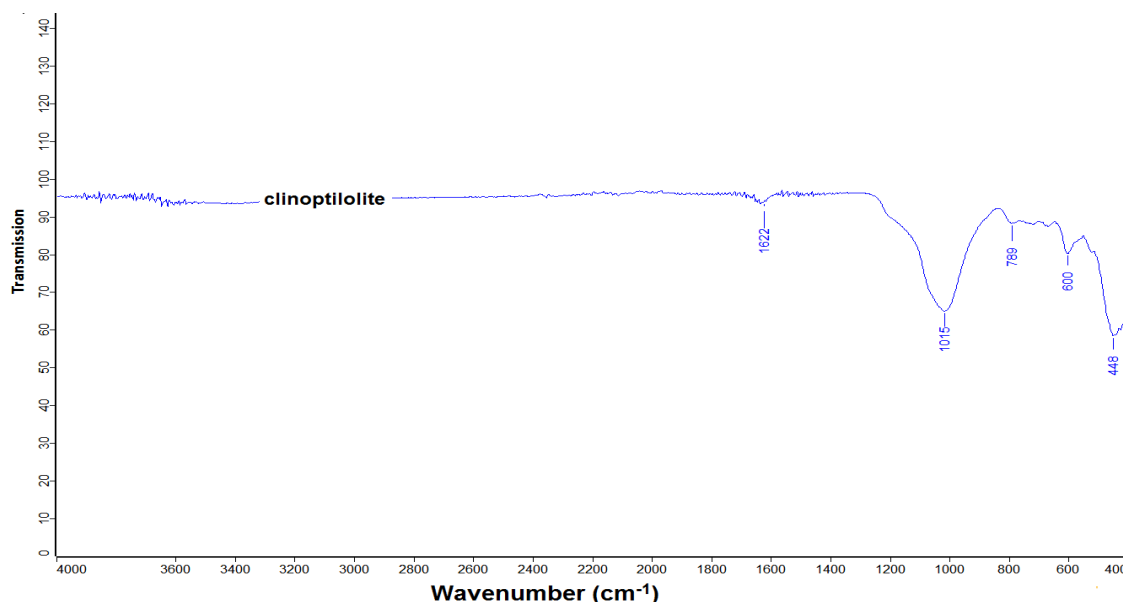


Figure 5.10: Shows the FT-IR spectra analysis of the as received clinoptilolite.

5.2.7. Inductively Coupled Plasma-Optical Emission Spectrometers (ICP-OES) analysis

The heavy metal ion concentrations in the waste water solution were determined using ICP-OES. The standard solutions for metal analysis using the ICP were prepared from standard metal solutions to determine the amount of Fe^{3+} , Cu^{2+} , Pb^{2+} and Zn^{2+} present in the solutions before and after the ion exchange.

Inductively Coupled Plasma-Optical Emission Spectrometers (ICP-OES) results

Results of both kinetic and equilibrium studies are presented in chapters 6 and 7, which shows the behaviour of adsorbents, factors that affect the rate of adsorption and maximum effective capacity of natural zeolite towards Fe^{3+} , Cu^{2+} , Pb^{2+} and Zn^{2+} ions removal. Every hour 15 ml of the sample was taken for metal ion concentration analysis using the ICP-OES. Microsoft office excel were used for data interpretation. After a mathematic calculation the results were presented either by plotting a chart or presenting data in a table.

5.3 . Conclusion:

In this study different analytical techniques were used in order to provide more information on the characteristics of natural zeolite samples. The technological properties of zeolite products depend on the physical, chemical and mineralogical characteristics of the natural zeolite, which also controls the overall processing treatment of polluted effluents.

The surface morphology of the different natural zeolite samples was determined using SEM. The micrographs of the “as received” natural zeolite show a number of different size macropores in the zeolite structure ($1\text{ }\mu\text{m} \leq d \leq 2\text{ }\mu\text{m}$). The micrographs mostly show well defined crystals of natural zeolite.

The SEM figures show some well-defined zeolite crystals at 200 °C but the surface of the crystals are shown to have lost some porosity and decomposition of some crystalline structure due to further thermal treatment.

NaCl acidic solutions were used for the chemical pre-treatment of the zeolite. The micrographs obtained after the application of chemical pre-treatment shows a clean surface and well defined crystal structures of clinoptilolite.

The result of both EDS and XRF analysis shows that SiO_2 , Al_2O_3 , Na_2O and K_2O were the main components of natural zeolite. While the analysis also shows that the predominant exchangeable cations in the natural zeolite structure were Na^+ , Mg^{2+} , K^+ and Ca^{2+} .

The result of TGA analysis showed continued mass loss during the thermal treatment process. Results show that, clinoptilolite samples are continually losing weight while undergoing dehydroxylation and dehydration.

CHAPTER 6

6. EQUILIBRIUM STUDIES

6.1. Introduction

The adsorption equilibrium can be defined as a completed state that takes place when the rates at which both molecules are adsorbed and desorbed onto a surface are equal (Richardson *et al.*, 2002).

In this chapter equilibrium studies were carried out to determine the maximum effective capacity of natural zeolite towards Cu^{2+} , Fe^{3+} , Pb^{2+} and Zn^{2+} ion removal under specific conditions. That was followed by a study of the selectivity comparison for these cations.

Two famous isotherm equations have been selected in the present investigation, namely; Freundlich and Langmuir (Sprynskyy *et al.*, 2006). The Langmuir and Freundlich isotherm models are the most well-known. They describe the sorption equilibrium used for environmental studies (Hashem, 2007; Erdem *et al.*, 2004; Inglezakis *et al.*, 2002; Kocaoba *et al.*, 2007).

6.2. Adsorption isotherms

An adsorption isotherm equation is an expression of the relation between the amount of solute adsorbed and the concentration of the solute in the liquid phase. Adsorption isotherms need to be studied well in order to investigate the characteristic performance of zeolite. Kocaoba *et al.* (2007) have described the use of these models to predict the behaviour of different adsorbates for adsorbents and the theoretical adsorption constants.

There are many factors that affect the equilibrium constant and experimental conditions including: the effect of system temperature; and the effect of the total initial concentration of the solution and the characteristics of the ion exchange system, such as mineral type, solution composition, and pH of the solution (Inglezakis *et al.*, 2002).

Equilibrium experiments were carried out using adsorbent masses of 4g. The adsorbent was mixed with 100 ml solution of the appropriate multi-component solution. The agitation speed of 150 rpm was used for 360 minutes. The particle size of the zeolite samples used was 250 μm . Three different solution pH were used, as follows: 2, 4 and 6 ± 0.1 . This experiment was initially done for Cu^{2+} , Fe^{3+} , Pb^{2+} and Zn^{2+} ions and the concentration range of cations was from 50 to 800 mg/l.

The Langmuir and Freundlich adsorption isotherms were adopted because they are the most widely used for heavy metal solutions and clinoptilolite systems (Altın *et al.*, 1998; Erdem *et al.*, 2004; Payne and Abdel-Fattah, 2004; Petrus and Warchoř, 2003; Peric *et al.*, 2004; Sheta *et al.*, 2003) since they are simple and capable of describing experimental results in a wide range of concentrations (Altın *et al.*, 1998).

6.2.1 Langmuir adsorption isotherm

The Langmuir equation (1918) makes the assumption that the maximum adsorption corresponds to a saturated mono-layer of adsorbate molecules into the adsorbent surface. Previous studies have been concerned that the Langmuir adsorption isotherm is based on a number of assumptions, including:

- Monolayer coverage of the adsorbent surface.
- Molecules are adsorbed at stable sites and do not transmigrate over the surface.
- All adsorption sites are energetically identical and the energy of adsorption is constant (Almaraz *et al.*, 2003; Richardson *et al.*, 2002; Tien, 1994, Gunay *et al.*, 2007; Motsi *et al.*, 2009).

The equilibrium data for heavy metal cations over the different concentration range of metal ions have been fitted with the Langmuir Isotherm (for solid – liquid systems) and use the following equation:

$$C_e/q_e = 1/Qb + C_e/Q$$

Where,

q_e is the amount of solute adsorbed per unit mass of adsorbent at equilibrium (mg/g),

C_e is the residual liquid phase concentration at equilibrium (mg/l),

Q and b are Langmuir constants related to sorption capacity and sorption energy, respectively. Maximum sorption capacity (Q) represents monolayer coverage of sorbent with sorbate and b represents enthalpy of sorption and should vary with temperature.

Data obtained from the kinetic adsorption tests was used to determine the loading capacity, q_e (mg/g) of the different adsorbents, using the following equation:

$$q_e = (C_o - C_e) \times V / m$$

The percentage removal of metal ions from solution was also determined using the equation below:

$$\text{Percentage Adsorbed (\% removal)} \quad q_e = \{(C_o - C_e) \times 100\} / C_o$$

Where,

q_e is the amount of solute adsorbed per unit mass of adsorbent at equilibrium (mg/g),

C_o is the initial concentration of heavy metal ions (mg/l),

C_e is the residual liquid phase concentration at equilibrium (mg/l),

V is the volume of solution from which adsorption occurs (l), and

m is the weight of the zeolite used (g).

Results and discussion

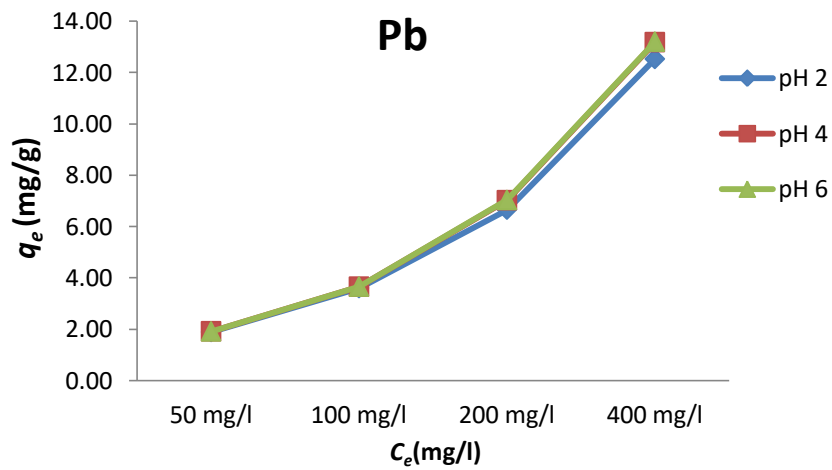
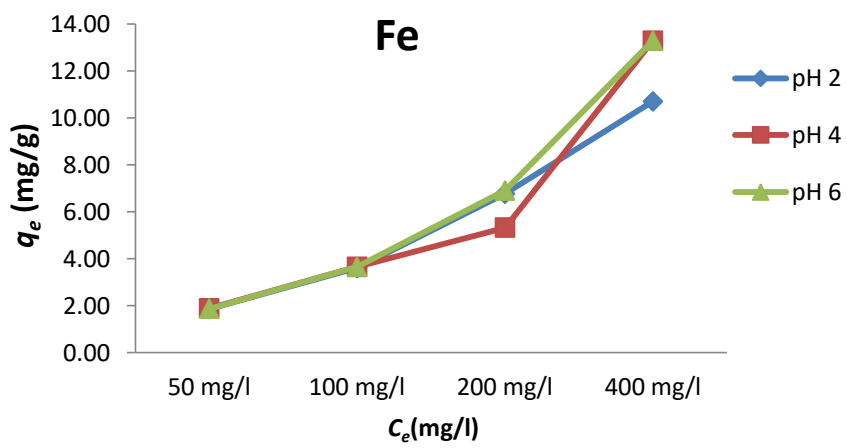
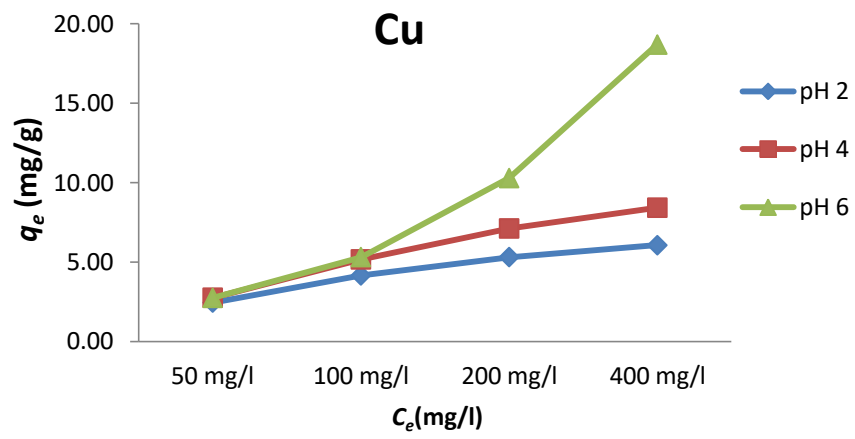
The experimental data obtained from the equilibrium studies were correlated with the Langmuir adsorption isotherms. A linear plot was obtained when C_e/q_e was plotted against C_e over the entire concentration range of metal ions from 50 to 800 mg/l. The values of the Langmuir model parameters for each cation are presented in Table 6.1.

Table 6.1: Calculated equilibrium adsorption Langmuir isotherm constants for the removal of copper, iron lead and zinc ions from solution.

composition of material	Initial pH	Langmuir		
		$Q(\text{mg/g})$	$b (\text{l/mg})$	Correlation coefficient (r^2)
Cu^{2+}	2	6.33	1.506	0.99
	4	8.896	2.155	0.99
	6	22.83	3.325	0.93
Fe^{3+}	2	8.13	2.414	0.99
	4	14.92	5.449	0.98
	6	14.71	7.131	0.99
Pb^{2+}	2	13.70	198.5	0.99
	4	1.039	0.28	0.99
	6	14.49	216.3	0.93
Zn^{2+}	2	13.33	3.07	0.93
	4	13.89	3.54	0.94
	6	17.54	6.34	0.96

Table 6.1 shows that the Langmuir isotherms for the adsorption of Cu^{2+} , Fe^{3+} , Pb^{2+} and Zn^{2+} from solution give a straight line. This means that the linear fits fairly good to the experimental results as revealed by the values of the correlation coefficients, r^2 , which range from 0.93 to 0.99. The Langmuir isotherm constants and their correlation coefficients r^2 are listed in table 6.1. The adsorption capacity generally increases when the initial solution pH increases. The maximum adsorption capacity, Q , which represents the monolayer coverage of the sorbent with sorbate according to the Langmuir model, occurred at pH6 in the range of 22.83, 14.49 and 17.54 mg/g of Cu^{2+} , Pb^{2+} and Zn^{2+} respectively. Meanwhile the maximum adsorption capacity, Q , of Fe^{3+} occurred at pH4; it was 14.92 mg/g. The Langmuir model effectively and significantly showed that the sorption data with all r^2 values >0.93 . According to the Q parameter, sorption on the zeolite produced the following sequence $\text{Cu}^{2+} > \text{Zn}^{2+} > \text{Fe}^{3+} > \text{Pb}^{2+}$.

Figure 6.1 shows that as the initial concentration of heavy metal increases, the amount of metal adsorbed into the natural zeolite surface (q_e) increases.



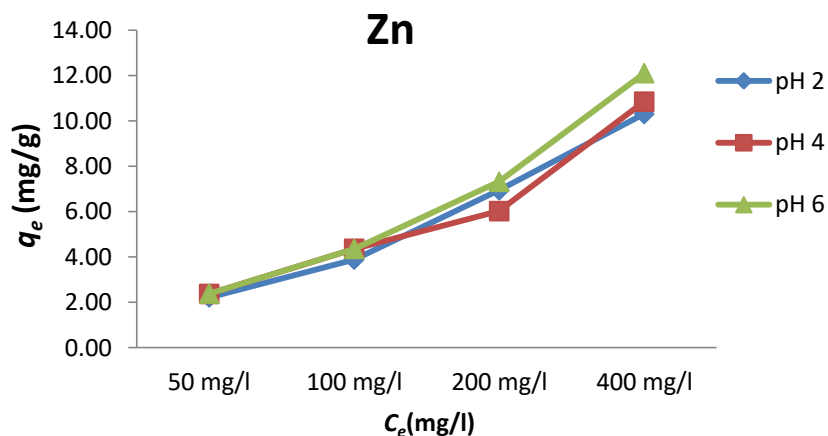
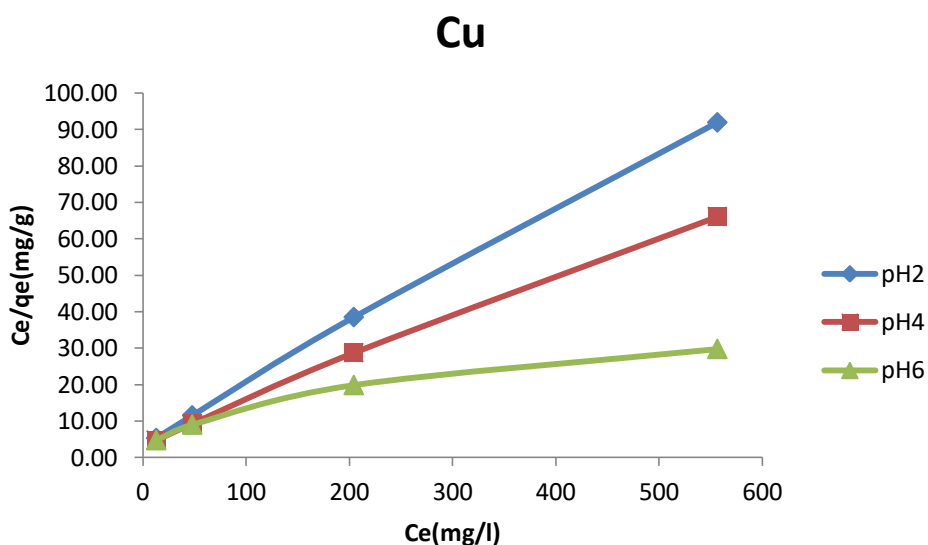


Figure 6.1: Showing the kinetic experimente data for the removal copper, iron, lead and zinc ions from solution at different pH values.

The adsorption capacity of natural zeolite for Cu^{2+} , Fe^{3+} , Pb^{2+} and Zn^{2+} at different initial solution pH levels is also shown graphically in figure 6.1. It can be observed that when the solution pH increases the adsorption capacity of the adsorbent increases. This is mainly due to the decrease in H^+ ion concentration. The effect of initial solution pH on the adsorption of heavy metals by natural zeolite is discussed in detail in section 7.3.3.



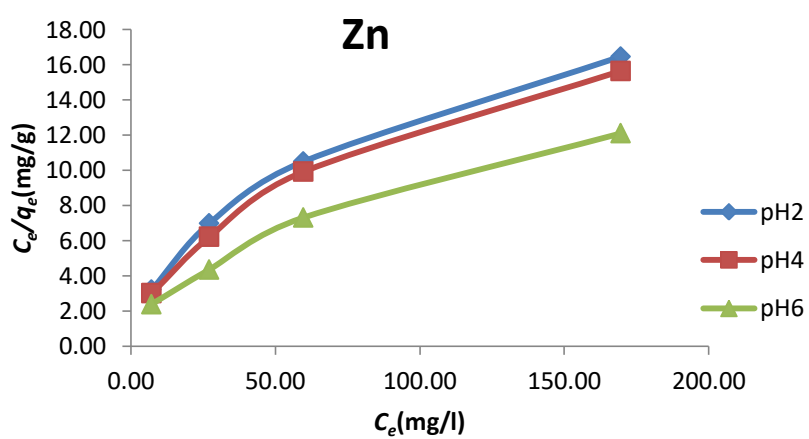
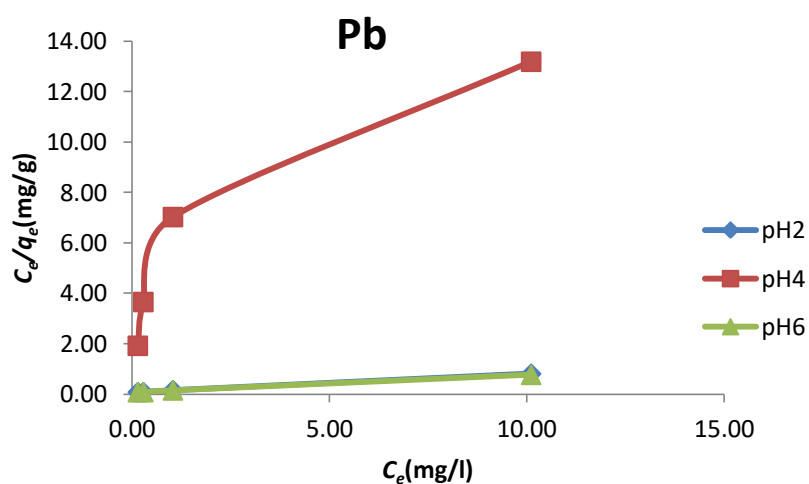
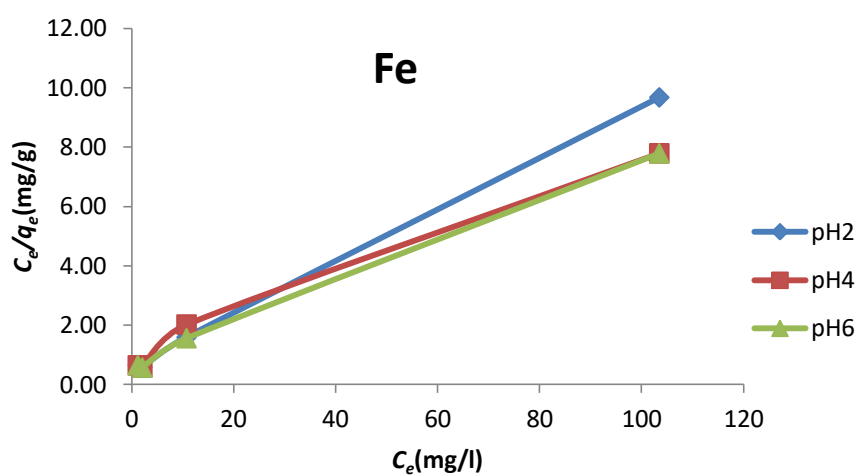


Figure 6.2: Equilibrium adsorption using Langmuir isotherm constants for the removal of copper, iron, lead and zinc ions from solution.

It can be observed from figure 6.2 that in each equilibrium study there is a variation in the equilibrium pH values with respect to the initially adjusted pH values. On the whole the equilibrium pH values are higher than the initially adjusted pH values. This may be due to the increasing initial Fe^{3+} , Cu^{2+} , Pb^{2+} and Zn^{2+} concentration. The highest experimental amount of Cu^{2+} , Fe^{3+} , Pb^{2+} and Zn^{2+} removed was in the range of 13.28, 18.69, 13.20 and 19.60 mg/g at initial pH6.

6.2.2 Freundlich adsorption isotherm

The Freundlich sorption isotherm was developed by Freundlich in 1926. This model is one of the most widely used isotherms. It can be correlated to the experimental data over a wide range of concentration (Motsi *et al.*, 2009). This isotherm gives an expression surrounding the surface heterogeneity and this model assumes that all adsorption sites are energetically unequal and that the energy of adsorption is irregular (Prasad and Saxena, 2008; Gunay *et al.*, 2007). It is a more realistic assumption than the Langmuir isotherm. The Freundlich isotherm describes equilibrium on heterogeneous surfaces that are more often seen in natural systems and can be written as follows:

$$q_e = kC_e^{1/n}$$

Where,

q_e is the amount of solute adsorbed per unit mass of adsorbent at equilibrium (mg/g),

C_e is the residual liquid phase concentration at equilibrium (mg/l),

k and n are empirical Freundlich constants that are dependent on experimental conditions.

k is an indicator of adsorption capacity while n is related to the adsorption intensity or binding strength.

The linear form of the Freundlich adsorption isotherm is:

$$\ln q_e = \ln k + \frac{1}{n} \ln C_e$$

As stated by Papageorgiou *et al.* (2006) values of $1/n < 1$ indicate heterogeneous adsorbents, while values closer to or equal to 1 indicate a material with relatively homogeneous binding sites due to its porosity. Natural zeolite can be classified as a heterogeneous adsorbent (Inglezakis *et al.*, 2002; Alvarez-Ayuso *et al.*, 2003; Gunay *et al.*, 2007).

Results and discussion

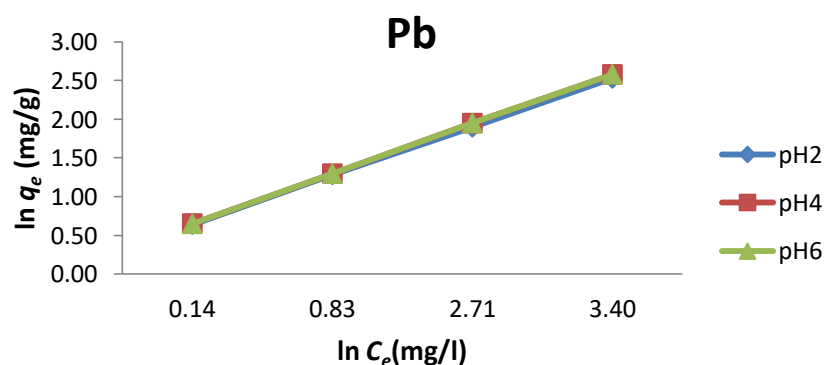
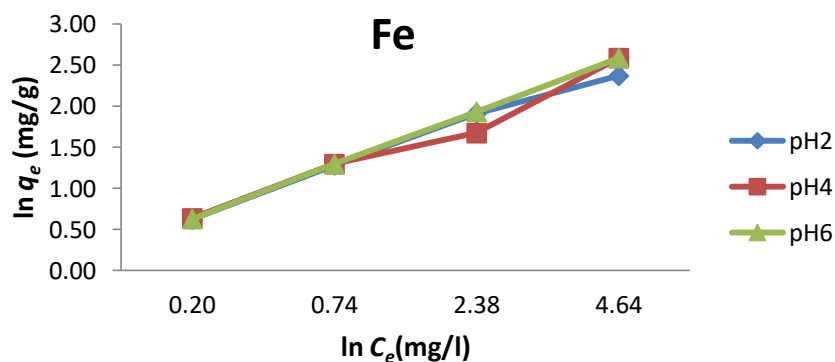
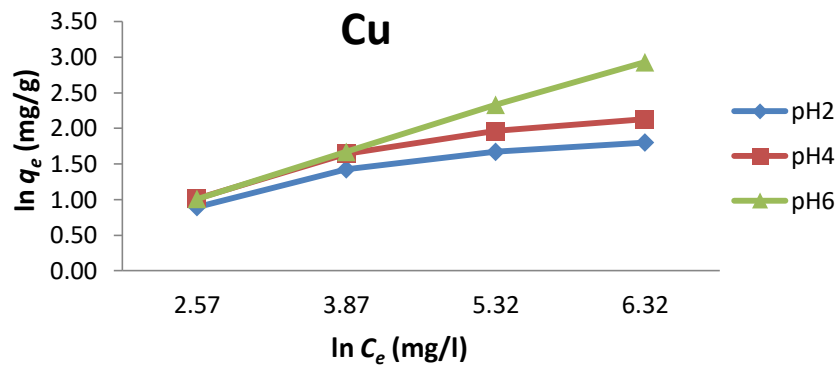
A linear plot is obtained when $\ln q_e$ is plotted against $\ln C_e$ over the entire concentration range of metal ions investigated and the values of k and n were calculated. The constants k and n were calculated for each cation (Table 6.2). The value of k is a measure of the adsorption capacity of zeolite and it increases as the amount of metal removed per unit weight increases.

Table 6.2: Calculated equilibrium adsorption Freundlich isotherm constants for the removal of copper, iron, lead and zinc ions from solution.

composition of material ppm	Initial pH	Freundlich		
		k (l/mg)	$1/n$	Correlation coefficient (r^2)
Cu^{2+}	2	1.47	0.24	0.93
	4	1.45	0.29	0.94
	6	1.33	0.50	0.99
Fe^{3+}	2	2.29	0.36	0.90
	4	2.13	0.95	0.95
	6	2.23	0.41	0.94
Pb^{2+}	2	3.22	1.85	0.95
	4	3.22	1.82	0.96
	6	3.20	1.81	0.96
Zn^{2+}	2	1.23	0.50	0.97
	4	1.10	0.47	0.99
	6	1.20	0.52	0.99

Table 6.2 shows that the Freundlich isotherms for the adsorption of Cu^{2+} , Fe^{3+} , Pb^{2+} and Zn^{2+} from solution gave good fits of the experimental results. This was clearly observed from the correlation coefficient, r^2 value, ranging from 0.90 to 0.99.

The results in table 6.2 show that all of the Fe^{3+} , Cu^{2+} , and Zn^{2+} metals have a numerical value of $1/n < 1$ apart of Pb^{2+} , which has a value of $1/n > 1$. The result shows that the value of n corresponds to good adsorption for zeolite because values of n between 2 and 10 correspond to good adsorption (Erdem *et al.*, 2004). The value of n is greater than unity, suggesting that the adsorption intensity is favourable at high concentrations but much less so at lower concentrations (Erdem *et al.*, 2004; Panday *et al.*, 1985).



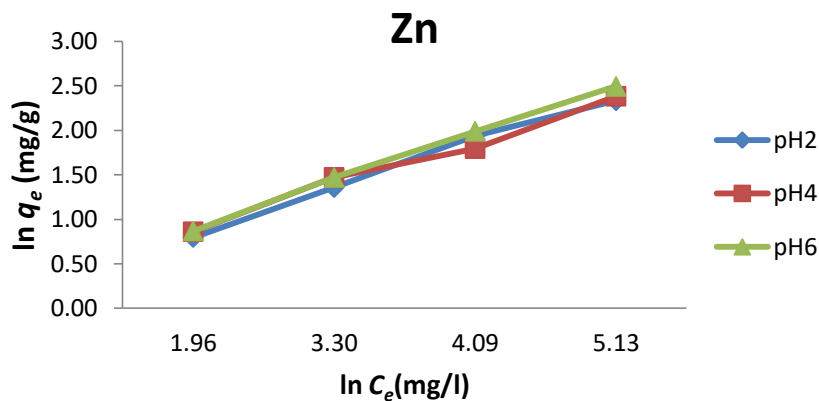


Figure 6.3: Equilibrium adsorption using Freundlich isotherm constants for the removal of copper, iron, lead and zinc ions from solution.

It is clear from figure 6.3 that as the initial concentration of heavy metal cations were increased, the amount of metal adsorbed by the natural zeolite (q_e) increased too.

As seen in tables 6.1 and 6.2, the Langmuir isotherm for the adsorption of Cu^{2+} from solution fits more correctly to the experimental data as revealed by the values of the correlation coefficients r^2 , which are 0.93, 0.99 and 0.99 for pH2, pH4 and pH6 respectively. Meanwhile the low correlation coefficient r^2 , which was 0.93, 0.94 to 0.99 for pH2, pH4 and pH6 respectively, shows less agreement of the Freundlich isotherm with the experimental data. The range of values of the correlation coefficient r^2 0.99, 0.98 and 0.99 of the Langmuir isotherm for the adsorption of Fe^{3+} from solution also fits correctly with the experimental data. However, the low correlation coefficient r^2 , which was 0.90, 0.95 and 0.94 for pH2, pH4 and pH6 respectively, shows less agreement of the Freundlich isotherm with the experimental data.

The Langmuir isotherm of the adsorption of Pb^{2+} from solution also fits more correctly to the experimental data as revealed by the values of the correlation coefficients r^2 , which were 0.99, 0.99 and 0.93 for pH2, pH4 and pH6 respectively. However, the low correlation coefficient r^2 , which was 0.95, 0.96 to 0.96 for pH2, pH4 and pH6 respectively, shows less agreement of the Freundlich isotherm with the experimental data. This indicates that the adsorption data of the Langmuir's isotherm data is more accurate than Freundlich isotherm

data, which indicates that the adsorption process is basically mono- layer coverage of these metal ions on the natural zeolite surface and chemisorption.

The value of the correlation coefficients r^2 0.93, 0.94 and 0.96 of the Langmuir isotherm for the adsorption of Zn^{2+} from solution is lower than the correlation coefficients r^2 range 0.97, 0.99 and 0.99 of the Freundlich isotherm. This indicates that the adsorption data of the Freundlich isotherm is more accurate than Langmuir's isotherm data, which in turn indicates that the adsorption process is basically heterogeneous.

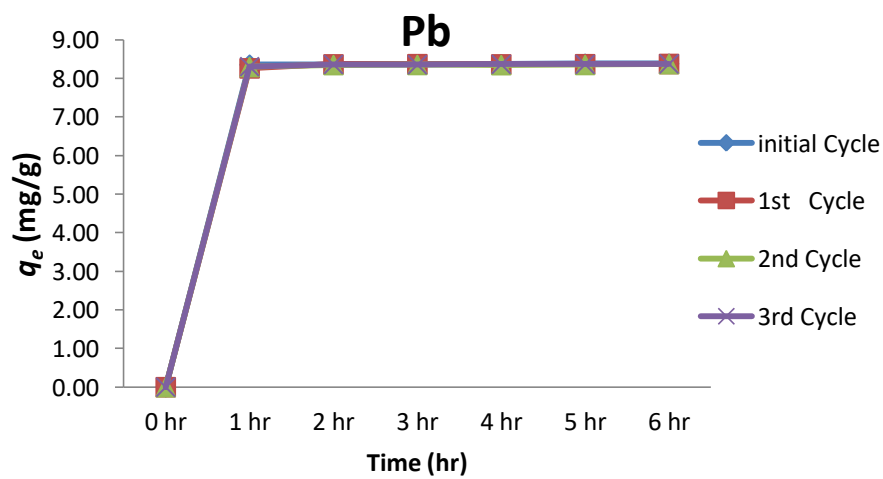
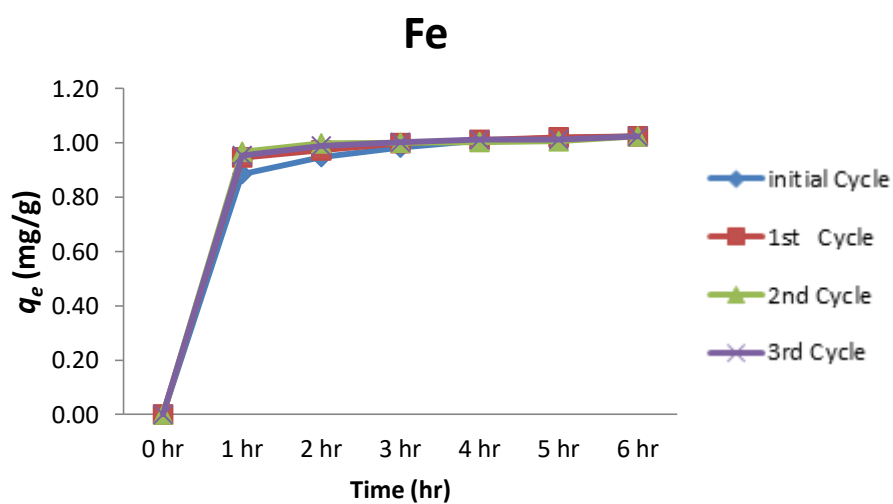
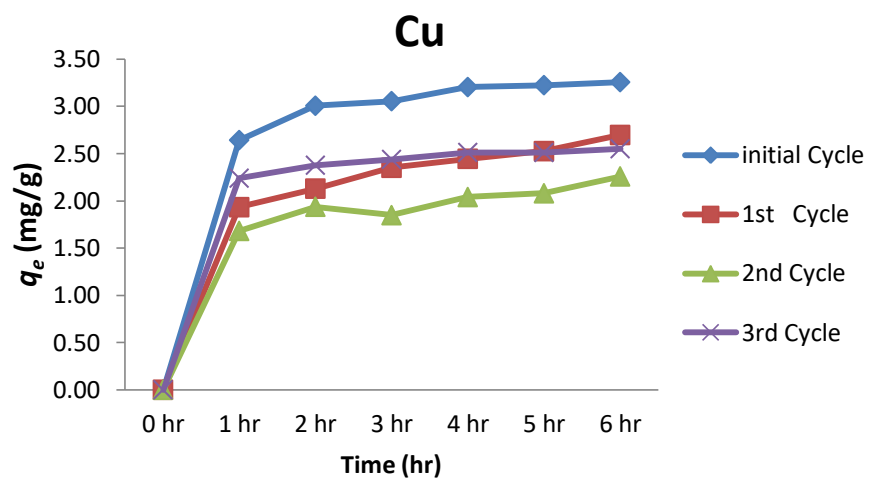
The results show that throughout the equilibrium experiments, the pH of the solutions continuously increased. Figures (6.1, 6.2 and 6.3) representing the change in pH with the equilibrium concentrations for Cu^{2+} , Fe^{3+} , Pb^{2+} and Zn^{2+} , respectively.

6.3 . Regeneration studies

The regeneration of adsorbent is one of the factors that can be taken into account since that makes the processes more economical and reduces the environmental impact. For these reasons, there is a strong motivation to understand the mechanisms leading to the reuse and regeneration of adsorbents, which makes the procedure cheaper and cleaner.

Regenerative capability is one of the characteristics that are considered when using zeolite as an adsorbent for any practical application (Richardson *et al.*, 2002). Zeolite can be regenerated and reused with little change in its adsorption efficiency after regeneration. Natural zeolite can be reused for a number of cycles before the structures are exhausted, which makes the processes economical and enables a decrease in the volume of waste material.

In this study, the regeneration of natural zeolite was carried out using 0.5M NaCl. The adsorption capacity of the natural zeolite was also investigated after each run. Used zeolite samples were regenerated and mixed with multi-component solutions of the heavy metal ions for cycles of 360 minutes each. The samples were washed with deionised water after each regeneration cycle in order to remove excess NaCl entrapped within the zeolite structure. Three adsorption cycles were carried out for all of the heavy metal ions as shown in figure 6.4.



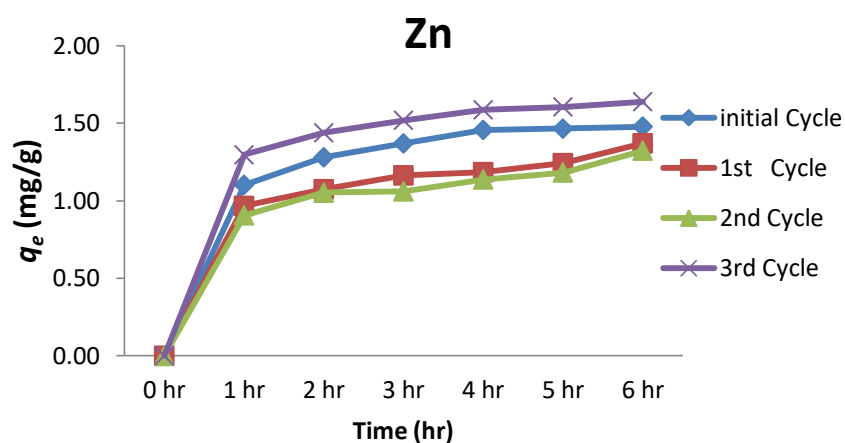
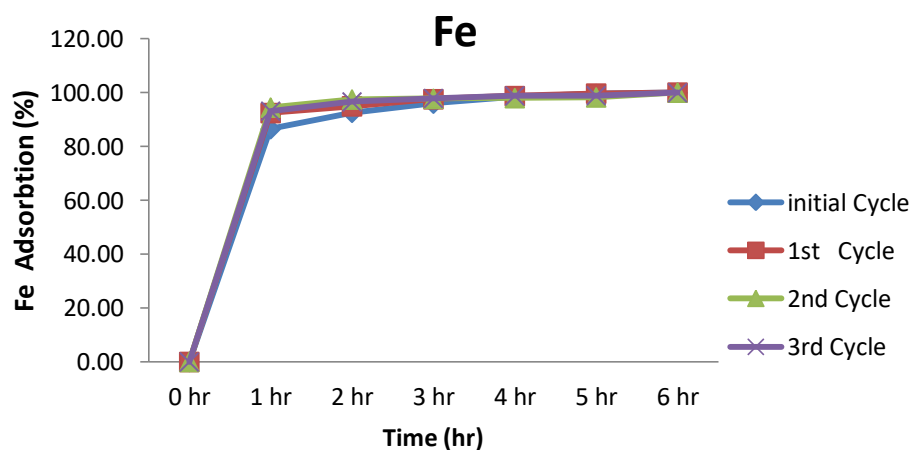
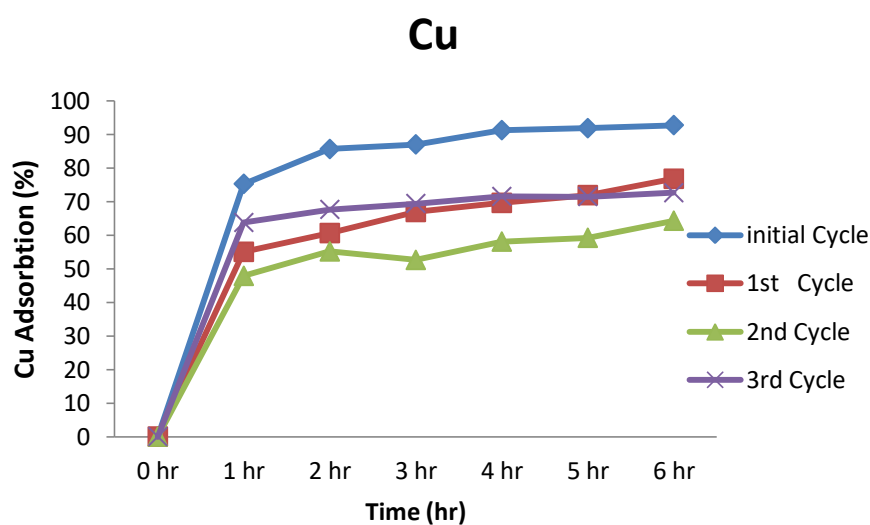


Figure 6.4: The amount of recovery of heavy metals from natural zeolite by regeneration.



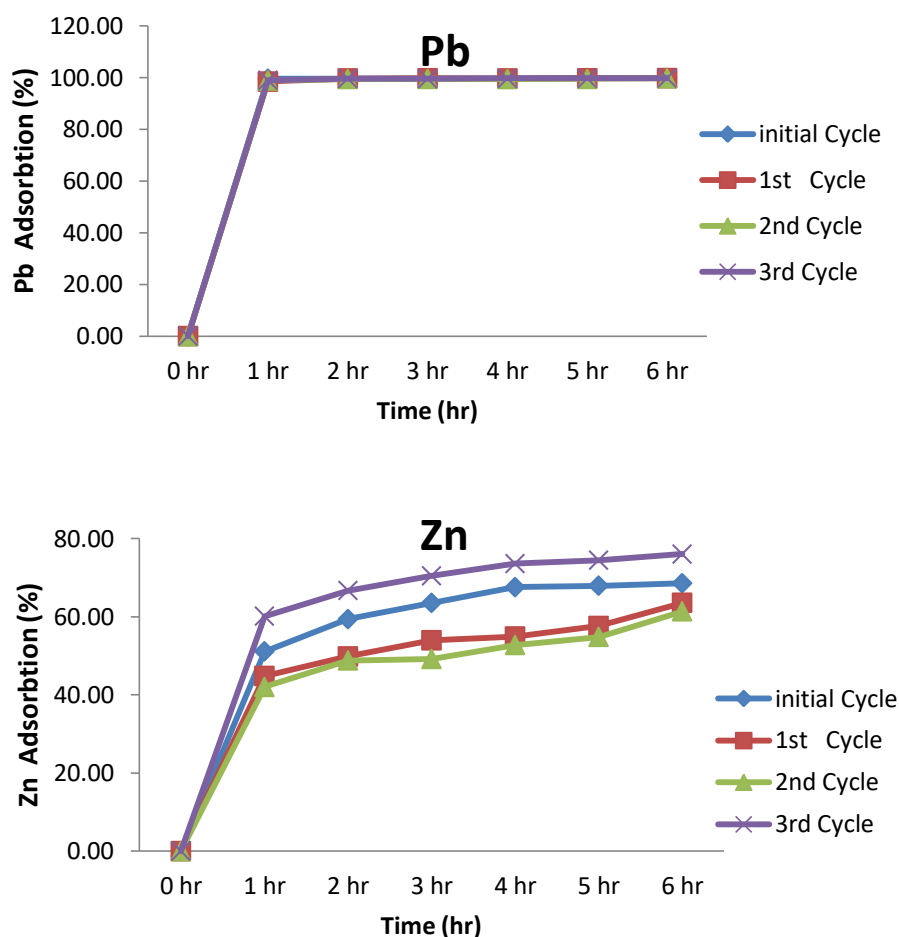


Figure 6.5: The percentage of recovery of heavy metals from natural zeolite by regeneration.

Figure 6.4 above shows that when the natural zeolite was initially used at concentration 141.41 mg/l, the loading capacity for Cu^{2+} ions was 3.26 mg/g, and after the first regeneration with 0.5M NaCl stripping solution, the loading capacity decreased to 2.70mg/g.

The second loading capacities for Cu^{2+} ions after regeneration were around 2.26 mg/g (lower than the first regeneration run and the initial run) and the third run had a loading capacity of 2.55 mg/g, which was slightly lower than the initial run but higher than the second regeneration run (Figure 6.4).

With an initial loading capacity of Fe^{3+} ions of 1.02 mg/g (Figure 6.4), it was observed that the first and second regeneration cycles recorded loading capacities were lower than the initial run. The subsequent third regeneration cycles recorded loading capacities slightly higher than the initial run.

According to figure 6.4 it is evident that the initial loading capacity of Pb^{2+} ions was 8.38 mg/g (Figure 4.27). The subsequent first, second and third regeneration cycles recorded loading capacities similar to the initial run.

The initial loading capacity of Zn^{2+} ions was 1.48 mg/g (Figure 6.4). It was observed that the first and second regeneration loading capacity decreased to 1.37 and 1.32 mg/g. The third run had a loading capacity of 1.64 mg/L, which was slightly higher than the initial run.

Desorption processes took place due to the displacement of the heavy metal ions from adsorption sites on the zeolite structure in the case of Na^+ ions from NaCl solution.

Throughout the regeneration experiments, it was observed as a general trend that the adsorption capacity of natural zeolite that has been regenerated was decreased slightly with each repeated three regeneration cycles. This concurs with the results obtained by Argun (2008) regarding the regeneration of natural zeolites, as he found that the zeolite capacity decreases with each repeated regeneration cycle. This decrease in zeolite adsorption capacity may appear for two reasons: first, it may be that some metal ions, once they are exchanged onto the zeolite, are rigidly fixed or become inaccessible to the incoming ions, and thus the ion exchange sites reduce with time. The second possible mechanism may be due to the removal of oxygen atoms from the lattice, when strongly held cationic species are removed during the regeneration step (Gottardi and Galli, 1985). This would result in the destruction of the zeolite lattice and loss of adsorption/ ion exchange sites.

6.4 . Selectivity of natural zeolite

Zeolite selectivity is a critical property for adsorbent/exchanger materials in wastewater treatment; they show different preferences for particular ions. Adsorption selectivity in various cation saturated zeolites can be affected by a number of factors such as the effect of negative charge density, saturated cation type, ordering of Si-O-Al linkage, Si/Al ratio and type of crystal structure (Armbruster, 200; Langella *et al.*, 2000).

Equilibrium studies have been carried out by many researchers to determine the selectivity of natural zeolite for heavy metals. Researchers have used different types of natural zeolite under different experimental conditions to determine the effectiveness and capacity of their

adsorbent materials in adsorbing heavy metal cations from solution (Bailey *et al.*, 1999; Alvarez-Ayuso *et al.*, 2003; Wingenfelter *et al.*, 2005; Inglezakis and Grigoropoulou, 2004). According to Armbruster (2001) and Langella *et al.* (2000) the selectivity of clinoptilolite towards heavy metal cations exists in the series: $Pb^{2+} > Cd^{2+} > Cu^{2+} > Co^{2+} > Cr^{2+} > Zn^{2+} > Mn^{2+} > Hg^{2+}$.

In this study the Langmuir adsorption isotherm was used to determine the selectivity of natural zeolite for heavy metals. This was done by comparing the maximum adsorption capacity (Q) of natural zeolite for the respective heavy metal cations. The results of the selectivity series obtained were different for equilibrium studies using solutions with an initial pH of 2, 4 and 6.

Table 6.3: Shows the selectivity series of natural zeolite towards Cu^{2+} , Fe^{3+} , Pb^{2+} and Zn^{2+} cations in solutions with a different initial pH.

composition of material ppm	Initial pH	Langmuir	
		Q (mg/g)	experimentally derived selectivity series
Cu^{2+}	2	6.33	$Pb^{2+} > Zn^{2+} > Fe^{3+} > Cu^{2+}$
Fe^{3+}		8.13	
Pb^{2+}		13.70	
Zn^{2+}		13.33	
Cu^{2+}	4	8.896	$Fe^{3+} > Zn^{2+} > Cu^{2+} > Pb^{2+}$
Fe^{3+}		14.92	
Pb^{2+}		1.039	
Zn^{2+}		13.89	
Cu^{2+}	6	22.83	$Cu^{2+} > Zn^{2+} > Fe^{3+} > Pb^{2+}$
Fe^{3+}		14.71	
Pb^{2+}		14.49	
Zn^{2+}		17.54	

Table 6.3 shows that the natural zeolite (clinoptilolite) samples have different unique selectivity series. The difference in the adsorption capacity values may correspond to the different experimental conditions such as the initial solution pH, the initial solution concentration and the zeolite particle size, as well as conditions such as the agitation speed and the pre-treatment of the zeolite. The chemical composition of the natural zeolite samples used may also affect the unique selectivity series (Inglezakis *et al.*, 2003).

6.5. Conclusion

The equilibrium studies illustrated that natural zeolite had a good capability in removing heavy metals from multi-component solutions. The maximum removal capacities Q were 22.83, 14.92, 14.49 and 17.54 mg/g natural zeolite for copper, zinc, iron and lead respectively. It was clearly observed that the adsorption capacity increased with an increase in initial solution pH, from 2 to 6.

The Langmuir and Freundlich isotherm models were used to represent the experimental data and the models fitted precisely. They were also used to evaluate the adsorption behaviour of natural zeolite towards removing copper, iron, lead and zinc. Finally, these models were able to give good fits to the experimental data.

Throughout the regeneration experiments, it was observed zeolite can be regenerated and reused while the adsorption capacity of natural zeolite that has been regenerated was decreased slightly with each repeated three regeneration cycles.

According to the Langmuir isotherm model, the selectivity series of natural zeolite for the adsorption of copper, iron, lead and zinc from solution was found to vary when the solution pH changed.

CHAPTER 7

7. KINETIC STUDIES

7.1. Introduction

Kinetic studies were performed in order to investigate the behaviour of adsorbents and understand the removal mechanisms involved in the adsorption process. Kinetic studies are critical processes that are used to obtain information about the process dynamics such as the adsorption rate, contact time and mass transfer parameters including external mass transfer coefficients and intraparticle diffusivity (Connors, 1990). Margeta *et al.* (2013) have divided the process of diffusion in the zeolite system into four phases: (I) Diffusion in solution, (II) Diffusion through the film, (III) Diffusion in pores, and (IV) Ion exchange (Figure 7.1). These parameters are important in the design and to optimise the operation of any adsorption experiment in wastewater treatment. Therefore, kinetic studies were used in this study to evaluate the suitability of natural zeolite for removing pollutants from solution. Kinetic studies also supply information about the nature of the ionic transport mechanisms that control the exchange rate (Harland, 1994).

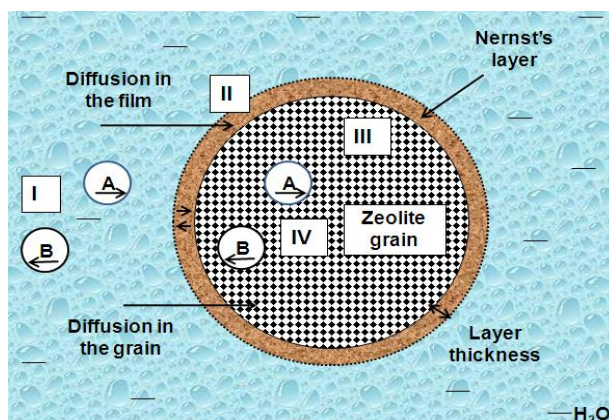


Figure 7.1: Diffusion processes in the system of zeolite/aqueous solution (Margeta *et al.*, 2013).

The uptake of heavy metal cations from solution using zeolite materials is affected by several factors; examples of such factors are the adsorbent mass, adsorbent particle size, initial solution pH, initial solution concentration, agitation speed and pre-treatment or modification of the adsorbent in the case of batch experiments. In this chapter, a number of these factors

and their effect on the efficiency of natural zeolite in removing Cu^{2+} , Fe^{3+} , Pb^{2+} and Zn^{2+} from solution will be investigated in detail.

7.2 . Kinetic study results

The results of the kinetic experiments were used to measure the adsorption capacities from solutions. Multi-component solutions were mixed with natural zeolite and agitated for 360 minutes at room temperature. The initial concentrations of the mixed component solutions were 141, 41, 336 and 88 mg/l for the Cu^{2+} , Fe^{3+} , Pb^{2+} and Zn^{2+} ions respectively.

In general the results show that the highest adsorption rate of Cu^{2+} , Fe^{3+} , Pb^{2+} and Zn^{2+} ions took place in the first hours followed by a slower adsorption rate later on. The first hour is an initial stage of adsorption when higher rates of adsorption take place; this may be due to the availability of more adsorption sites and the fact that the metal ions exchange easily on the surface of the zeolite grains (Inglezakis *et al.*, 2002). The driving force for adsorption is very high in the initial stage of the adsorption process and this also results in a higher initial adsorption rate. After that, a slower adsorption rate follows due to slower diffusion of the metal ions into the interior channels. Consequently, these metal ions occupy the exchangeable positions within the crystal structure of the natural zeolite (Amarasinghe and Williams, 2004; Myroslav *et al.*, 2006).

The data obtained from the kinetic adsorption tests were used to determine the removal capacity, q_e (mg/g) of the different adsorbents using the following equation:

$$q_e = (C_o - C_e) \times V / m$$

The percentage removal of metal ions from solution was also determined using the equation below:

$$\text{Percentage Adsorbed (\% removal)} \quad q_e = \{(C_o - C_e) \times 100\} / C_o$$

where,

q_e amount of adsorbate adsorbed per unit weight of adsorbent (mg/g)

C_o and C_e are the initial and final metal ion concentrations in solution (mg/l) respectively, V is the solution volume (l) and m is the weight of the zeolite used (g).

7.3 . Factors that affect the rate of adsorption

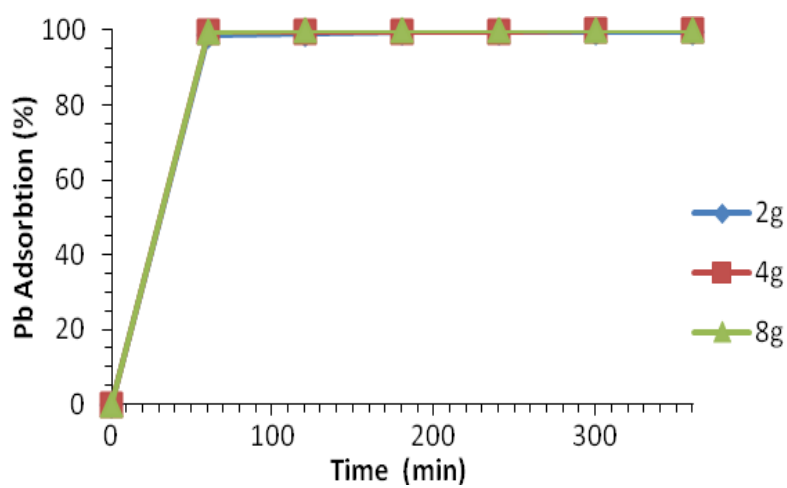
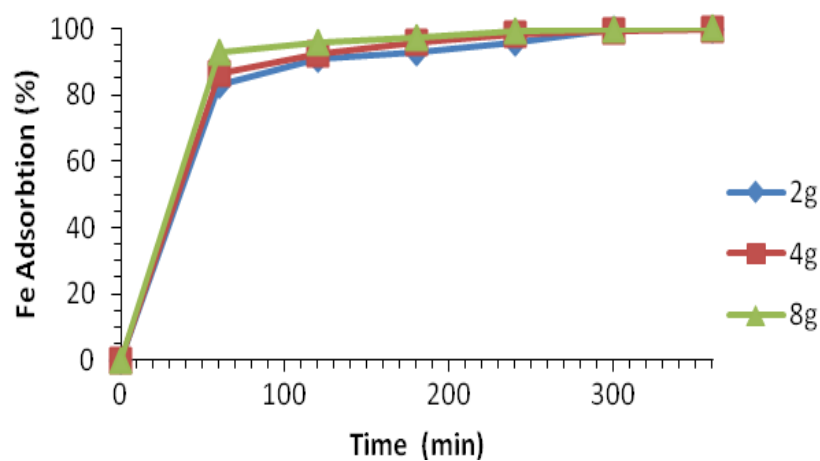
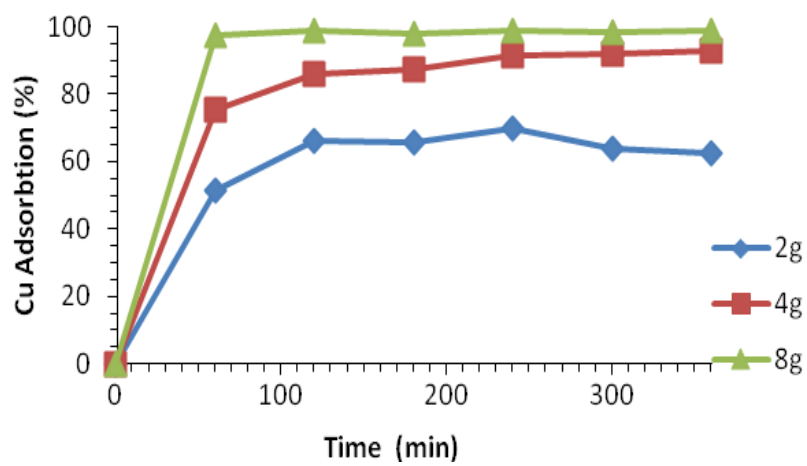
A numbers of parameters that affect the rate of adsorption were studied and described in detail. These include: effect of adsorbent mass, effect of adsorbent particle size, effect of initial solution pH, effect of initial solution concentration, effect of agitation speed and effect of pre-treatment of adsorbent.

7.3.1. Effect of adsorbent mass

Kinetic experiments were carried out using three different adsorbent masses, 2g, 4g and 8g. The adsorbent was mixed with 100 ml solution of the appropriate multi-component solution. An agitation speed of 150 rpm was used for 360 minutes and samples were collected every hour and analysed. The particle size of the zeolite samples used was 250 μm . The pH was adjusted to 4 ± 0.1 . This experiment was initially carried out for Cu^{2+} , Fe^{3+} , Pb^{2+} and Zn^{2+} ions using fixed initial metal concentrations. The results in table 7.1 clearly show that when the adsorbent mass was increased, this resulted in an increase in the adsorption of the heavy metal ions. The main reason for this is that as the adsorbent mass increases more adsorption sites are available per mass of adsorbent surface and thus the total amount of metal that is removed increases. This result indicates that the mineral mass in the solution can affect the adsorption capacity for the removal of heavy metals as it determines the availability of adsorption sites. The removal of Cu^{2+} , Fe^{3+} , Pb^{2+} and Zn^{2+} ions mostly occurs in the early stage, while the percentage of adsorbed Fe^{3+} and Pb^{2+} reached 90% in the first hour (Figure 7.2).

Table 7.1: Shows the effect of natural zeolite mass on the removal of heavy metals from solution.

Heavy metal ions	Adsorbent Mass (g)	Percentage Adsorbed (%)
Copper	2g	62.51
	4g	92.85
	8g	99.02
Iron	2g	99.88
	4g	99.98
	8g	100.00
Lead	2g	99.70
	4g	99.91
	8g	99.99
Zinc	2g	41.02
	4g	69.14
	8g	98.02



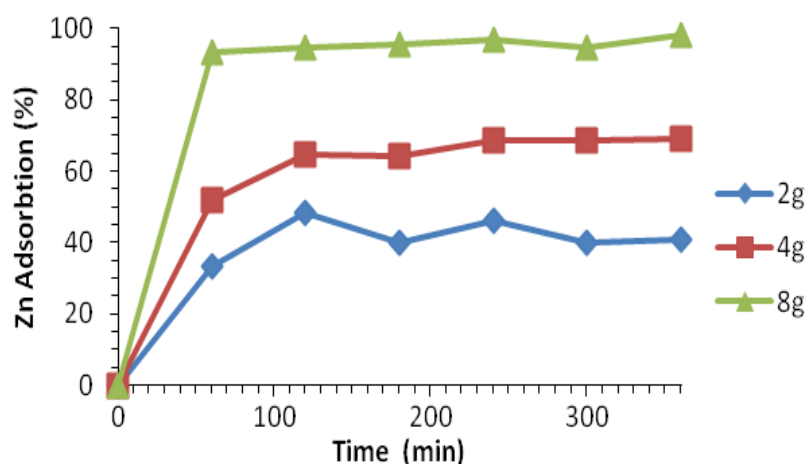


Figure 7.2: Shows the effect of the mass of natural zeolite on the adsorption of copper, iron, lead and zinc from solution.

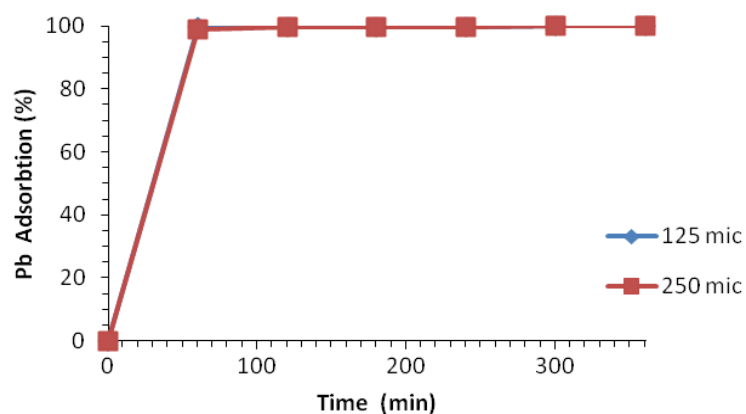
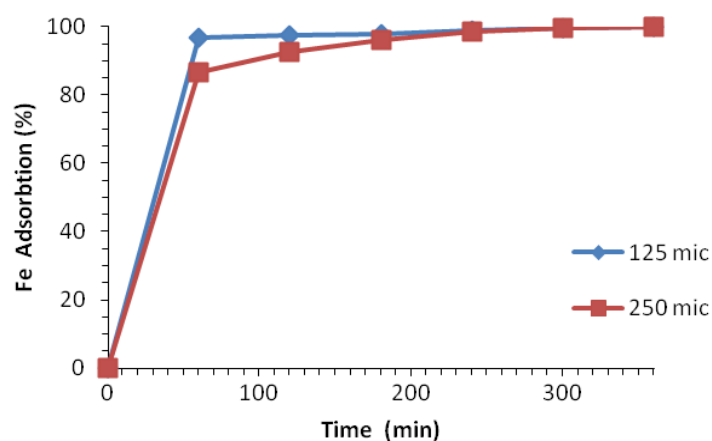
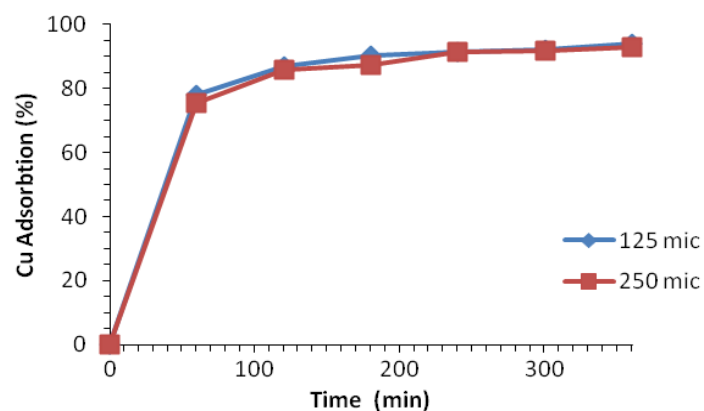
7.3.2. Effect of adsorbent particle size

The effect of adsorbent particle size on adsorption capacities from solutions was investigated. Two different sizes were used, 125 and 250 μ m. The adsorbent was mixed with 100 ml solution of the appropriate multi-component solution. This experiment was initially carried out for Cu^{2+} , Fe^{3+} , Pb^{2+} and Zn^{2+} cations, using fixed initial metal concentrations. The results obtained are presented in figure 7.3. Zeolite weights of 4g were used at an agitation speed of 150 rpm for 360 minutes and samples were collected every hour and analysed.

It was observed that the smaller particle sized samples adsorbed more of the Cu^{2+} , Fe^{3+} , Pb^{2+} and Zn^{2+} ions. This indicates that any decrease in adsorbent particle size causes an increase in the adsorption of the heavy metals ions. This is because as the adsorbent particles get smaller more adsorption sites are available for metal uptake and more contacts are taking place. On the other hand smaller particle sizes result in the shortening of the diffusion distance that ions have to travel in order to get to an active site; thus adsorption is enhanced and requires a shorter time to reach equilibrium. This is in agreement with the results obtained by Sprynskyy *et al.* (2006) and Inglezakis *et al.* (2004). They concluded that the larger particle size adsorbent had lower adsorption capacities than the smaller particle sizes.

Although particle size can affect the adsorption capacity mostly at the initial stage, as the contact time increases there is a decrease in the level of the effect of particle size on

adsorption and the adsorption process gets slower. The same results were found by Malliou *et al.* (1994) and Erdem *et al.* (2004). The use of very fine particles can also cause some operational problems such as difficulty in the filtration of the zeolite from solution in batch studies (Inglezakis *et al.*, 2001).



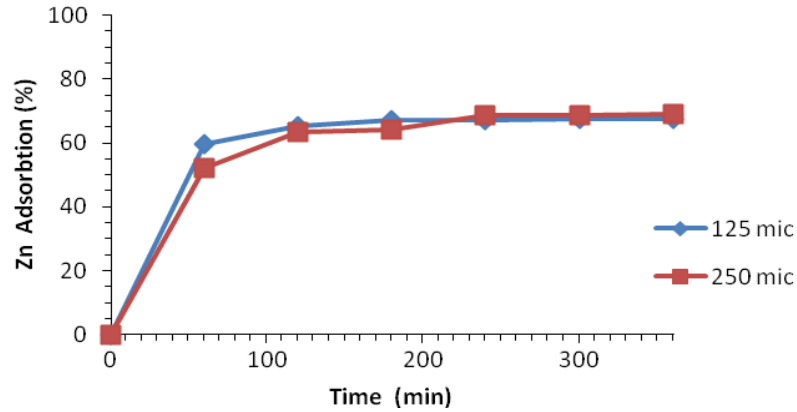


Figure 7.3: Shows the effect of particle size on the adsorption of iron, copper, lead and zinc from solution.

7.3.3. Effect of initial solution pH

Initial solution pH is a critical parameter for adsorption experiments. This parameter has a significant impact on heavy metal removal processes since it can influence and impact on adsorbent ability to remove metals and is connected with the competition of hydrogen (H^+) ions with heavy metal cations for active sites on the adsorbent surface (Dimirkou, 2007; Inglezakis *et al.*, 2003; Hui *et al.*, 2005). An acidic solution can impact on both the character of the exchanging ions and the character of the adsorbent.

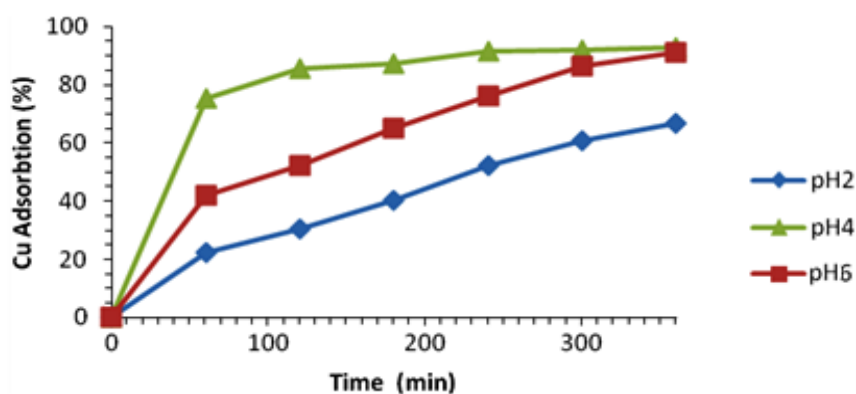
Solutions with different pH values were used as follows: 2, 4 and 6 ± 0.1 for the multi-component solutions. 100ml of the solution was contacted with 4g of natural zeolite for 360 minutes. The particle size of the zeolite samples used was 250 μm . The agitation speed was 150 rpm at room temperature. This experiment was initially done using fixed metal concentrations of Cu^{2+} , Fe^{3+} , Pb^{2+} and Zn^{2+} cations. The results obtained are presented in figure 7.4.

The results show that as the solution pH increases, the heavy metal removal efficiency also increases. This is due to the competition between the hydrogen ions and heavy metal cations for the same exchange sites (Inglezakis *et al.*, 2001; Wingenfelder *et al.*, 2005; Alvarez-Ayuso *et al.*, 2003) and electrostatic repulsion between the heavy metal cations in solution; as more hydrogen ions are adsorbed, the number of protonated zeolite surfaces increases (Cabrera *et al.*, 2005). Figure 7.4 shows how the initial solution pH influences the adsorption

capacity of natural zeolite. This has been confirmed by Wingenfelder *et al.* (2005). He concluded that as the initial pH increases, more negatively charged surface becomes available thus facilitating greater heavy metal removal. Thus an increase in the initial pH resulted in an increase in the adsorption efficiency of natural zeolite for Cu^{2+} , Fe^{3+} , Pb^{2+} and Zn^{2+} ions. Moreno *et al.* (2001) and Alvarez-Ayuso *et al.* (2003) observed the same behaviour using clinoptilolite and stated that the efficiency of metal adsorption depends on the solution pH levels. However, metal precipitates at high pH values above pH7 and low values below pH2 inhibit the contact of metal ions with the adsorbent.

The results show that the ion exchange process increases with an increase in pH up to a maximum value and the best heavy metal removal efficiency value was obtained between pH values of 4 and 6, while pH values below pH4 or above pH6 decreased the heavy metal removal efficiency, as shown in figure 7.4.

As concluded by Ragnarsdottir *et al.* (1996) and Oren and Kaya (2006), a low pH value (< 4) solution can cause dissolution of the zeolite crystal structure. Oren and Kaya (2006) assumed that pH values between pH4 and pH6 are fundamental in the ion exchange process. Previous studies have shown that at higher pH values (> 7) the zeolite structure can be affected and this can result in the reduction of the ion exchange process (Alvarez – Ayuso *et al.*, 2003; Dal Bosco *et al.*, 2005; Yu *et al.*, 2003; Oren and Kaya 2006; Argun, 2008). This is in agreement with outcomes obtained by Mier *et al.* (2001), who also concluded that the pH of the solution can affect the removal efficiency by affecting the integrity of the natural zeolite. Tsitsishvili (1992) also added that the natural zeolite structure is known to be partially degraded and lose its ion exchange capacity in alkaline media while in highly acidic solutions the natural zeolite structure breaks down. Thus ion exchange processes increase with an increase in pH up to 7, and decrease slowly thereafter.



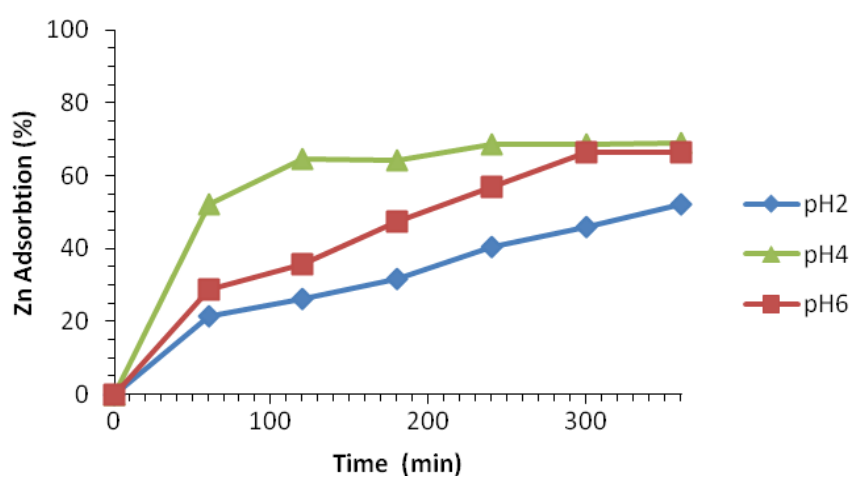
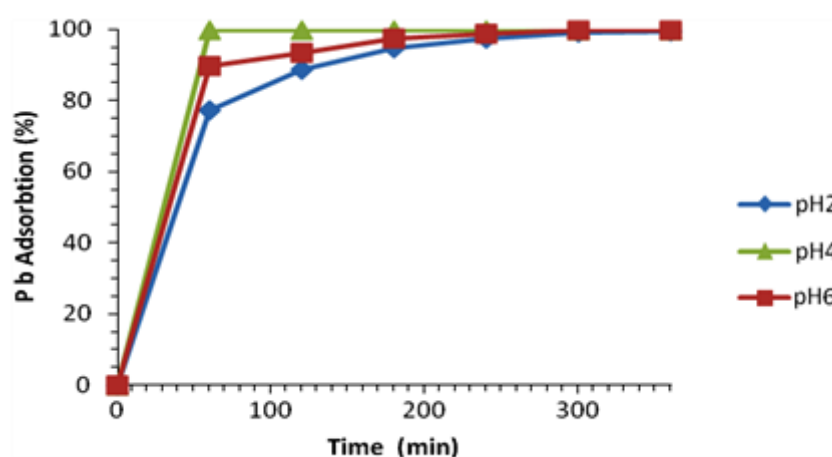
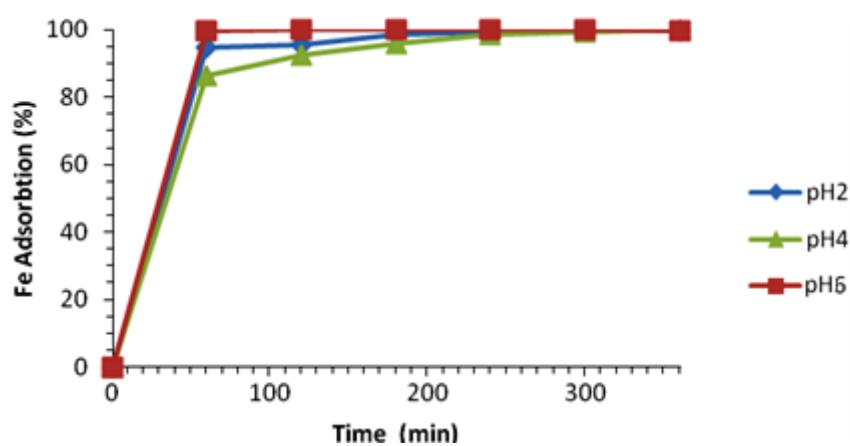


Figure 7.4 : Shows the effect of initial solution pH on the adsorption of copper, iron, lead and zinc from solution.

7.3.4. Effect of initial solution concentration

The initial solution concentration of the solution significantly impacts on the heavy metal removal process. Several studies have reported that an increase in the initial concentration resulted in an improvement in the adsorption capacity at the initial stage and a decrease in the overall heavy metal removal efficiency, which depends on the availability of active sites (Coruh and Ergun, 2009; Cabrera *et al.*, 2005; Peric *et al.*, 2004; Erdem *et al.*, 2004; Ören and Kaya, 2006; Akgu *et al.*, 2006).

The effect of the initial solution concentration on the adsorption process was determined using multi-component solution concentrations in the range of (50, 100, 200 and 400) mg/l. 100 ml solutions at pH4 were contacted with 4g of zeolite samples of size 250 µm. The experiments were run for 360 minutes and samples were collected and analysed. An agitation speed of 150 rpm was used at room temperature.

Table 7.2: Shows the effect of initial solution concentration on the adsorption capacity of natural zeolite

Heavy Metals	Initial Concentration (mg/l)	Amount Adsorbed, q_e (mg/g)
Copper	50	0.37
	100	0.76
	200	1.30
	400	2.30
Iron	50	0.0
	100	0.46
	200	1.13
	400	2.78
Lead	50	0.62
	100	1.29
	200	2.89
	400	6.68
Zinc	50	0.19
	100	0.56
	200	0.80
	400	1.37

The results in table 7.2 show that generally any increase in the initial solution concentration results in an increase in the heavy metal removal efficiency and the rate of adsorption, as shown in figure 7.5. This may be a result of the concentration driving force since it is responsible for overcoming the mass transfer resistance associated with the adsorption of metals from solution by the zeolite (Barrer, 1982). Therefore, as the initial concentration increases, the driving force also increases, resulting in improved efficiency of the heavy metal removal process. Then after the system reaches saturation point, the initial solution concentration does not show any significant change in the amount adsorbed due to a decrease in the number of active sites (Connors, 1998).

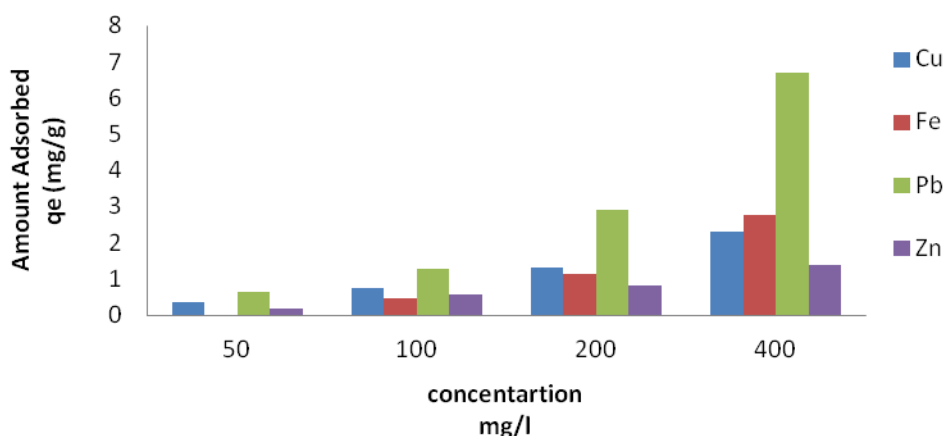
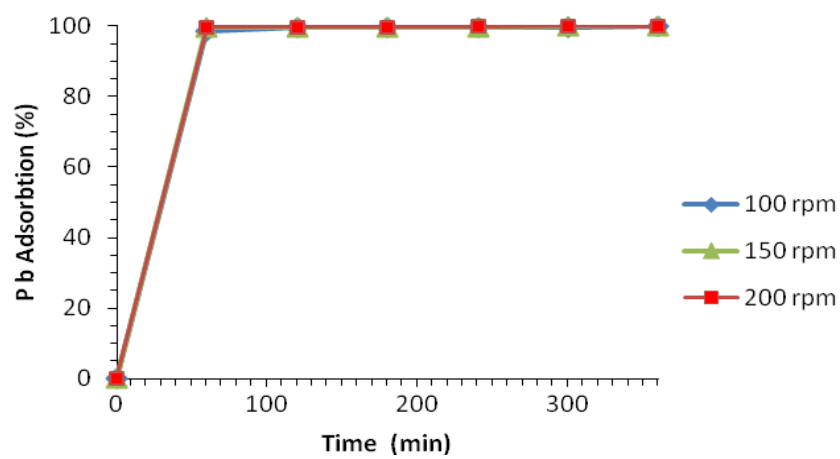
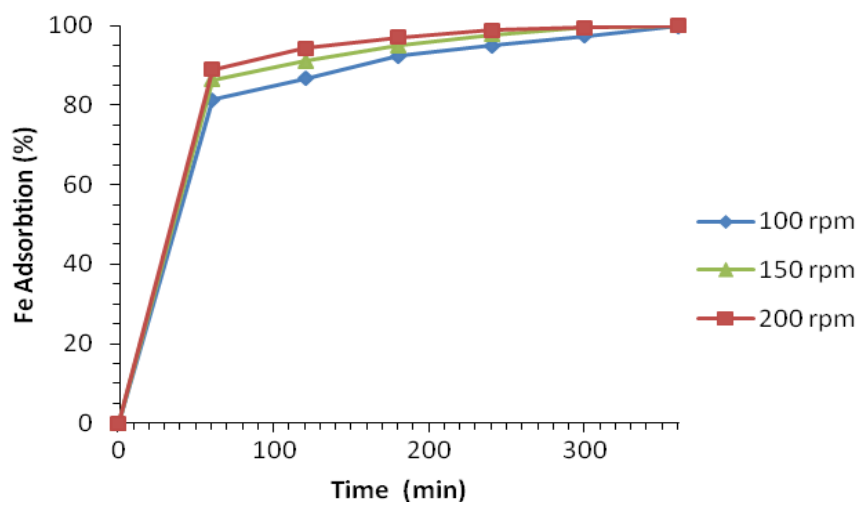
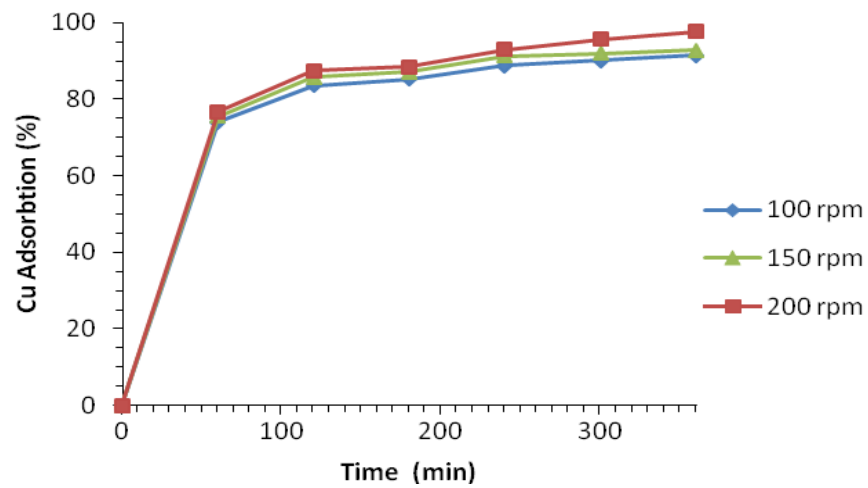


Figure 7.5: Shows the effect of initial solution concentration and the amount of heavy metals adsorbed q_e (mg/g) by natural zeolite.

7.3.5. Effect of agitation speed

The effect of agitation speed on the removal of the cations from the solution was determined using a magnetic stirrer at speeds of 100, 150 and 200 rpm. The mixture was contacted with 4g of zeolite samples and agitated for 360 minutes. The particle size of the zeolite samples used was 250 μm at room temperature. The pH was adjusted to 4 ± 0.1 . This experiment was initially done for Cu^{2+} , Fe^{3+} , Pb^{2+} and Zn^{2+} ions, using fixed initial metal concentrations. The results of the effect of agitation are shown in figure 7.6.



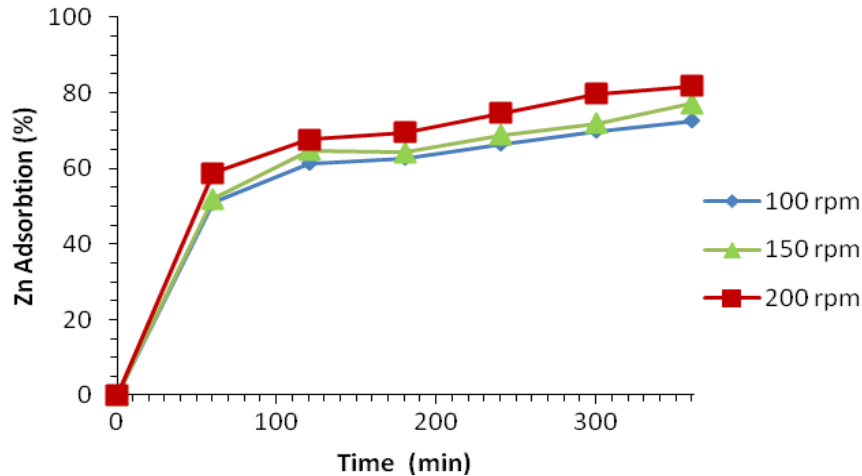


Figure 7.6: Shows the effect of agitation speed on the adsorption of heavy metals by natural zeolite.

The results show that the metal removal efficiency increased as the speed of agitation increased. This is in agreement with the results obtained by Ören and Kaya, (2006). They concluded that an increase in the speed of agitation resulted in higher adsorption capacities. The agitation helps in overcoming the external mass transfer resistance, which controls the rate of adsorption. Hence, an increase in the speed of agitation generally results in an increase in ion mobility in the solution and reduces the mass transfer resistance. At high agitation speed, the external diffusion coefficient increases and the boundary layer becomes thinner, which usually improves the rate of solute diffusion through the boundary layer (Trgo and Peric, 2003).

Agitation of the mixture also results in abrasion and the production of more broken natural zeolite particles. This means that fresh smaller size zeolite particles are produced and more activate sites are available on the surface. So this mechanical procedure leads to an increase in the surface area, which significantly improves the efficiency of the heavy metal removal from solution (Trgo and Peric, 2003).

7.3.6. Effect of pre-treatment

Natural zeolite can be modified by a single or combined treatment such as thermal and chemical modification (Karmen *et al.*, 2013). The pre-treatment of natural material is carried out to increase the metal removal efficiency from solution. For this purpose, both hydrothermal and chemical pre-treatment of natural zeolite were carried out in order to investigate whether pre-treatment could increase the adsorption capacity of natural zeolite.

7.3.6.1 . Thermal treatment of natural zeolite

Thermal treatment processes depend on the adsorbent structure and rate of temperature used. Thermal treatment processes can enhance the pore volume by removing water and organics from the pore channels, which leads to an increase in the number of active sites and promotes the adsorption process. Thus thermal treatment processes can improve the efficiency of heavy metal removal from solution. To determine the adsorption capacity of natural zeolite in wastewater treatment, it is important to study the dehydration procedure and structural stability of natural zeolitic materials. Table 7.3 shows the stability of the structure of different types of natural zeolites, presented by Breck (1974).

Table 7.3: Shows the structural stability of some natural zeolites (Breck, 1974).

Natural zeolite	Structural stability
Heulandite	up to 300 °C
Laumontite	up to 500 °C
Analcime	up to 700 °C
Erionite	up to 750 °C
Clinoptilolite	up to 750 °C
Mordenite	up to 800 °C

Thermal analysis methods were used to gain information about the mass loss change and adsorption or crystallization. The results obtained from the TG/DTG analysis clearly show that the zeolite structure was stable up to 750 °C and that zeolite water was removed to 400°C continually. The DTG pattern of clinoptilolite displays a new diffraction peak at 750-800°C (Figure 5.9, chapter 5), which could be attributed to the formation of sodalite. Figure 7.7 shows the dehydration and dehydroxylation process of clinoptilolite and their mass loss rate (13 wt. %).

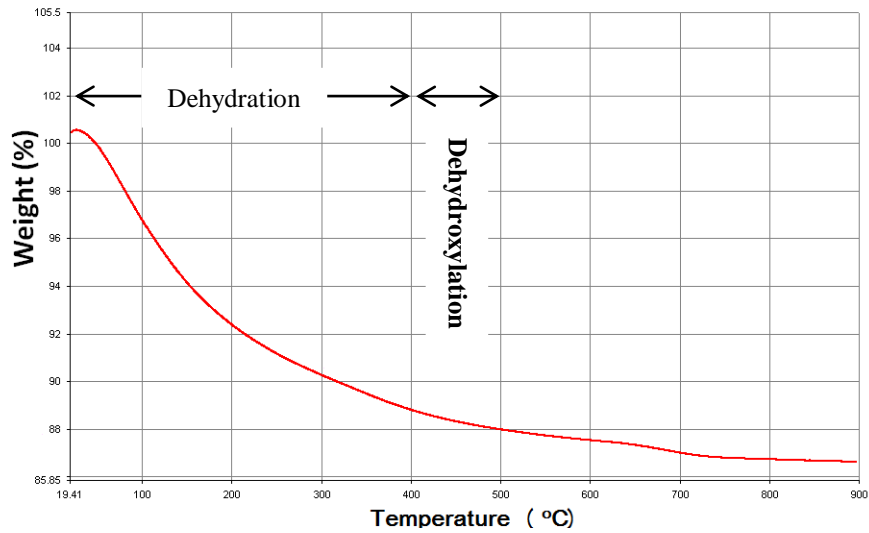
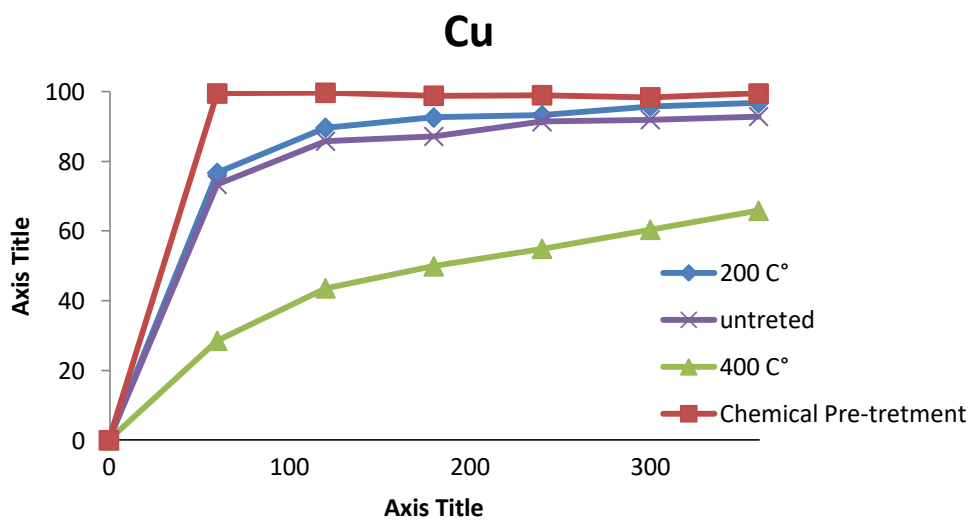


Figure 7.7: Shows the loss of mass of clinoptilolite by thermogravimetric analysis (TGA) which show curves between 20-900°C.

The effect of the thermal treatment on the removal of cations from the solution by natural zeolite was determined by contacting 100 ml of multi-component solutions with 4g of pre-treated zeolite samples. The experiments were run for 360 minutes. An agitation speed of 150 rpm was used at room temperature. The results of the effect of the thermal pre-treatment on the removal of the cations from the solution are shown in figure 7.8.



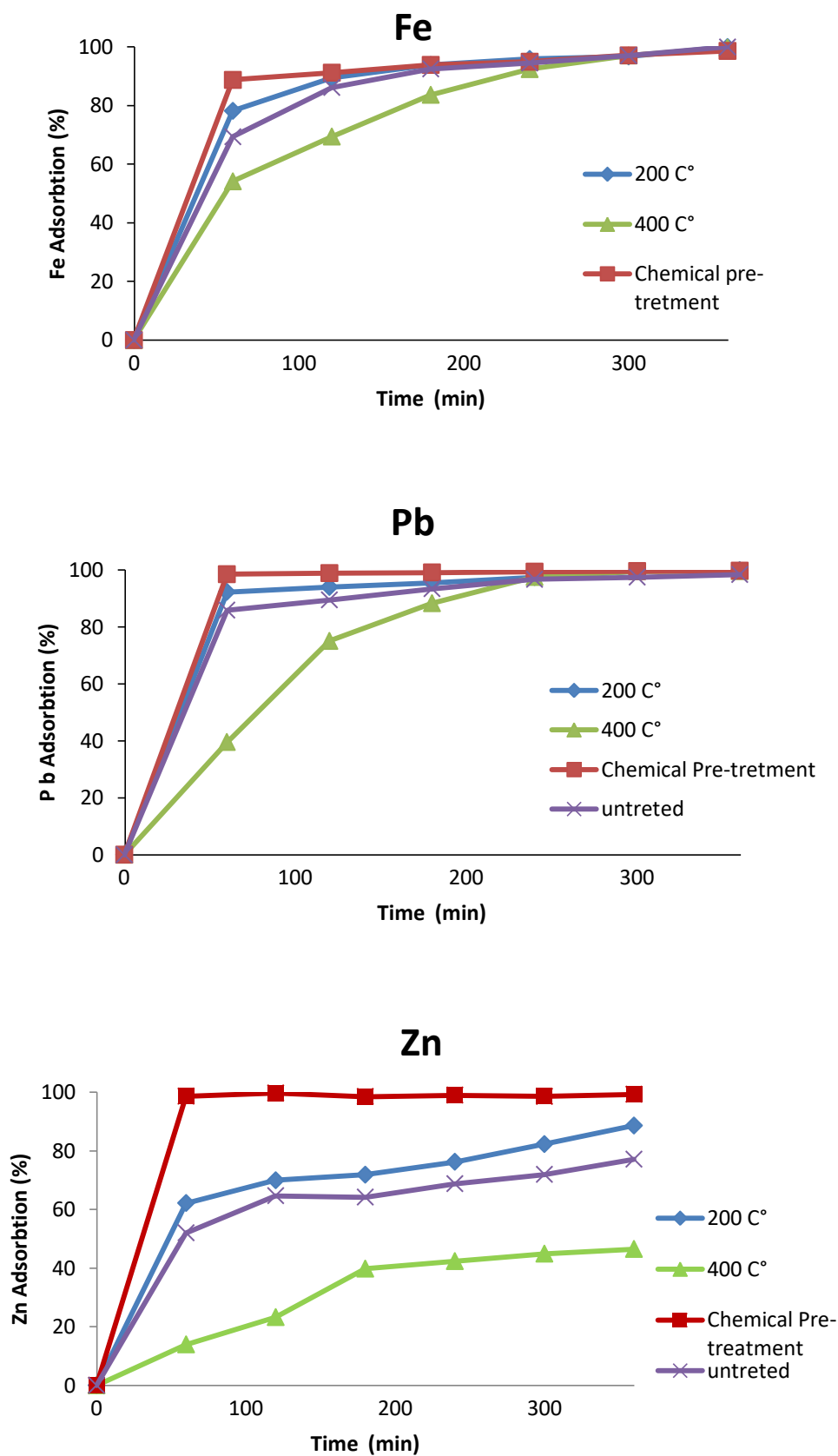


Figure 7.8: Shows the comparison of natural and thermally treated natural zeolite.

The thermal treatment process of natural zeolite was performed by heating the natural zeolite sample in a furnace for 30 minutes at 200 and 400°C. Although the thermal treatment process can affect the adsorption capacity, mostly up to 200°C, as the temperature rate increases more, there is a decrease in the level of the effect of the thermal treatment process on adsorption and the adsorption process gets slower.

It was observed that the thermal treatment samples at 200°C adsorbed more metal ions of Cu^{2+} , Fe^{3+} , Pb^{2+} and Zn^{2+} ions from solution, around %50 better than the thermal treatment samples at 400°C adsorbed less metal ions as shown in figure 7.8. Also, the rate of adsorption by calcined zeolite up to 200°C was %10 better compared to the untreated zeolite, but the efficiency decreased when zeolite was treated at very high temperatures.

The increase in the efficiency of heavy metal removal from solution as a result of thermal treatment may be due to the removal of water and hydroxyl groups from the natural zeolite structure. This removal of water and hydroxyl group results in a change in the surface area of the samples and also leaves the channels more vacant and available. Hence the adsorption capacity is improved since the heavy metal ions had better access to exchangeable sites within the natural zeolite (Turner *et al.*, 2000; Tatsuo and Nagae, 2003). However, the decline in the efficiency for zeolite treated at very high temperatures was related to the possible collapse of the zeolite structure and the loss of porosity, which reduced the activated surface area (Akdeniz *et al.*, 2007; Tatsuo and Nagae, 2005).

7.3.6.2 . Modification of zeolite with solution of inorganic salts

The chemical modification was carried out using inorganic salts (NaCl) to activate the zeolite and increase its efficiency in water treatment (Kumar and Hayashi 2009; Cerjan *et al.*, 2007; Li *et al.*, 2007). For successful modification 0.5M NaCl solutions were used to modify the natural zeolite. Inglezakis *et al.* (2001) investigated the effect of NaCl concentration on the effective capacity of the conditioned clinoptilolite in fixed-bed reactors and found that raising the concentration above 0.4 M/L had practically effect on the effective capacity. The most widely used concentration ranges are 0.5-2.0 M NaCl (Çulfaz and Yagız, 2004; Ouki *et al.*, 1994; Curkovic *et al.*, 1997; Cincotti *et al.*, 2006; Langella *et al.*, 2000). Washing the zeolite samples after the pre-treatment process using deionised water is essential in order to remove

excess NaCl entrapped within the zeolite structure (Ouki and Kavannagh, 1999). NaCl is the most commonly used pre-treatment agent for the conversion of clinoptilolite to harmonic or near harmonic form (Çulfaz and Yagız, 2004; Bektas and Kara, 2004; Semmens and Seyfarth, 1988; Inglezakis *et al.*, 2001).

The chemical treatment processes were carried by contacting 4g of natural zeolite with 200 ml of 0.5M NaCl. The mixture was agitated in a beaker using a stirrer at a speed of 150 rpm for 24 hr at room temperature. Thereafter the sample was rinsed three times in ample deionised water for a total period of 15 mins and dried in an oven at 100°C.

The adsorption capacity as a result of the chemical treatment processes was higher compared to the untreated zeolite or thermal pre-treatment zeolite as shown in figure 7.8. This may be due to the removal of all unwanted waste material from the zeolite surface. After the contact of zeolite with NaCl, decationization process occurs which is exchange of cations (H^+ or Na^+) from solution with exchangeable cations (Na^+ , K^+ , Ca^{2+} , Mg^{2+}) from the zeolite framework which led to competition of hydrogen (H^+) ions with heavy metal cations for the active sites on the adsorbent surface.

7.4. Conclusion

Kinetic studies of the removal of Cu^{2+} , Fe^{3+} , Pb^{2+} and Zn^{2+} ions from synthetic wastewater were carried out using natural and modified zeolite. Experiments were carried out in order to investigate the impact of several parameters on the efficiency of zeolite for the removal of heavy metals from industrial wastewater. The results obtained may be summarized as follows:

- The study indicated the suitability of the zeolite used for the removal of Cu^{2+} , Fe^{3+} , Pb^{2+} and Zn^{2+} ions from synthetic wastewater, while considering the economic aspects of wastewater treatment.
- The adsorbent mass, adsorbent particle size, initial solution pH, initial solution concentration and agitation speed as well as pre-treatment or modification of the adsorbent in the case of batch experiments are usually the most influential parameters.
- The efficiency of heavy metal removal was enhanced with increased initial solution pH, increased agitation speed, increased solution concentration, decreased particle size and greater mass of adsorbent as well as the application of pre-treatments.
- The results suggest that the adsorption of Cu^{2+} , Fe^{3+} , Pb^{2+} and Zn^{2+} ions on the selected adsorbents involves a complex mechanism and a number of possible rate controlling steps can determine the process efficiency such as boundary layer diffusion due to external mass transfer effects (external solution phase surrounding the particle), intraparticle diffusion within the exchanger itself, and chemical reaction kinetic control.
- In general the results show that adsorption is a heterogeneous process as the removal rate of Cu^{2+} , Fe^{3+} , Pb^{2+} and Zn^{2+} ions mostly occurred early on, but as the contact time increased, there was a decrease in the level of the effect of the parameters on adsorption and the adsorption process became slower.

CHAPTER 8

8.SYNTHESIS AND CHARACTERIZATION OF ZEOLITE A BY HYDROTHERMAL TRANSFORMATION OF NATURAL KAOLINITE

8.1 . Introduction

This chapter discusses the results obtained after activation of kaolinite and metakaolinite followed by different thermal and chemical treatments. The conversion of the raw materials into zeolitic materials was carrying on by hydrothermal transformation. The kaolinite clay used in the present investigation was supplied from Iraq. The adsorption behaviour of zeolite type A as a low-cost adsorbent was studied in order to consider its application for the removal of Cu^{2+} , Fe^{3+} , Pb^{2+} and Zn^{2+} ions from industrial wastewater. The batch method was employed in order to investigate the behaviour of synthetic zeolite and understand the metal removal efficiency from solution.

8.2. Kaolinite framework structure

Kaolinite is also known as “china clay” and “kaolin”. It was discovered in the year 1867 and the word “kaolin” is derived from the name of the Chinese town Kao-Ling located in the Jiangxi Province of southeast China (Schroeder, 2003; Pohl, 2011). Kaolinite ($\text{Al}_2\text{Si}_2\text{O}_5(\text{OH})_4$) is one of the most common clay minerals. It primarily occurs in abundance in soils that are formed from the decomposition of aluminium silicate minerals like feldspar and is usually a white mineral.

The basic kaolin mineral structure comprising the minerals kaolinite, dickite, nacrite, and halloysite is a layer of a single silica (SiO_4) tetrahedral sheet and a single alumina $\text{Al}(\text{O}, \text{OH})_6$ octahedral sheet (Murray, 2007). Then both sheets are combined to form the kaolinite unit layer which are joined by sharing a common layer of oxygens and hydroxyls and these unit layers are stacked one over the other, as shown in figure 8.1 (Grim, 1968; Murray, 2007; Deer *et al.*, 1992). It is strongly hydrogen bonded to the plates above and below. All of the apical oxygens of the silica tetrahedrons point in the same direction so that these oxygens and/or hydroxyls are shared by the silicons in the tetrahedral sheet and the aluminum in the

octahedral sheet (Murray, 2007). Kaolinite has a low adsorption capacity and a lower ion exchange capacity compared to zeolite, which are directly related to the low surface charge on the particle. Since kaolinite particles have an oxygen surface on one side and a hydroxyl surface on the other (Murray, 2007; Deer *et al.*, 1992).

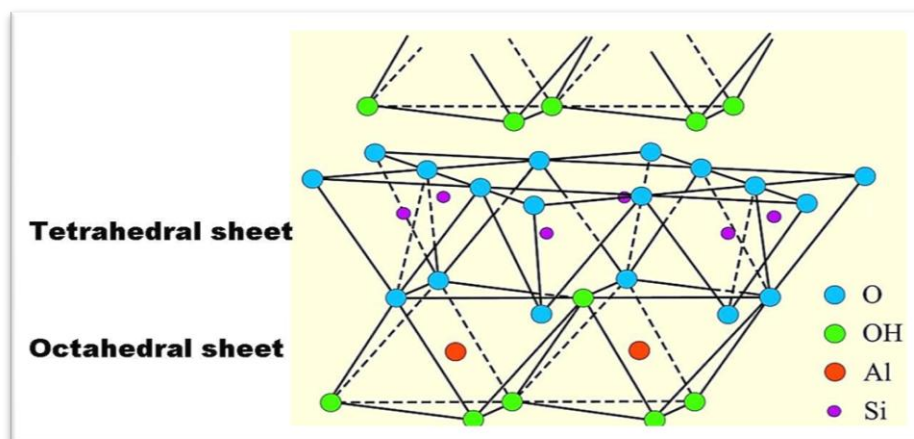


Figure 8.1: Diagrammatic sketch of the kaolinite structure and representation of (SiO_4) tetrahedral or $\text{Al}(\text{O},\text{OH})_6$ octahedral (Grim, 1968).

Kaolinite undergoes a series of phase transformations when thermally treated. The formation of metakaolinite during the thermal treatment of kaolinite is a very important stage that consists of three processes. These processes include the destruction of the kaolinite sheet structure, dehydroxylation and the recombination of silica and alumina into the structure of metakaolinite (Rios *et al.*, 2007). The run of these steps is significantly affected by the heating rate. The mechanism and influence of the heating rate in the course of these processes was investigated using the methods of thermal analysis DTG and XRD.

During calcinations of kaolinite, the silicon atoms experience a range of reactions of differing distortion due to dehydroxylation (Bellotto *et al.*, 1995). The aluminium atoms mostly transform from octahedral to tetrahedral geometry. As the calcination temperature increases, the structure becomes more distorted and amorphous silica is then liberated (Bellotto *et al.*, 1995).

The dehydroxylation process might result in the disturbance of the $\text{Al}(\text{O},\text{OH})_6$ octahedral

sheet by the outer hydroxyls, but it does not have much effect on the SiO_4 tetrahedral sheet due to the more stable inner-hydroxyl groups (Rios *et al.*, 2007). The outer hydroxyls of the octahedral sheets may be more easily removed by heating than the inner ones, which will maintain a more ordered SiO_4 tetrahedral group in the structure during dehydroxylation (Rios *et al.*, 2007). After heating at 950°C , the SiO_4 groups combine with the AlO_6 group to form the Al–Si spinel phase, which has a short range order structure (Bellotto *et al.*, 1995).

In recent years, there has been much interest in producing synthetic zeolite using low-cost raw materials such as kaolinite (natural clays) (Ayele *et al.*, 2015; Georgiev *et al.*, 2009; Ibrahim *et al.*, 2010; Rondón *et al.*, 2013; Doaa and Mohamed, 2014; Jamil *et al.*, 2010). Nowadays, synthetic zeolites are used commercially more often than natural zeolites due to the homogeneity of their particle sizes and the purity of crystalline products, which results in significantly higher efficiency in heavy metal removal (Breck, 1982; Szoztak, 1998). Another advantage of synthetic zeolites in comparison to natural zeolites is that synthetic zeolites can be engineered with a wide variety of chemical properties and pore sizes and that they have greater thermal stability (Petrov and Michalev, 2012). Previous experiments have established that the preparation of synthetic zeolites from chemical sources of silica and alumina can be expensive, while the conversion of raw materials (natural sources of silica and alumina) into zeolitic materials synthesised by hydrothermal transformation is much cheaper (Kovo and Holmes, 2010; Petrov and Michalev, 2012; Adamczyk and Bialecka, 2005; Querol *et al.*, 1997; Saija *et al.*, 1983; Tanaka *et al.*, 2004; Ayele *et al.*, 2015; Walek *et al.*, 2008; Wang *et al.*, 2008).

Thus in the present study, Iraqi natural kaolinite was used as a starting material to produce zeolite A. The zeolite synthesis from natural kaolinite was carried out using a hydrothermal synthesis technique considering the economic aspects.

8.2 . Kaolinite structural transformations

The Kaolinite structure undergoes a series of phase transformations when thermally modified at atmospheric pressure as indicated below:

8.2.1. Drying phase

During the kaolinite thermal treatment process, below 100 °C, exposure to dry air will slowly remove adsorbed water from the kaolinite structure (Frost *et al.*, 2003). Then at temperatures between 100 °C and about 400 °C, the dehydration process appears and any remaining water is expelled from the kaolinite pores. At this stage a weight loss takes place. This may be due to the reorganisation in the octahedral layer that can be correlated with a dehydration process (Balek and Murat, 1996). After dehydration, the kaolinite goes through a dehydroxylation in the range 450– 600 °C (Frost *et al.*, 2003).

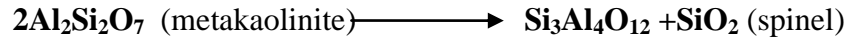
8.2.2. Metakaolinite phase

The dehydroxylation of kaolinite is an endothermic process in which the removal of chemically bonded hydroxyl ions takes place. Kaolinite can be transformed into metakaolinite above temperature of 550 °C. Endothermic dehydration of kaolinite begins at 550–600 °C producing disordered metakaolinite, while continuous hydroxyl loss is observed up to 900 °C (Petrov and Michalev, 2012; Rios *et al.*, 2007). There is a disagreement concerning the nature of the metakaolinite formation phase. Previous studies have generally concluded that metakaolinite is not only amorphous silica (SiO₂) and alumina (Al₂O₃), but rather it can be a complex amorphous structure that retains some longer-range order due to the stacking of its hexagonal layers (Alkan *et al.*, 2005). According to Kakali *et al.* (2001), kaolinite dehydroxylation occurs at temperatures from 400–650 °C, which is the transformation stage to metakaolinite. Frost *et al.* (2003) considered that this kaolinite dehydroxylation process occurs between 450°C and 550°C. However, in this study a dehydroxylation process occurred between 450°C and 600 °C. This reaction series includes the formation of highly disordered metakaolinite, as shown below:



8.2.3. Spinel phase

On further calcinations metakaolinite converts to spinel, this is also referred to an alumina-silica structure, at temperatures from 925–950 °C. The exothermic peak observed at 1000 °C can also be attributed to the formation of spinel with mullite-like composition, as described by Chakravorty and Ghosh (1991). A progressive decomposition of metakaolinite occurs up to 950 °C, as shown below:



8.2.4. Platelet mullite phase

The spinel transforms to a more stable material called platelet mullite and highly crystalline cristobalite at calcinations above 1050 °C. The exothermic peak at ~1000 °C suggests the breakdown of the metakaolinite structure. Breck (1974) considered the decomposition of metakaolinite and the formation of mullite as the result of two stages according to the reactions:



8.2.5. Needle mullite phase

Calcinations up to 1400 °C produce a new form of mullite called "needle mullite", which contributes to significant increases in structural strength and heat resistance (Rios *et al.*, 2007). This is a structural but not chemical transformation.

8.3. Characterization of the untreated and thermally treated kaolinite

8.3.1. Scanning Electron Microscopy (SEM)

The surface morphology of the kaolinite and zeolite A samples was determined using SEM under the following analytical conditions: EHT = 10.00 kV and 20.00 kV, Signal A = SE1 and VPSE, WD = 6.0, 6.5, 7.0 and 8.5mm at different magnifications. SEM micrographs (Figure 8.2) show the occurrences of the kaolinite products obtained before and after hydrothermal treatment of kaolinite and metakaolinite. Kaolinite can be recognized by its platy morphology. It is formed of small hexagonal plates that are loosely packed (Mousa and Buhl 2014).

The micrograph of the “as received” kaolinite samples represented below were obtained from SEM analysis under the following SEM analytical conditions: EHT =10.00 kV, Signal A =SE1, WD 6.0 mm at a magnification of 20000x. Figure 8.2 shows a micrograph of kaolinite. It presents crystals of kaolinite that are not well defined.

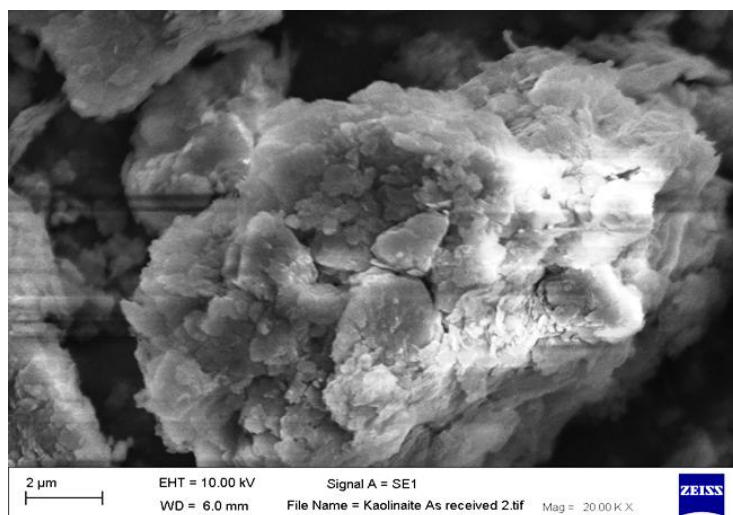


Figure 8.2: SEM micrograph of the as-received kaolinite at a magnification of 20000x.

Figure 8.3 shows the micrographs of the kaolinite samples under the following SEM analytical conditions: EHT =20.00 kV, Signal A =VPSE, WD = 8.5 mm at a magnification of 2000x. The micrograph displays the randomly oriented crystallites and in particular indicates the crystalline nature of kaolinite before any modification.

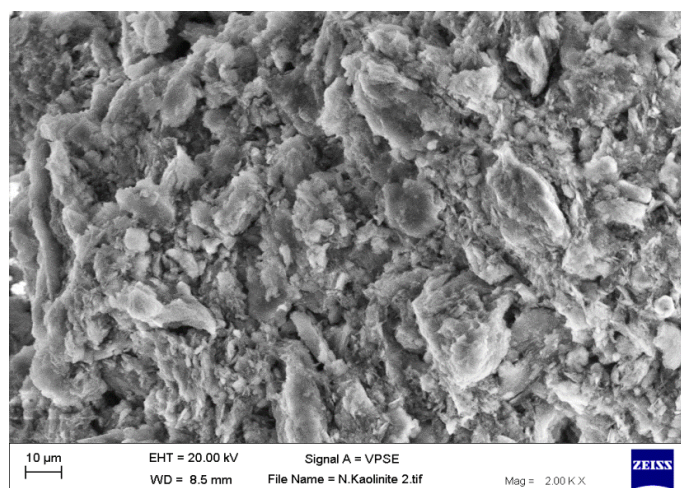


Figure 8.3: The SEM micrograph of kaolinite showing the crystalline nature of kaolinite at a magnification of 2000x.

The micrographs of the metakaolinite samples were studied under the following SEM analytical conditions: EHT =10.00 kV, Signal A =SE1, WD = 6.5 mm at a magnification of 20000x and 10000x (Figure 8.4). The sample was calcined at 600°C for 3hr. The micrographs show the randomly oriented crystallites and in particular indicate the appearance of the partly crystalline.

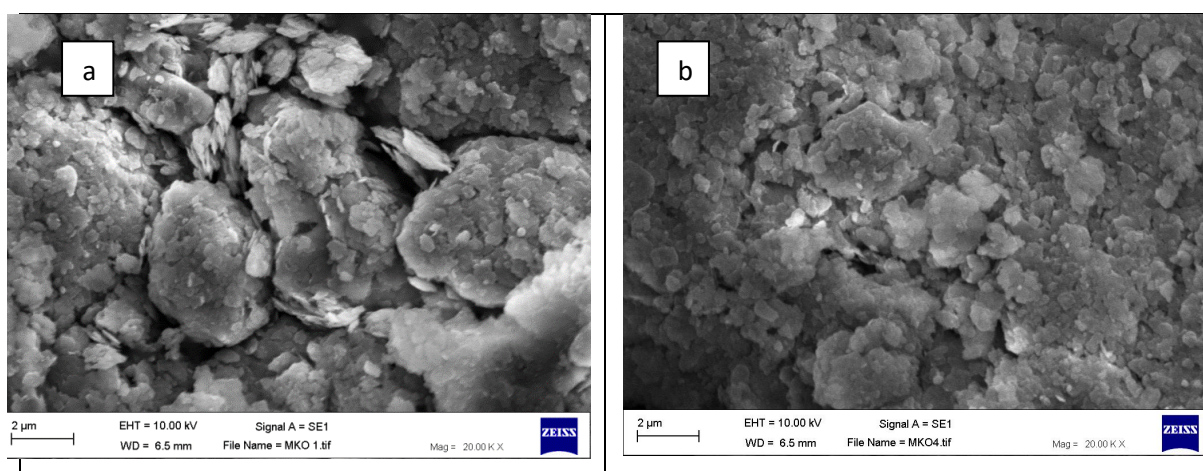


Figure 8.4: SEM micrograph showing the crystalline nature of metakaolinite at a magnification of (a) 20000x and (b) 10000x.

The micrographs of the synthesised zeolite A samples were taken under the following SEM analytical conditions: EHT =10.00 kV, Signal A =SE1, WD = 7 mm at magnifications of

5000x, 10000x and 20000x. As shown in figure 8.5, the micrograph indicates in particular the well-formed typical cubic shaped crystals of zeolite A with an average particle size of 3.1 μm . Figures 8.5 and 8.6 shows the crystalline nature of the zeolite synthesised by a conventional hydrothermal synthesis reaction at a magnification of 5000x and 1000x. Figures 8.7 and 8.8 show the crystalline nature of the zeolite synthesised by alkaline fusion followed by hydrothermal reaction.

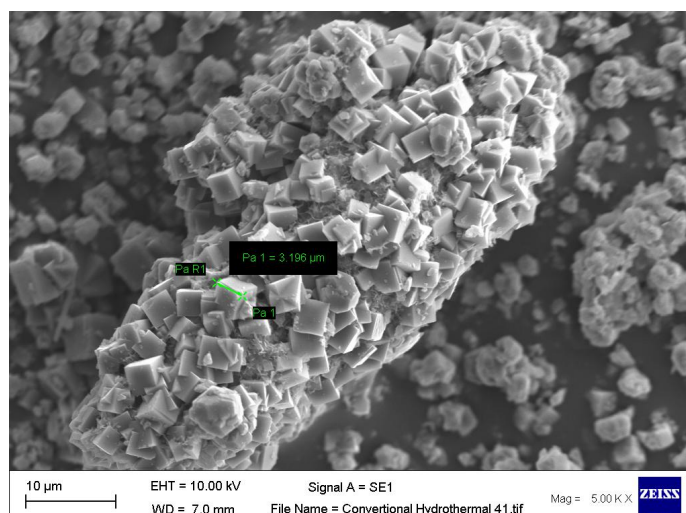


Figure 8.5: SEM microstructure showing the oriented crystallites conducted by conventional hydrothermal synthesis reaction at a magnification of 5000x.

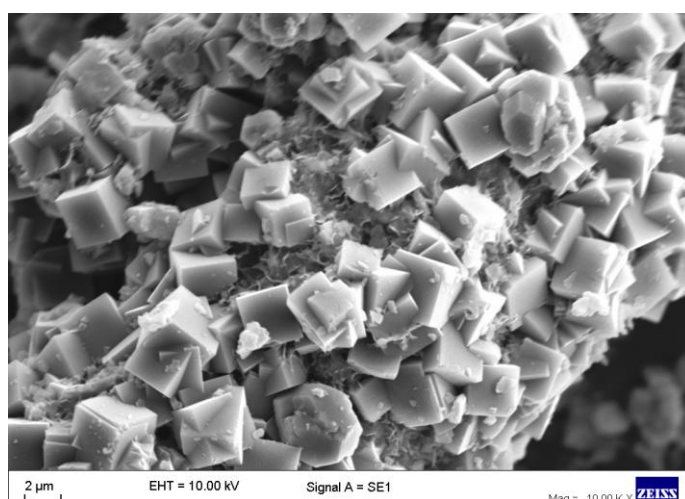


Figure 8.6: SEM microstructure showing the oriented crystallites conducted by conventional hydrothermal synthesis reaction at a magnification of 10000x.

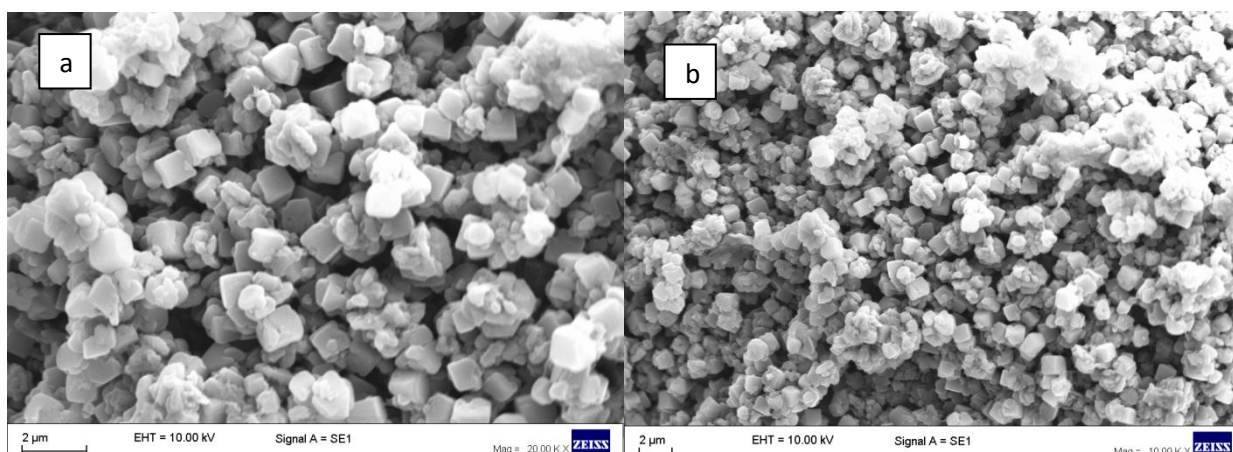


Figure 8.7(a,b): SEM microstructure showing the oriented crystallites synthesised by alkaline fusion followed by hydrothermal reaction.

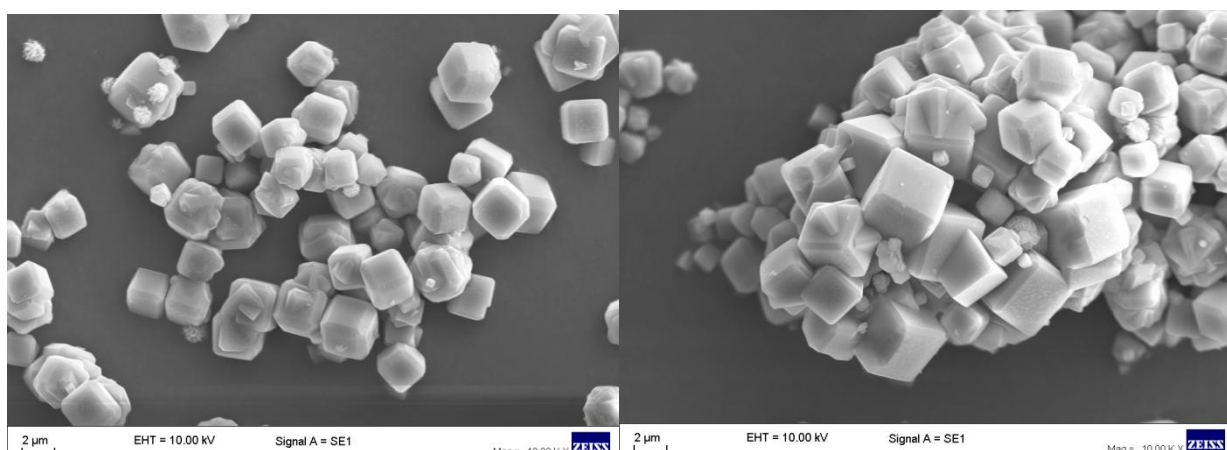


Figure 8.8: SEM microstructure showing the oriented cubic shaped crystals of zeolite A with rounded edges at a magnification of x 10000.

The results from the SEM micrographs show that most of the kaolinite transformation phases which were obtained by hydrothermal fusion. The SEM micrographs clearly show poorly formed crystal of metakaolinite and very well developed cubic shaped crystals of zeolite A. Figures (8.5, 8.6, 8.7 and 8.8) show the typical cubic shaped crystals of zeolite A. Once optimised the conditions resulted in the synthesis of zeolite A with high crystallinity (about 90%). The crystals were cubic.

8.3.2. Energy Dispersive Spectroscopy (EDS)

The Energy Dispersive Spectroscopy (EDS) analytical technique was used in this study for the elemental composition or chemical characterisation of the kaolinite and zeolite A samples. The main elements and their corresponding oxides were determined by EDS. The localisation of four analysed sites designated by numbers and a typical EDS curve are shown in appendix A.

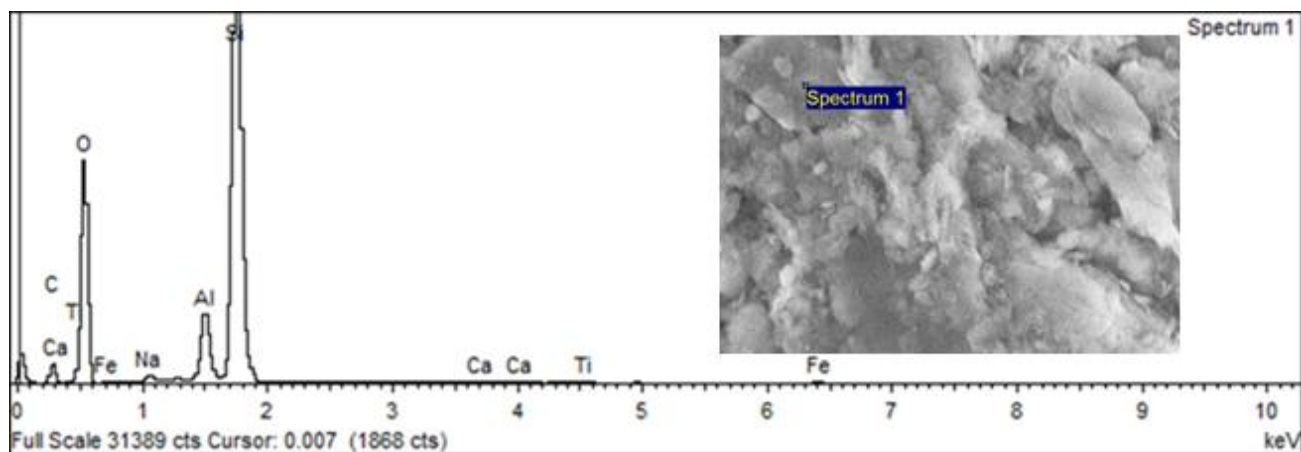


Figure 8.9: EDS analysis showing the elemental composition and the scanned image for kaolinite.

The results of the EDS analysis show that the predominant exchangeable cations in the kaolinite structure were Na^+ , Mg^{2+} , K^+ and Ca^{2+} .

Table 8.1: EDS analysis showing the elemental composition and the scanning method for the “as received” kaolinite.

Element	$\text{Na}_2\text{O}\%$	$\text{MgO}\%$	$\text{Al}_2\text{O}_3\%$	$\text{SiO}_2\%$	$\text{K}_2\text{O}\%$	$\text{CaO}\%$	$\text{TiO}_2\%$	$\text{Fe}_2\text{O}_3\%$
wt.%	1.64	0.23	13.49	15.72	0.22	0.76	0.70	1.04

8.3.3. X-ray diffraction (XRD)

X-ray diffraction (XRD) is an analytical technique used for phase identification of natural kaolinite materials. Figure 8.10 shows the XRD pattern of raw kaolinite. The raw kaolinite contained quartz as a major impurity. Kaolinite can be identified by its characteristic XRD peaks. It has highest peaks at 2θ value of 12.23° and 24.82° , which are the characteristic peaks of kaolinite as reported by Zhao *et al.* (2004) and Gougazeh and Buhl (2010). However, kaolinite contains the minor impurities illite, muscovite and halloysite.

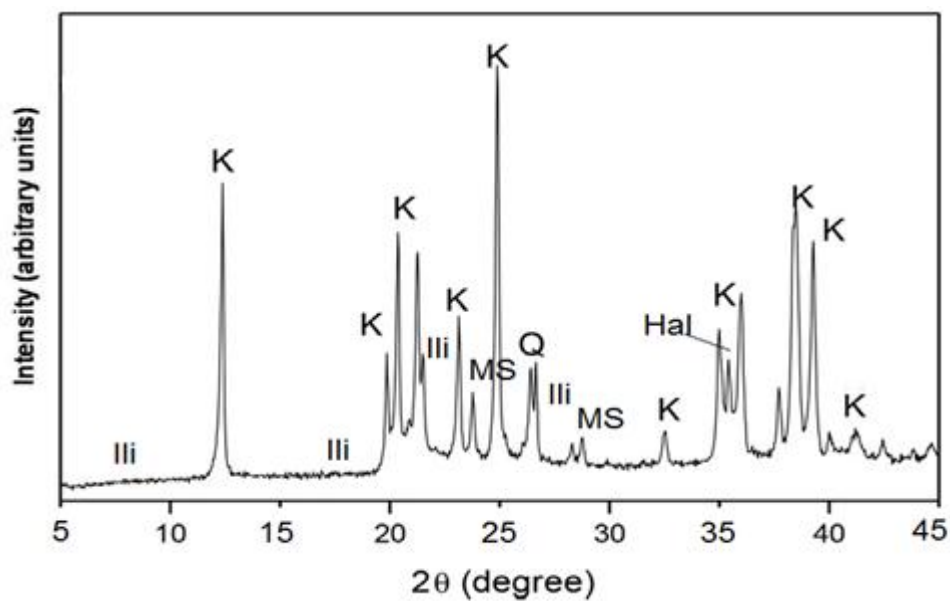


Figure 8.10: Shows the XRD pattern of kaolinite. Kaolinite (K); illite(Illi); muscovite(Ms); quartz(Q); halloysite (Hal).

Figure 8.11 shows a variety of XRD patterns of the kaolinite transformation phases at different temperatures including untreated “as received” and thermally treated kaolinite materials at 600, 950 and 1000 °C. The XRD patterns show the significant change in comparison to the untreated kaolinite sample, which was characterised by the disappearance of the diffraction peaks of kaolinite, with the appearance of amorphous aluminosilicate patterns (Gougazeh and Buhl 2014). Metakaolinite is an amorphous material and the highest diffraction peaks correspond to the presence of quartz (SiO_2), which is the crystalline phase, in metakaolinite (Gougazeh and Buhl 2014).

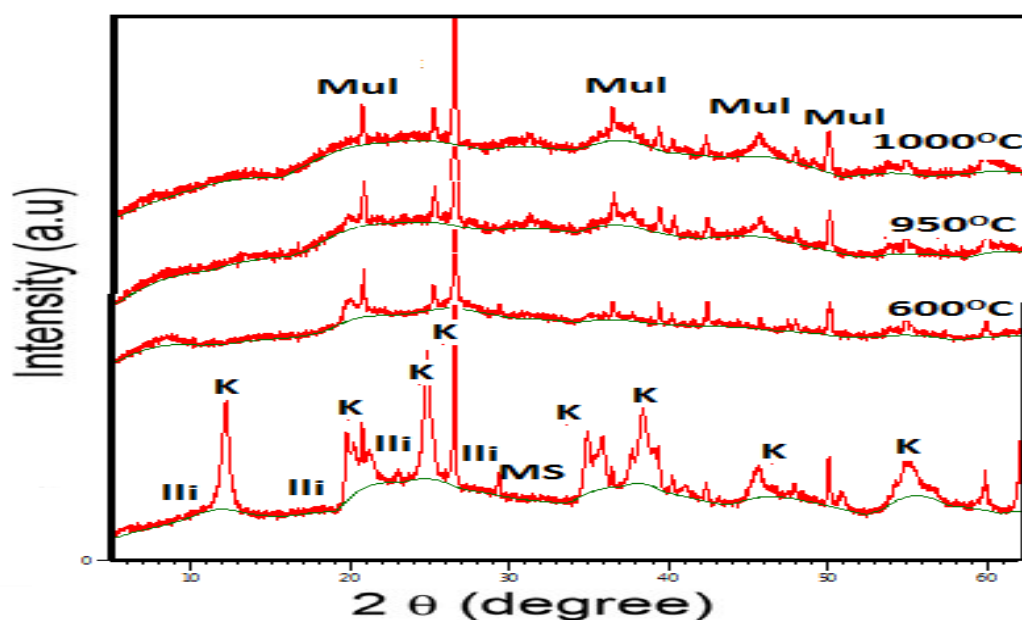


Figure 8.11: XRD patterns of uncalcined and calcined kaolinite at different temperatures. Ili (illite), K (kaolinite), Ms (muscovite), Mul (mullite).

The XRD pattern from zeolite type A, prepared by the conventional hydrothermal synthesis method is more pure (figure 8.12) than alkaline fusion prior to the hydrothermal synthesis method (figure 8.13). The results show that the synthetic zeolites contained major quantities of zeolite A.

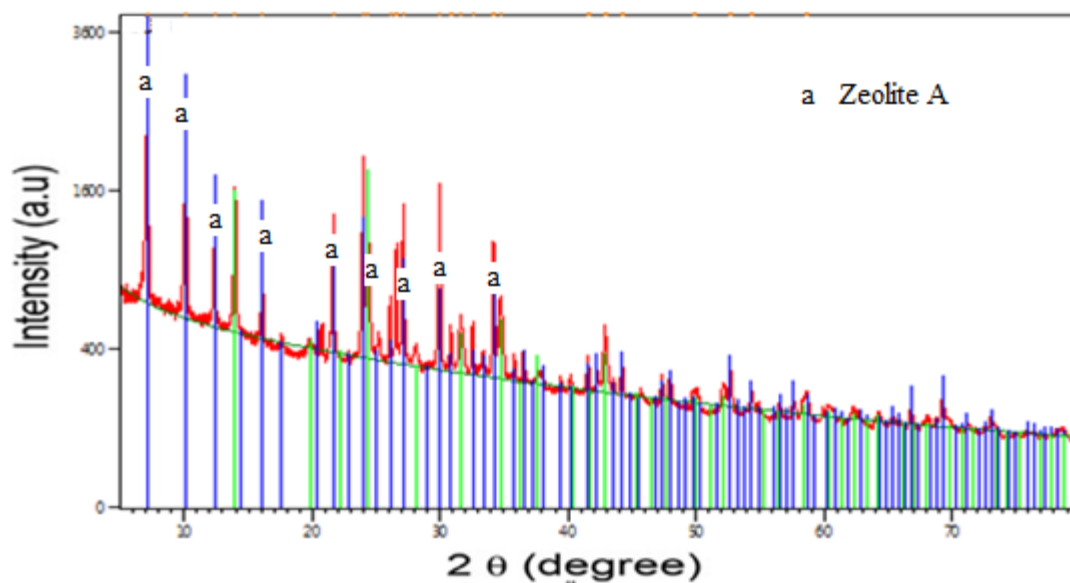


Figure 8.12: XRD analysis showing the mineralogical analysis of zeolite A (conventional hydrothermal synthesis).

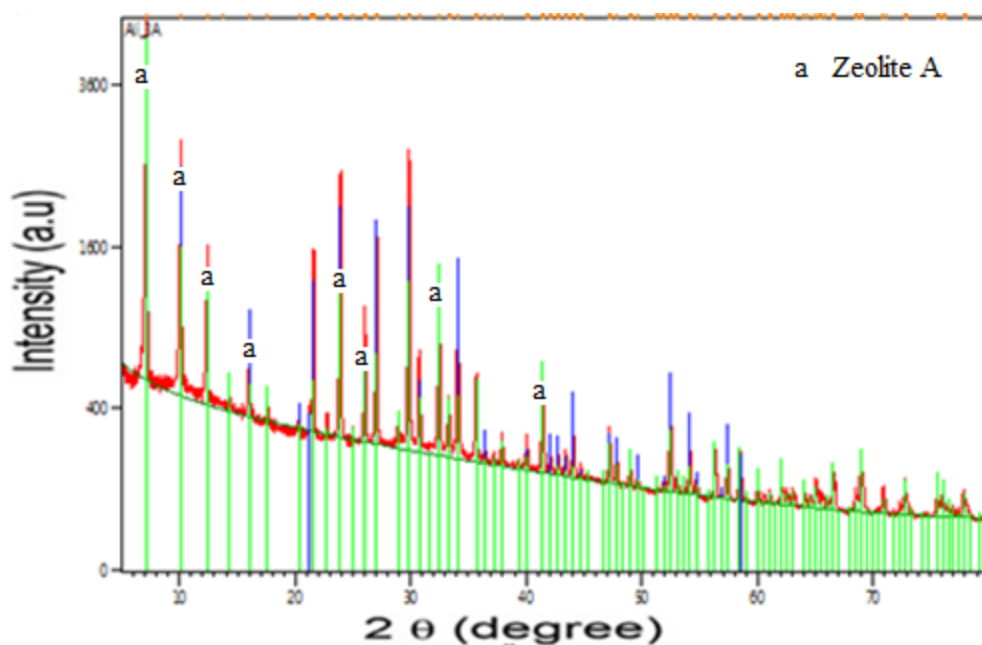


Figure 8.13: XRD analysis showing the mineralogical analysis XRD of zeolite A (alkaline fusion prior to hydrothermal synthesis).

8.3.4. X – Ray Fluorescence (XRF)

The elemental composition analysis of the raw kaolinite and prepared zeolite was obtained using XRF. The chemical analysis of the Iraqi kaolinite in the “as-received” form was determined. The main chemical composition of kaolinite and the existence of SiO_2 and Al_2O_3 in the raw kaolinite as an aluminosilicate source used in this study are presented in table 8.2.

Table 8.2: The chemical composition (wt.%) of the Iraqi kaolinite used in the preparation of zeolite type A.

Element	$\text{Na}_2\text{O}\%$	$\text{MgO}\%$	$\text{Al}_2\text{O}_3\%$	$\text{SiO}_2\%$	$\text{K}_2\text{O}\%$	$\text{CaO}\%$	$\text{TiO}_2\%$	$\text{Fe}_2\text{O}_3\%$
wt.%	1.74	0.21	30.17	39.37	0.48	0.89	0.78	1.49

The result of the chemical analysis of zeolite type A that was obtained after the conversion of the raw materials into zeolitic materials is presented below. Table 8.3 shows the chemical analysis of zeolite A synthesised by conventional hydrothermal transformation. The chemical analysis of zeolite A synthesised by alkaline fusion prior to the hydrothermal synthesis route is presented in table 8.4. The results indicate that the major components of zeolite are present

in the structure, in addition to trace amounts of impurities associated with the raw kaolinite used in the preparation, which could not be removed with the preparation procedure used. The predominant exchangeable cations for zeolite A were found to be Na^+ , K^+ , Mg^{2+} and Ca^{2+} . Previous studies show that the chemical analysis values for zeolite A were Al_2O_3 and SiO_2 were around 32% and 50% (Al-Dwairi, 2009; Ayele et al., 2015; Ibrahim et al., 2010).

Table 8.3: The chemical composition (wt.%) of zeolite A using the conventional hydrothermal synthesis route.

Element	$\text{Na}_2\text{O}\%$	$\text{MgO}\%$	$\text{Al}_2\text{O}_3\%$	$\text{SiO}_2\%$	$\text{K}_2\text{O}\%$	$\text{CaO}\%$	$\text{TiO}_2\%$	$\text{Fe}_2\text{O}_3\%$
wt. %	4.744	0.114	16.47	23.95	0.179	0.69	0.66	1.26

Table 8.4 : The chemical composition (wt.%) of zeolite A using alkaline fusion prior to the hydrothermal synthesis route.

Element	$\text{Na}_2\text{O}\%$	$\text{MgO}\%$	$\text{Al}_2\text{O}_3\%$	$\text{SiO}_2\%$	$\text{K}_2\text{O}\%$	$\text{CaO}\%$	$\text{TiO}_2\%$	$\text{Fe}_2\text{O}_3\%$
wt. %	4.877	0.114	14.465	20.731	0.105	0.872	0.67	1.38

8.3.5. Thermogravimetric analysis (TGA)

The thermal stabilities of the starting kaolinite and metakaolinite were obtained using thermogravimetric analysis (TGA). Thermal analysis methods were used to explore information about the mass loss change and adsorption or crystallization. The transition of kaolinite to metakaolinite was observed near 570 °C. The results describe the regular mass loss change and structural transformations of kaolinite, and indicate the main changes pointed out by DTA/ TGA during the heating of the Iraqi kaolinite sample from 30-1000°C. In the first stage, when the kaolinite was heated, the dehydration process took place. The adsorbed water was liberated below 400°C and the weakest part of the chemical bond was broken or perturbed. Then dehydroxylation took place in the range 450– 600 °C. At this stage of the transformation, the kaolinite was transformed to the metakaolinite phase with the loss of structural hydroxyl groups.

At a temperature of 925-950°C a progressive decomposition of metakaolinite occurs (metakaolinite converts to spinel). The DTG curve of the kaolinite sample (Figure 8.14) shows a peak at 570 °C due to dehydroxylation and at 980°C due to the formation of a new solid phase. The total loss calculated from the thermogravimetric analysis was 23.5%.

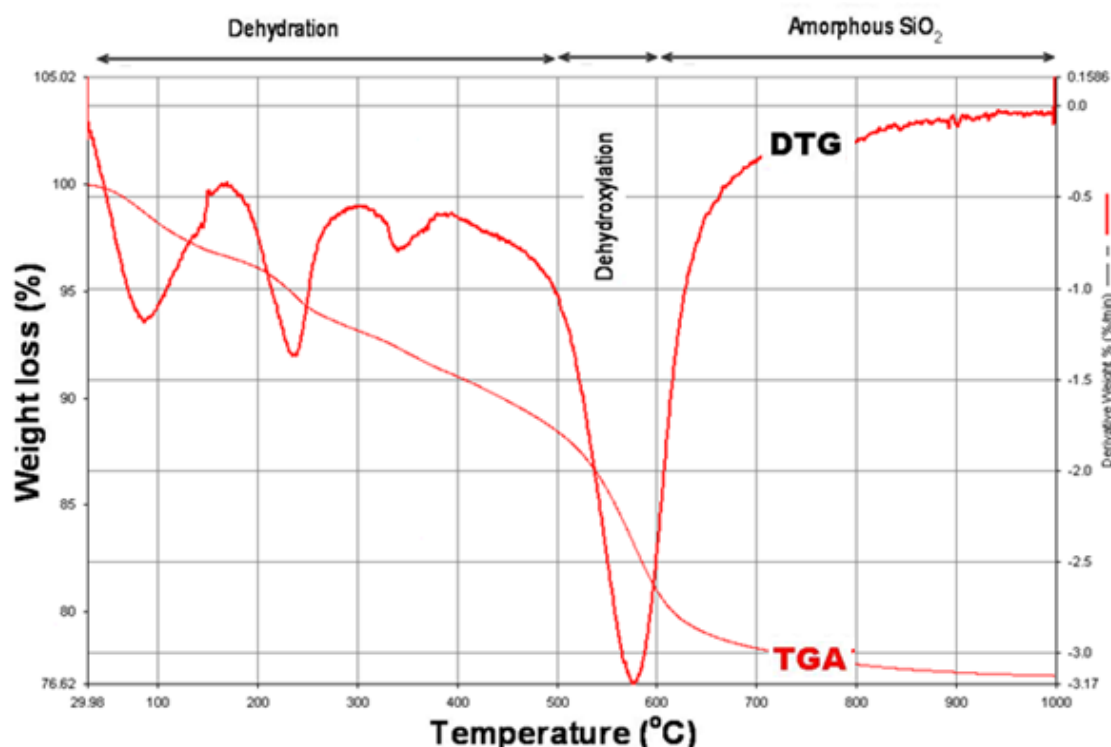


Figure 8.14: Thermogravimetric analysis (TGA/DTG) of Iraqi kaolin showing curves between 30-1000°C.

The results from the TGA/DTG show that the zeolite type A sample underwent continuous weight loss while it was heated to 900 °C. The main reason for this loss in weight appears to be dehydration and dehydroxylation (Figure 8.15 and 8.16). The DTG curve shows a peak at 170°C. According to Perraki and Orfanoudaki (2004), weight losses at below 200 °C are due to hygroscopic water and loosely bonded water, respectively. Figure 8.16 shows a peak at 160°C due to dehydration. There are another two endothermic peaks, at 530 °C due to dehydroxylation and at 850°C due to the formation of a new solid phase. The hydration point of zeolite A was higher than that of natural zeolite.

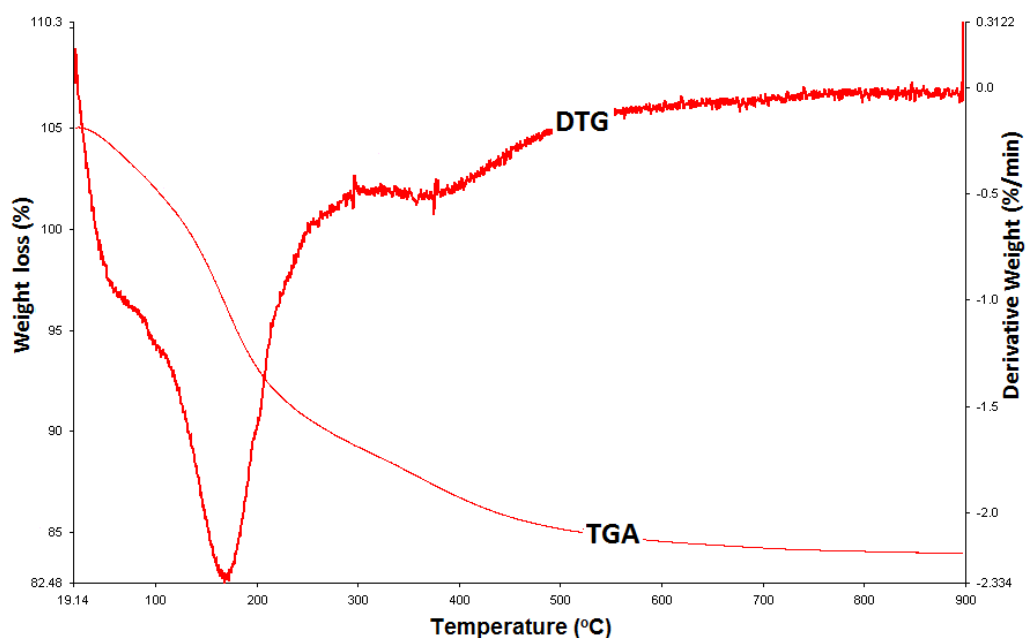


Figure 8.15: Thermogravimetric analysis (TGA/DTG) of zeolite A prepared by conventional hydrothermal synthesis routes, showing curves between 20-900°C.

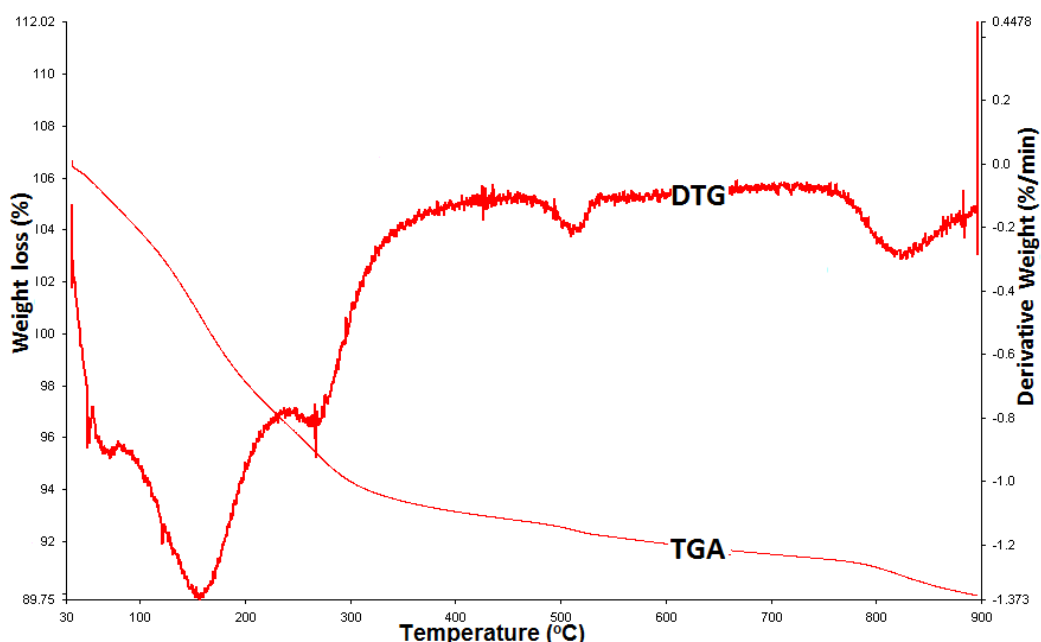


Figure 8.16: Thermogravimetric analysis (TGA/DTG) of zeolite A prepared by alkaline fusion prior to hydrothermal synthesis routes, showing curves between 30-900°C.

8.3.6. Fourier Transform Infrared (FT-IR) Spectroscopy

FT-IR spectra of the raw materials were recorded in the range 4000-400 cm^{-1} . FT-IR spectra of the original and thermally treated kaolinite were investigated at 600, 950 and 1000 $^{\circ}\text{C}$. Figure (8.17) shows the FT-IR spectra analysis of the as received kaolinite before calcination. The 3692 and 3620 cm^{-1} peaks can be attributed to the stretching vibration of the hydroxyl groups in the kaolinite structure (Saikia *et al.*, 2003; Alkan *et al.*, 2005; Liu *et al.*, 2001). The 3620 cm^{-1} peaks were assigned to the stretching vibration modes of the inner-hydroxyl groups, which can be referred to OH groups located in the octahedral and tetrahedral sheets. The band at 3692 cm^{-1} corresponds to the stretching vibration modes of the inner-surface OH groups, which are positioned at the surface of the octahedral sheets of the adjacent kaolinite layer (Kristof *et al.*, 1993).

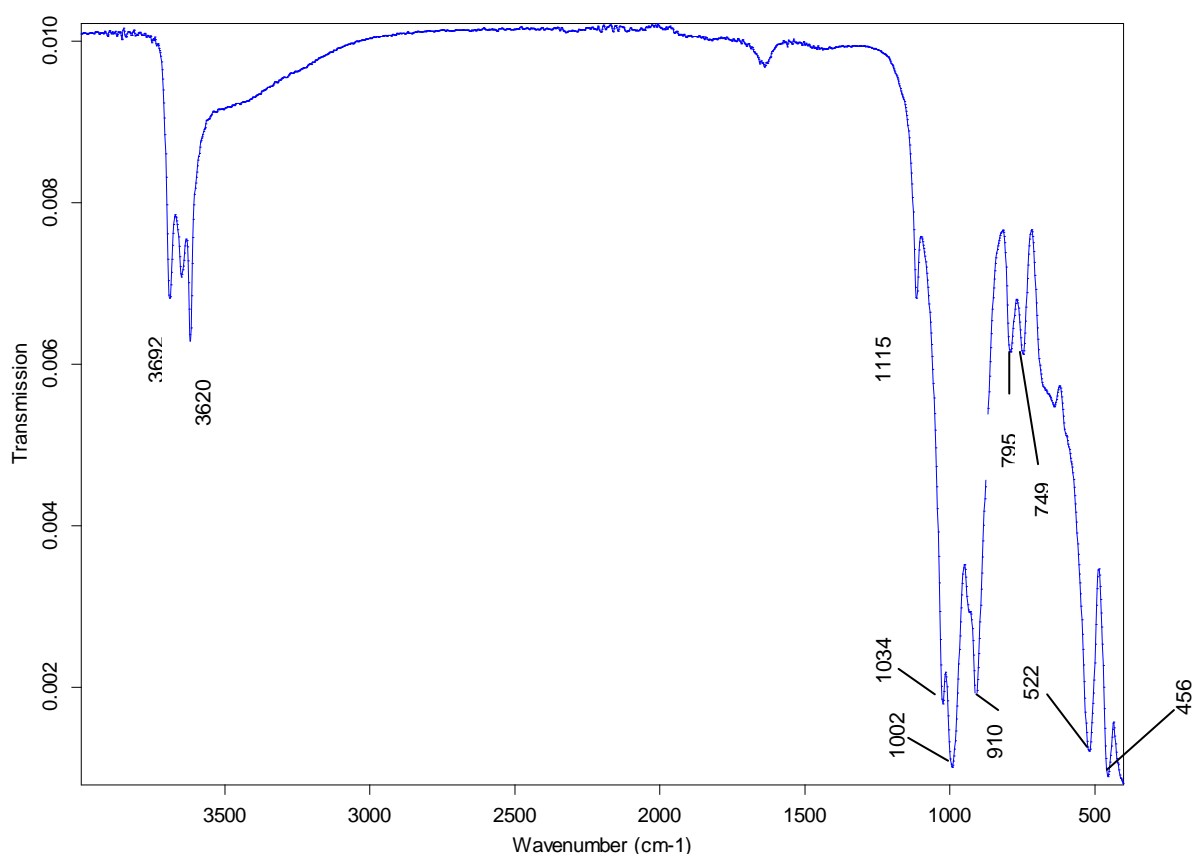


Figure 8.17: Shows the FT-IR spectra analysis of the as received kaolinite before calcination.

The 1115 cm^{-1} peak can be referred to the stretching vibration of Si-O in the kaolinite structure, while the peaks at 1034 cm^{-1} and 1002 cm^{-1} are caused by lattice vibrations of both Si-O-Si and Si-O-Al (van der Marel and Beutelspacher, 1976). Frost *et al.* (2002) assigned the bending vibrations of OH at 910 cm^{-1} and 942 cm^{-1} to the ‘surface OH bends’ and ‘inner

OH bends'. According to Marel and Beutelspacher (1976), these bending vibrations of OH are mainly caused by Al-OH groups. The peaks at 795 cm^{-1} and 749 cm^{-1} were assigned to Si-O and Al-O vibrations and finally, the 456 cm^{-1} and 522 cm^{-1} peaks were assigned to the deformation vibration of $\text{Al}(\text{O},\text{OH})_6$ octahedra.

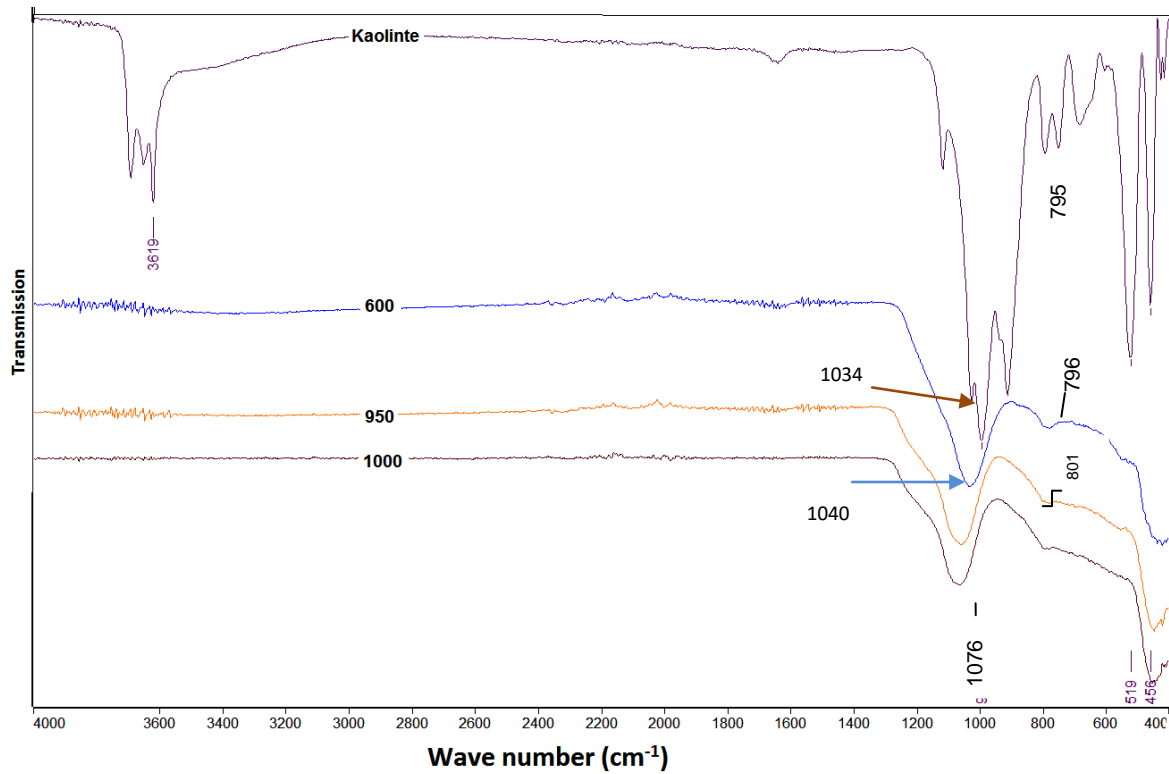


Figure 8.18: FT-IR spectra of kaolinite and metakaolinite obtained after calcination of kaolinite at 600, 950 and 1000 °C.

Figure 8.18 shows the transformation process of kaolinite into metakaolinite. The conversion of kaolinite to metakaolinite is revealed by the disappearance of these characteristic bands. A significant shift of the Si-O vibration bands at 1034 in kaolinite to a higher frequency band at 1040 cm^{-1} and 1076 cm^{-1} in metakaolinite was observed, which has been assigned to amorphous SiO_2 . The band of metakaolinite, located at 796 cm^{-1} and 801 cm^{-1} , which is splitting from 795 cm^{-1} band, can be attributed to the formation of mullite from Al-Si-spinel. (Lambert *et al.*, 1989). The vibration band at 1076 cm^{-1} for metakaolinite was assigned to the stretching Si-O-Si bonds, as reported by Sinha *et al.* (1995), Valcke *et al.* (1997) and Qiu *et al.* (2004). These bands proved the conversion of kaolinite to the metakaolinite phase, which was obtained from the calcined kaolinite. These FT-IR results are in good agreement with those obtained from the XRD data.

8.4. The synthesis of zeolite A from kaolinite materials

The synthesis of zeolite A from kaolinite involves two basic steps: metakaolinitization, which is the thermal treatment of the raw kaolinite at a high temperature to change the chemically stable kaolinite into a very reactive but amorphous material (metakaolinite). The second step is chemical treatment of the obtained metakaolinite with sodium hydroxide (Georgiev *et al.*, 2009). Metakaolinite with a Si/Al ratio of 1 is a convenient starting material for the synthesis of zeolite type A (Georgiev *et al.*, 2009). The metakaolinitization process is usually performed between 550 and 900°C (Hui, 2006), while in this study the metakaolinitization process was carried out at 600 °C.

8.4.1. Synthetic zeolite procedure

The kaolinite samples were dried and sieved and then ground as finely as possible (size of < 125 µm) using a mortar and pestle. The conversion of the raw materials into zeolitic materials was synthesised using conventional hydrothermal synthesis methods and alkaline fusion prior to hydrothermal synthesis methods. Both procedures were described in section 4.4.

FT-IR spectra of zeolite type A were recorded in the range 4000-400 cm⁻¹ (Figure 8.19). The 1034 cm⁻¹ band of metakaolinite (Figure 8.18) was shifted to 960 cm⁻¹ (Figure 8.19), which could be assigned to antisymmetric stretching of Si-O-Si or Si-O-Al bonds in aluminosilicates with a zeolite structure (Nesse, 2000). A band of weak intensity was observed around 549 cm⁻¹. It could represent the beginning of the crystallization of a zeolite with double rings (Alkan *et al.*, 2005). The bands at 456 cm⁻¹ correspond to the internal linkage vibrations of the Si-O-Si or Si-O-Al tetrahedral structure and to the asymmetric stretching, respectively, of zeolite A. The transformation of kaolinite to zeolite A can be clearly observed from FT-IR spectrum in the lattice region 960 - 456 cm⁻¹ (Figure 8.19). The kaolinite starting material gives well-defined FT-IR spectra bands in this region due to Si-O, Si-O-Al, and Al-OH vibrations.

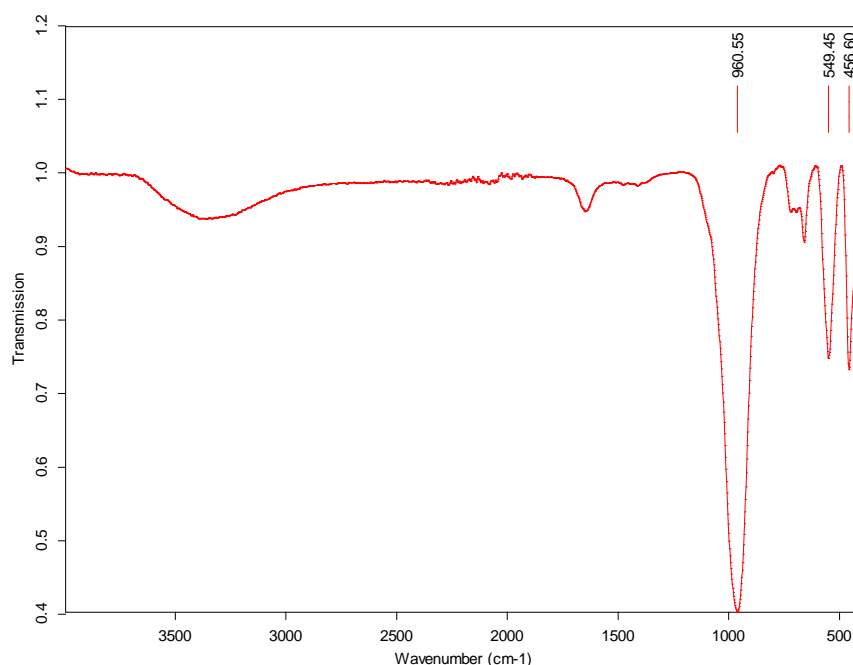


Figure 8.19: Show the FT-IR spectra of zeolite A obtained from kaolinite after treatment.

8.4.2. Synthetic zeolite experimental Procedure

Batch adsorption tests were carried out using 4g of synthetic zeolite type A which prepared via conventional hydrothermal synthesis method. The adsorbent was mixed with 100 ml of the appropriate multi-component solution for 360 minutes and samples were collected every hour and analysed. The mixtures were agitated in a 100 ml beaker using a stirrer at a speed of 150 rpm at room temperature. The particle size of the dry synthetic zeolite samples used was 75-150 μm . The pH was adjusted to 4 ± 0.1 .

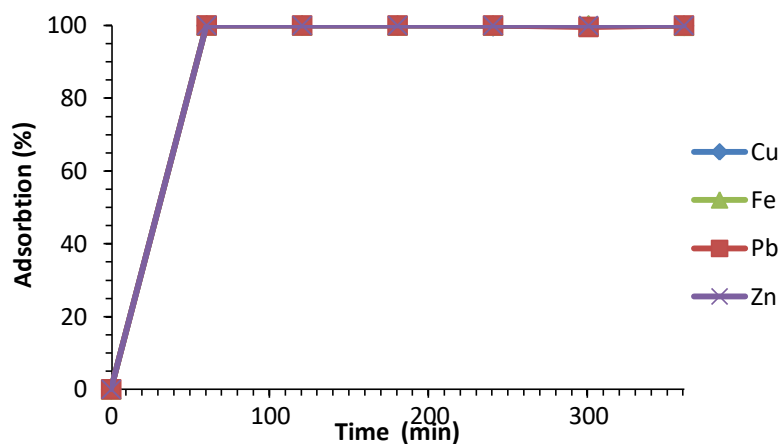


Figure 8.20: Shows the adsorption of copper, iron, lead and zinc from solution by zeolite A.

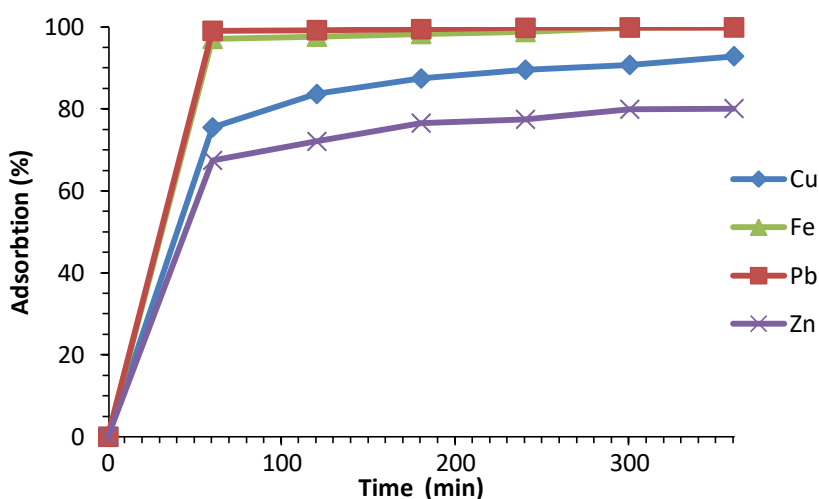


Figure 8.21: Shows the adsorption of copper, iron, lead and zinc from solution by natural zeolite.

Batch studies were used in order to investigate the behaviour of both natural zeolite and synthetic zeolite A and to understand the metal removal efficiency from solution. The results show that the uptake of heavy metal cations from solution using synthetic zeolite mostly occurs in the first hour and the highest removal ratio of Cu^{2+} , Fe^{3+} , Pb^{2+} and Zn^{2+} ions was achieved $> 99\%$ in the first hour (Figure 8.20). The percentage adsorbed value of heavy metal cations from solution using natural zeolite passed 90% in the first hour (Figure 8.21). Hence, the metal removal efficiency from solution of synthetic zeolite is higher than that of natural zeolite.

8.5 . Conclusions

The following observations could be made from the experimental results:

- The main aim of using kaolinite to produce zeolite type A is to provide a cheaper silica and alumina source material; in the meantime it can reduce material waste.
- The raw kaolinite contains quartz as a major impurity, which can be identified by its characteristic XRD peaks at 12.23° and at 24.82° , the characteristic peaks of kaolinite.
- The result of both the EDS and XRF analysis shows that SiO_2 , Al_2O_3 , Na_2O and K_2O were the main components of kaolinite and zeolite A. The analysis also shows that the predominant exchangeable cations in the kaolinite and zeolite A structure were found to be Na^+ , Mg^{2+} , K^+ and Ca^{2+} .
- The result of XRD analysis show that the synthetic zeolites contained major quantities of zeolite A.
- The DTG curve of the kaolinite sample shows a strong peak at 570°C due to dehydroxylation (formation of metakaolinite) and at 980°C due to the formation of a new solid phase. Dehydroxylation of kaolinite results in a mass loss of 23.5%.
- The findings from the FT-IR spectra as well as the DTA/TGA measurements showed that metakaolinite phase was obtained by heating the kaolinite at 600°C for 3 h.
- From the physicochemical characterisation results, it can be generally considered that the raw materials used in this study have properties suitable for zeolite synthesis and could be, in principle, a useful source of silica and alumina.
- Finally, considering new applications for these raw materials, zeolite A could be used as a good adsorbent material for the uptake of heavy metal cations from wastewater.

CHAPTER 9

9. GENERAL CONCLUSIONS AND RECOMMENDATION FOR FUTURE WORK

In this chapter the specific aims of this study are reviewed to present an overview of the conclusions of the study and to make a critical evaluation. In this study, the potential of natural zeolite as a low cost adsorbent material was assessed for the removal of copper, iron, zinc and lead from synthetic industrial waste metal solutions. In order to determine this potential a number of experiments were carried out such as the characterisation of zeolites, as well as equilibrium, and kinetic experiments.

This study also involved the development of synthetic zeolite from Iraqi kaolinite as a source of production for these important industrial materials. The application of zeolites and synthetic zeolite, especially in the areas of ion exchange, is well known; hence the use of local raw materials such as Iraqi kaolinite is meant to offer an alternative and cheaper means of producing this unique and functional material. A summary of the experimental results will be presented in this chapter.

9.1. Critical overview

9.1.1. Characterisation of natural zeolite

- The results from the SEM micrographs indicated that the natural zeolite samples used had a heterogeneous and porous structure, with defined clinoptilolite crystals. The SEM micrographs obtained from the chemically treated natural zeolite revealed that the NaCl acidic solution removed all of the undesired volatile matter and obtained a clean surface. The micrographs of the thermally treated natural zeolite showed that the natural zeolite crystals were affected. With an increase in thermal temperature there was a loss of porosity, while the natural zeolite exposed to extreme temperatures lost most of its porosity with amorphous crystals.

- The results of the EDS analysis show that SiO_2 , Al_2O_3 , Na_2O and K_2O were the main components of the natural zeolite, while the predominant exchangeable cations in the natural zeolite structure were Na^+ , Mg^{2+} , K^+ and Ca^{2+} .
- The X-ray diffraction (XRD) analytical technique was used for phase identification of the natural zeolite samples and characterization of the crystalline materials. The XRD results illustrated that the natural zeolite samples mainly contained clinoptilolite.
- The XRF analytical technique was used for chemical analysis of the natural zeolite to determine the chemical composition of the samples. The XRF results illustrated that the zeolite samples mainly contained Na^+ , K^+ , Mg^{2+} and Ca^{2+} exchangeable cations, and this concurs with the results obtained from the EDS analysis.
- The thermal stability of the natural zeolite was studied using TGA. The results of the TGA/DTG show that the clinoptilolite samples continually lost weight after being heated up to 1000 °C. This is due to dehydration and dehydroxylation processes.

9.1.2. Equilibrium studies

- The results from the equilibrium studies positively demonstrated that natural zeolite can be used as an excellent adsorbent for removing heavy metals from multi-component solutions. The results showed that the maximum removal capacities Q of natural zeolite were 22.83, 14.92, 14.49 and 17.54 mg/g for copper, iron, zinc, and lead respectively. In the meantime the results indicated that with an increase in initial solution pH the adsorption capacity was increased.
- Both the Langmuir and Freundlich isotherm models were used to characterize the experimental data and to assess the adsorption behaviour of natural zeolite for copper, iron, lead and zinc. The experimental data were slightly better suited to the Langmuir isotherm than the Freundlich isotherm. The value of the correlation coefficients r^2 ranged from 0.93 to 0.99 for the Langmuir isotherm and from 0.90 to 0.99 for the Freundlich isotherm.
- Natural zeolite has the ability to be regenerated and re-used for subsequent runs before it

begins to lose its capacity. The results obtained show that natural zeolite can be regenerated and reused with a small change in its adsorption efficiency after regeneration. That makes the processes more economical and reduces the amount of waste material.

- Finally, the results established from the equilibrium studies show that according to the Langmuir isotherm the selectivity series of natural zeolite for the adsorption of copper, iron, lead and zinc from solution was found to vary when the solution pH changed.

9.1.3. Kinetic studies

- The kinetic study indicated the suitability of the natural zeolites used for the removal of Cu^{2+} , Fe^{3+} , Pb^{2+} and Zn^{2+} ions from synthetic wastewater. Zeolite material was selected as a useful adsorbent while considering the economic aspects of wastewater treatment.
- The adsorbent mass, adsorbent particle size, initial solution pH, initial solution concentration and agitation speed as well as pretreatment or modification of the adsorbent in the case of batch experiments were found to influence the efficiency of natural zeolite in the removal of heavy metals from the industrial wastewater.
- The results from the kinetic study indicated that the heavy metal removal capacity increased with an increase in initial solution pH, an increase in agitation speed, an increase in solution concentration and a greater mass of adsorbent as well as the application of a pre-treatment.
- The results indicate that the adsorption of Cu^{2+} , Fe^{3+} , Pb^{2+} and Zn^{2+} ions on the selected adsorbents involves a complex mechanism and a number of possible rate controlling steps can determine the process efficiency such as boundary layer diffusion due to external mass transfer effects (external solution phase surrounding the particle), intraparticle diffusion within the exchanger itself, and chemical reaction kinetic control.
- In general, the results show that the highest rate of Cu^{2+} , Fe^{3+} , Pb^{2+} and Zn^{2+} ion adsorption took place in the first hours followed by a slower adsorption rate later on.

9.1.4. Characterisation of synthetic zeolite

- Another objective of this study has largely been achieved. The conversion of the raw materials into zeolitic materials was carried out using two methods: first conventional hydrothermal synthesis and second alkaline fusion prior to hydrothermal synthesis. The results from both routes show that zeolite A was synthesised successfully.
- The SEM micrographs revealed that the kaolinite samples used in this study show the morphology of crystals of kaolinite that are not well defined. The micrograph also displays the randomly oriented crystallites and in particular indicates the crystalline nature of the kaolinite before any modification.
- The SEM micrographs of the metakaolinite samples studied show the randomly oriented crystallites and in particular indicate the appearance of the crystalline nature of the metakaolinite.
- The SEM micrographs of zeolite A reveal the typical cubic shaped crystals. This can be optimised so the conditions resulted in the synthesis of zeolite A with good crystallinity of about 90% cubic crystal structures. The particles obtained were well-developed and had a mainly cubic monocrystallite framework shape.
- The results of the EDS analysis show that the predominant exchangeable cations in the raw materials structure were Na^+ , Mg^{2+} , K^+ and Ca^{2+} .
- The XRD results show that the raw kaolinite contained quartz as a major impurity; it had a layered structure at 12.23° and at 24.82° 2θ , which are the characteristic peaks of kaolinite. In the meantime the synthesized zeolite samples mainly contained zeolite A.
- The XRF analytical technique was used for the chemical analysis of the raw materials and zeolite A samples. The predominant exchangeable cations for both the raw materials and zeolite A samples were found to be Na^+ , Mg^{2+} , K^+ and Ca^{2+} , and this concurs with the results obtained from the EDS analysis.

- The thermal stability of the raw materials and zeolite A samples was obtained using TGA/DTA analysis. The DTA curve of the kaolinite sample shows a peak at 570°C due to dehydroxylation (formation of metakaolinite) and at 980°C due to the formation of a new solid phase. Dehydroxylation of kaolinite results in a mass loss of 23.6%.
- The DTG curve of the zeolite A samples shows a peak at 170°C due to the loss of molecular water. The DTG curve also shows a strong endothermic peak at 530 °C due to dehydroxylation and at 700-850°C due to the formation of a new solid phase.
- The findings from the FT-IR spectra as well as the DTA/TGA measurements show that the metakaolinite phase was obtained by heating the kaolinite at 600 °C for 3 h.
- The results confirm the findings observed in the characterization analysis in terms of the successful zeolitization of the starting materials and effectively prove one of the major theories of this research, that zeolites have advantages over other ion exchangers, based on their low- cost, as well as their ion selectivity, generated by their rigid porous structures.
- In the second method an alkaline fusion step was introduced prior to the hydrothermal treatment, because it plays an important role in enhancing the hydrothermal conditions for zeolite synthesis. On the other hand, this approach was adopted in this study because larger amounts of aluminosilicates can be dissolved by employing this method.
- Finally, the experiments show that both natural and synthetic zeolites can be available in commercial quantities. However, synthetic zeolites are more attractive for some specific applications, while the cheapness of a natural zeolite may favour its use (Sherman, 1999). This is why this research concentrated on using cheap and available materials such as kaolinite for zeolite synthesis, which can promote green technologies and reduce the operating costs and energy requirements and reduce the amount of the waste material. That makes the processes more economical and decreases the environmental impacts.

9.2 . Future work and recommendation

The experiments presented in this thesis have shown that both natural zeolite and synthetic zeolite have the potential for use in treating wastewater. Although, the initial objectives were achieved in this study, there are some other aspects that were not within the scope of this study due to the limitations of time and availability of equipment. Therefore, further research and studies are needed, taking into account that modern industrial technologies require the use of zeolitic materials and sorbents with very precisely specified parameters. There are several areas of research that could give better perspectives in terms of possible applications. Some recommendations for further studies are presented below:

- As a part of the kinetic study, the adsorbent mass, adsorbent particle size, initial solution pH, initial solution concentration and agitation speed as well as pre-treatment or modification of the adsorbent in the case of batch experiments was studied while the effect of temperature on heavy metal removal capacity was not included. However, for applied purposes on a large scale, the actual impact of all of these factors needs to be covered since they act simultaneously in solution and obviously have an effect on each other.
- Kinetic and equilibrium studies were performed throughout this study while in practice they are not economical and the data obtained from these are not sufficient to give accurate adsorptions that can be scaled up for industrial use. Therefore, as a further study, column studies could be realised to simulate full scale applications.
- Natural zeolite was chemically (using NaCl) and thermally treated in this study. However other modifications of zeolite with solutions of H_2SO_4 , HCl, NaNO_3 , NH_4Cl , HNO_3 , CaCl_2 , and NaOH can be used to increase the capacity and efficiency of natural zeolite in treating industrial wastewaters. This could be a potential area of further study.
- The determination of the best regenerating solution is very important. Hence, as a further study, the effectiveness of other regenerating solutions such as H_2SO_4 , HCl, NaNO_3 , NH_4Cl , HNO_3 , CaCl_2 , and NaOH could be investigated at various solution concentrations and temperatures.

- In this study equilibrium studies were carried out using synthetic industrial wastewaters that contained Cu^{2+} , Fe^{3+} , Pb^{2+} and Zn^{2+} only. In practice, industrial wastewater may contain a mixture of different cations in various concentrations; taking this point into account is important in order to get a clear picture of the maximum adsorption capacity of natural zeolite when treating industrial wastewaters.
- This study has only focused on the removal of cations and did not investigate the effect of anions on the capacity and effectiveness of natural zeolite. Industrial wastewaters contain both metal cations and anions such as sulfate (SO_4^{2-}), phosphoric acid (H_2PO_4^-), chloride (Cl^-) and nitrate (NO_3^-). To remove anions from the water Zeolite surface has to be modified with a solution of inorganic salts (for example FeCl_3). Further studies could be carried out to determine whether zeolite can remove anions from solution and how the anions affect the heavy metal uptake capacity and efficiency of natural zeolite in treating industrial wastewaters.
- While zeolite A was successfully synthesised from the kaolinite, the process of producing synthetic zeolite should pay attention to a wide range of experimental parameters and conditions such as the effect of crystallization time, the effect of alkalinity (NaOH), the effect of gel temperature and the gel formation condition, the solid/solution ratio and the effect of aging time, which may influence the production process and need to be investigated in detail.
- In this study the regeneration of natural zeolite was investigated and the results show that natural zeolite can be reused for a number of cycles before the structures are exhausted. In future work the possible regeneration of synthetic zeolite and reducing the disposal of zeolitic materials can be considered to make the processes more economical and feasible.
- In this study the equilibrium studies focused on the Langmuir and Freundlich isotherms models only, while other isotherms models were not investigated. There are other isotherm models available that could be used to describe the equilibrium sorption such as: the Sips, Temkin, Toth, Redlich-Peterson and Dubinin-Kaganer-Radushkevich (DKR) isotherms. These isotherms models are more general and do not presume a homogeneous surface or stable sorption potential.

- The most interesting thing about zeolites is the composition pattern of their crystal structure, which means they can be used as molecular sieves. But in the meantime, the sorption processes of zeolite particles are very different and complex because of their unique porous structures, mineralogical heterogeneity, outer and inner charged surfaces, broken bonds and the existence of crystal edges as well as the other imperfections on the surface. Therefore, more research needs to be done on clinoptilolite and its behaviour in regard to heavy metals removal.
- In this study only the clinoptelolite was investigated supplied from USA. Future work could be expanded to include comparison with clinoptelolite from other geographical regions. Also, could include experiments at neutral pH. Also include structural studies to investigate changes in crystallinity and lattice parameters during pre-treatment, exchange and regeneration. This would be important to see in the zeolite degraded. It would also help determine the nature of the uptake of ions (adsorption vs ion-exchange). Surface area measurements would also help determine if the process was ion-exchange or surface adsorption.
- Finally, a wide range of successful environmental applications of zeolite materials are available. On this basis a variety of contaminated soil, polluted air and wastewater treatment technologies could be developed. The improvement of the long-term chemical and physical stability of modified zeolitic materials and the combination of their sorption properties with contaminant destruction could also be the subject of further academic and industrial research.

BIBLIOGRAPHY

- Abusafa A., Yücel H. (2002) Removal of ^{137}Cs from aqueous solutions using different cationic forms of a natural zeolite: clinoptilolite. *Separation and Purification Technology*, **28**, pp.103 – 116.
- Ackley M.W., Rege S.U., Saxena H. (2003) Application of natural zeolites in the purification and separation of gases. *Microporous and Mesoporous Materials*, **61**, pp.25 – 42.
- Adamczyk, Z. and Bialecka, B. (2005) Hydrothermal synthesis of zeolites from polish coal fly ash. *Polish Journal of Environmental Studies*, **14**(6), pp. 713–719.
- Ahmaruzzaman, M.D. (2008) Adsorption of phenolic compounds on low-cost adsorbents: A review. *Colloid and Interface Science*, **143**, pp.48–67.
- Akdeniz, Y., and Ulku, S. (2007) Microwave effect on ion-exchange and structure of clinoptilolite. *Journal of Porous Materials*, **14**(1), pp.55-60.
- Akgu, M., Karabakan, A., Acar, O. and Yurum, Y. (2006) Removal of silver (I) from aqueous solutions with clinoptilolite. *Microporous and Mesoporous Materials*, **94**, pp. 99–104.
- Al-Dwairi, R.A. (2009) The Use of Expendable Local Zeolite Deposits for NH_4 Removal in Municipal Wastewater. *Jordan Journal of Civil Engineering*, **3**(3), pp. 256 -263.
- Alkan, M., Hopa, C., Yilmaz, Z. and Guler, H. (2005) The effect of alkali concentration and solid/liquid ratio on the hydrothermal synthesis of zeolite NaA from natural kaolinite. *Microporous and Mesoporous Materials*, **86**, pp.176-184.
- Almaraz, V., Trocellier, P., Da´vila and Rangel, I. (2003) Adsorption of aqueous Zn(II) species on synthetic zeolites. *Nuclear Instruments and Methods in Physics Research Section*, **210**, pp.424–8.
- Altin, O., Ozbelge, H.O., and Dogu, T. (1998) Use of general purpose adsorption isotherms for heavy metal-clay mineral interactions. *Journal of Colloid and Interface Science*, **198**, pp.130– 40.

Alvarez-Ayuso, E., Garcia-Sanchez, A., and Querol, X. (2003) Purification of metal electroplating waste waters using zeolites. *Water Research*, **37**, pp. 4855-4862.

Amarasinghe, B.M.W. and Williams, R.A. (2004) Tea waste as a low cost adsorbent for the removal of Cu and Pb from wastewater. *Chemical Engineering Journal*, **132**, pp.299 – 309.

Andras, P., Turisova, I. Marino A. and Buccheri G. (2012) Environmental hazards associated with heavy metals at Lubietová Cu-deposit (Slovakia) *Chemical Engineering Transactions*, **28**, pp.259 – 264.

Anne, M. H. (2014) *Molecular Sieve Definition - Definition of Molecular Sieve - What Is a Molecular Sieve?*". [Online].available at :< *Chemistry.about.com*>.

Argun, M.E. (2008) Use of clinoptilolite for the removal of nickel ions from water: Kinetics and thermodynamics. *Journal of Hazardous Materials*, **150**(3), pp. 587 – 595.

Armbruster, T. (2001) Clinoptilolite-heulandite:applications and basic research. *Studies in Surface Science and Catalysis*, **135**, pp.13-27.

Armbruster, T. and Gunter, M. E. (2001) Crystal structures of natural zeolites. In D.L. Bish and D.W. Ming (eds) Natural Zeolites: Occurrence, Properties, Applications. *Reviews in Mineralogical Society of America*, **45**, pp.1-68.

Ayele, L., Perez-Pariente, J., Chebude, Y. and Diaz, I.(2015) Synthesis of zeolite A from Ethiopian kaolin. *Microporous and Mesoporous Materials*. **215**, pp.29-36.

Axente D., Abrudean M., Bâldea A. (1983) Adsorption on romanian natural clinoptilolite. *Zeolites*, **3**(3), pp. 259 – 260.

Babel, S. and Kurniawan, T.A. (2003) Low-cost adsorbents for heavy metals uptake from contaminated water: a review. *Journal of Hazardous Materials*, **97**(1), pp.219 – 243.

Baccouche, A., Srasra, E. and Maaoui, M.E. (1998) Preparation of Na-P1 and sodalite octahydrate zeolites from interstratified illite-smectite. *Applied Clay Sciences*, **13**, pp.255-273.

Bailey, S.E., Olin, T.J., Bricka, R.M. and Adrian, D.D. (1999) A review of potentially low-cost sorbents for heavy metals. *Water Research*, **11**(33), pp. 2469 – 2479.

Balek, V. and Murat, M. (1996) The emanation thermal analysis of kaolinite clay minerals. *Thermochimica Acta*, **282**, pp. 385–397.

Bansal, R.C. and Goyal, M. (2005) Activated carbon adsorption, *CRC Press, Taylor & Francis Group*, pp.145-196. < <https://www.crcpress.com/Activated-Carbon-Adsorption/Bansal-Goyal/p/book/9780824753443>>.

Barrer, R. M. and Rev, Q. (1949) Molecular-sieve action of solids. *Journal of the American Chemical Society*, **3**, pp.293.

Barrer, R.M. (1982) *Hydrothermal chemistry of zeolite*. London: Academic Press INC.

Basaldella, E.I. and Tara, J.C. (1995) Synthesis of LSX zeolite in the Na/K system. Influence of the Na/K ratio. *Zeolites*, **11**, pp. 243-248.

Basaldella, E.I., Boneno, R.D. and Tara, J.C. (1993) Synthesis of NaY zeolite on preformed kaolinite spheres. Evolution of zeolite content and textural properties with the reaction time. *Industrial and Engineering Chemistry Research*, **32**, pp. 751-757.

Basaldella, E.I., Kikot, A. and Tara, J.C. (1995) Effect of pellet pore size and synthesis conditions in the in situ synthesis of LSX zeolite. *Industrial and Engineering Chemistry Research*, **34**, pp. 2990-2996.

Bauer, A. and Berger, G. (1998) Kaolinite and smectite dissolution rate in high molar KOH solutions at 35 ° and 80 °C. *Applied Geochemistry*, **13**, pp. 905-916.

Bekkum, H.V., Flanigen, E.M. and Jansen J.C. (2001) *Introduction to Zeolite Science and Practice. Studies in Surface Science and Catalysis*, **137** , Pages ix–x

Bektas, N. and Kara, S. (2004) Removal of lead from aqueous solutions by natural clinoptilolite: equilibrium and kinetic studies. *Separation and Purification Technology*, **39**, pp.189 – 200.

- Bellotto, M., Gualtieri, A., Artioli, G. and Clark, S.M. (1995) Kinetic study of the kaolinite-mullite reaction sequence. Part I: kaolinite dehydroxylation. *Physics and Chemistry of Minerals*, **22** (4), pp.207–214.
- Bish, D.L. and Ming, D.W. (2001) Applications of natural zeolites in water and wastewater treatment, Natural Zeolites: Occurrence, Properties, Applications. *Reviews in Mineralogy and Geochemistry*, **45**, pp.519-550.
- Blanchard, G., Maunaye, M. and Martin, G. (1984) Removal of heavy metals from waters by means of natural zeolites. *Water research*, **18**(12), pp. 1501 -1507.
- Boukadir, D., Bettahar N. and Derriche, Z. (2002) Synthesis of zeolites 4A and HS from natural materials. *Annales de Chimie - Science des Materiaux*. **27**,pp. 1-13.
- Breck, D.W. (1974) *Zeolite Molecular Sieves: Structure, Chemistry and Use*, 1st ed. John Wiley: New York.
- Brindley, G.W and Nakahira, M. (1959) The Kaolinite-Mullite Reaction Series: I, A Survey of Outstanding Problems. *Journal of the American Ceramic Society*, **42**, pp 311-314.
- Cabrera, C., Gabaldon, C. and Marzal, P. (2005) Sorption characteristics of heavy metal ions by a natural zeolite. *Journal of Chemical Technology and Biotechnology*, **80**, 477-481.
- Cama, J., Ayora, C., Querol, X. And Ganor, J. (2005) Dissolution kinetics of synthetic zeolite NaP1 and its implication to zeolite treatment of contaminated waters. *Environmental Science and Technology*, **39**(13), pp.4871-4877.
- Cañizares, P., Durán, A., Dorado, F. and Carmona, M. (2000) The role of sodium montmorillonite on bounded zeolite-type catalysts. *Applied Clay Science*, **16**, pp. 273–287.
- Chiang, A.S.T. and Chao, K. J. (2001) Membranes and films of zeolite and zeolite-like materials. *Journal of physics and chemistry of solids*, **62**, pp. 1899-1910.
- Cincotti, A., Mameli, A., Locci, M. A., Orru, R. and Cao, G. (2006) Heavy metal uptake by Sardinian natural zeolites: Experiment and modelling. *Industrial and Engineering Chemistry Research*. **45**, pp.1074-1084.

Cincotti A., Lai N., Orrù R., Cao G. (2001) Sardinian natural clinoptilolites for heavy metals and ammonium removal: experimental and modeling. *Chemical Engineering Journal*, **84**, pp.275 – 282.

Colella, C. (1999) Natural zeolites in environmentally friendly processes and applications. *Studies in Surface Science and Catalysis*. **125**, pp. 641–655.

Colella, C. (2007) Environmental applications of natural zeolitic materials based on their ion exchange properties. *Natural Microporous Materials in Environmental Technology*, **362**, pp 207-224.

Colella, C. and Wise, W.S. (2014) The IZA Handbook of Natural Zeolites: A tool of knowledge on the most important family of porous minerals. *Microporous and Mesoporous Materials*, **189**, pp.4–10.

Connors, K. (1998) *Chemical Kinetics: The study of reaction rates in solution*. John Wiley & Sons:USA.

Coruh, S. and Ergun, O.N. (2009) Ni²⁺ removal from aqueous solutions using conditioned clinoptilolites : kinetic and isotherm studies. *Environmental Progress & Sustainable Energy*, **28**, pp. 162–172.

Crini, G. (2005) Recent developments in polysaccharide-based materials used as adsorbents in wastewater treatment. *Progress in Polymer Science*, **30**, pp.38-70.

Crini, G. (2006) Non-conventional low-cost adsorbents for dye removal: a review. *Bioresource Technology*, **97**, pp.1061–1085.

Crittenden, B. and Thomas J. W. (1998) *Adsorption Technology and Design*, 1st ed. Butter Worth, UK: Elsevier Science and Technology.

Culfaz, M. and Yagiz, M. (2004) Ion exchange properties of natural clinoptilolite: lead-sodium and cadmium-sodium equilibria. *Separation and Purification Technology*, **37**(2), pp. 93-105.

Curkovic, L., Cerjan-Stefanovic, S. and Filipan, T. (1997) Metal ion exchange by natural and modified zeolites. *Water Research*, **31**(6), pp. 1379 - 1382.

DalBosco, S.M., Jimenez, R.S. and Carvalho, W.A. (2005) Removal of toxic metals from wastewater by Brazilian natural scolecite. *Journal of Colloid and Interface Science*. **281**, pp. 424 – 431.

Deer, W.A., Howie, R.A. and Zussman, J. (1992) *An introduction to the rock-forming minerals*. 2 ed. Harlow: Longman.

Deunert, R., Lennart, B. and Tiemeyer, B. (2007) Legislative effects on the development of surface water quality in rural areas in Northern Germany. *Cleaner Production*, **15**(16), pp. 1507 – 1513.

Dimirkou, A. (2007) Uptake of Zn^{2+} ions by a fully iron exchanged clinoptilolite. *Water Reserch.*, **41**, pp. 2763–2773.

Division for Sustainable Development (2016) *Sustainable Development Goals*. [online]. [Accessed 5th November 2016]. Available at: <<http://www.un.org/sustainabledevelopment/water-and-sanitation>>.

Doaa, M. and Mohamed, S. (2014) Removal of Pb^{2+} from water by using Na-Y zeolites prepared from Egyptian kaolins collected from different sources, *Journal of Environmental Chemical Engineering*, **2**, pp.723–730.

Duff M.C. (2002) Uranium Sorption on Sodium Aluminosilicates and Gibbsite. availabl at [<http://www.osti.gov/bridge>] (last date accessed: November, 2005).

Dyer, A. (1988) *An introduction to zeolite molecular sieves*. GB: John Wiley& Sons Ltd.

Dyer, A. and Zubair, M. (1998) Ion-exchange in chabazite. *Microporous and Mesoporous Materials*. **22**, pp. 135-150.

Erdem, E., Karapinar, N. and Donat, R. (2004) The removal of heavy metal cations by natural zeolites. *Journal of colloidal and Interface Science*, **280**(2), pp. 309 – 314.

Faghihian H., Marageh M.G., Kazemian H. (1999) The use of clinoptilolite and its sodium form for removal of cesium and strontium from nuclear wastewater and Pb^{2+} , Ni^{2+} , Cd^{2+} , Ba^{2+} from municipal wastewater. *Applied Radiation and Isotopes*, **50**, pp.655 – 660.

Flanigen, E. M. (1991) Zeolites and Molecular Sieves an historical perspective. *Studies in Surface Science and Catalysis*, **58**, pp.13–34.

Freitas, P., Iha, K., Felinto, M., and Su´arez-Iha, M. (2008) Adsorption of di-2-pyridyl ketone salicyloylhydrazone on Amberlite XAD-2 and XAD-7 resins: Characteristics and isotherms. *Journal of colloidal and Interface Science*, **323**, pp.1-5.

Frost, R.L., Horváth, E., Makóc, E., Kristóf, J. and Rédey, A. (2003) Slow transformation of mechanically dehydroxylated kaolinite to kaolinite - an aged mechanochemically activated formamide - intercalated kaolinite study. *Thermochimica Acta*, **408**, pp.103-113.

Frost, R.L., Mako, E., Krsitof, J. and Klopogge, J.T. (2002) Modification of kaolinite surfaces through mechanochemical treatment - a mid-IR and near-IR spectroscopic study. *Spectrochimica Acta Part A*. **58**, pp. 2849-2859.

Galli, E., Gottardi, G., Mayer, H., Preisinger, A., Passaglia, E. (1983) crystallography journals,[online].**B 39**, pp.189.< <http://journals.iucr.org>>.

Gedik, K and Imamoglu, I. (2008) Removal of cadmium from aqueous solutions using clinoptilolite: Influence of pretreatment and regeneration. *Journal of Hazardous Material*, **155**(2), pp. 385 – 392.

Gennaro B., Colella A., Aprea P., Colella C. (2003). Evaluation of an intermediatesilica sedimentary chabazite as exchanger for potentially radioactive cations. Microporous and Mesoporous Materials, **61**,pp.159 – 165.

Georgiev, D., Bogdanov, B., Angelova, K., Markovska,I. and Hristov, Y. (2009) Synthetic zeolites - structure, classification, current trends in zeolite synthesis review. International Science conference. Stara Zagora, Bulgaria.

Gottardi, G. and Galli, E. (1985) *Natural Zeolites*. Berlin Heidelberg: Springer Verlag.

Gougazeh, M. and Buhl J.C. (2014) Synthesis and characterization of zeolite A by hydrothermal transformation of natural Jordanian kaolin. *Journal of the Association of Arab Universities for Basic and Applied Sciences*, **15**, pp. 35–42.

Grim, R.E. (1968) *Clay Mineralogy, Technology & Engineering*. 2nd ed., McGraw-Hill, New York.

Grimshaw, R.W. and Harland, C.E. (1975) *Ion exchange: Introduction to theory and practice*. London: The Chemical Society.

Gunay, A., Arslankaya, E. and Tosun, I. (2007) Lead removal from aqueous solution by natural and pretreated clinoptilolite: Adsorption equilibrium and kinetics. *Journal of Hazardous Materials*, vol. **146**(2), pp. 362 – 371.

Gupta V.K., Carrott P.J.M., Ribeiro M.M.L., and Suhas T.L. (2009) Low-cost adsorbents: growing approach to wastewater treatment—a review. *Critical Reviews in Environmental Science and Technology*, **39**, pp. 783–842.

Halimoon H. and Yin S. (2010) Removal of Heavy Metals from Textile Wastewater using Zeolite, The international journal published by the Thai Society of Higher Education Institutes on Environment Environment Asia 3(special issue), pp.124-130.

Hamdaoui, O. (2009) Removal of copper (II) from aqueous phase by Purolite C100 – MB cation exchanger resin in fixed bed columns: Modeling. *Journal of Hazardous Materials*, **161**(2 – 3), pp. 737 – 746.

Hameed, B. H. (2009) Grass Waste: A Novel Sorbent for the Removal of Basic Dye from Aqueous Solution. *Hazardous Materials*, **166**, pp.233-238.

Han, R., Zou, W., Li, H., Li, Y. and Shi, J. (2006) Copper (II) and lead (II) removal from aqueous solution in fixed – bed columns by manganese oxide coated zeolite. *Journal of Hazardous Materials*, **B137**(1), pp. 934 – 942.

Harland, C.E. (1994) *Ion Exchange: Theory and Practice*, 2nd ed. The Royal Society of Chemistry: London.

Harrison, R.M. (1993) *Pollution: Causes, Effects and Control*, 4th ed. Royal Society of Chemistry: Great Britain.; Reprinted from edition (20 July 2001).

Hashem, M.A. (2007) Adsorption of lead ions from aqueous solution byokra wastes. *Nuclear Instruments and Methods in Physics Research Section*, **2**(7), pp.178–84.

Hey, M.H. (1930) Studies on the zeolites. I. General review. *Mineralogical Magazine*. **22**, pp.422-437.

Huang, W.L. (1993) The formation of illitic clays from kaolinite in KOH solution from 225 °C to 350°C. *Clays and Clay Minerals*, **41**, pp. 654.

Hui, K.S., Chao, C.Y.H. and Kot, S.C. (2005) Removal of mixed heavy metal ions in wastewater by zeolite 4A and residual products from recycled coal fly ash. *Journal of Hazardous Materials*, **127**, pp. 89 -101.

Ibrahim, H. S., Jamil, T., and Eman Z. H. (2010) Application of zeolite prepared from Egyptian kaolin for the removal of heavy metals: II. Isotherm models. *Journal of Hazardous Materials*, **182**, pp.842–847

Imhoff, K., Muller, W.J. and Thistlethwayte, D.K. (1971) *Disposal of sewage and other waste-borne wastes*, 2nd ed, Ann Arbor Science Publishers: London.

In Depth Tutorials and Information (2017) Bioaccumulation of Heavy Metals (Water Science)available at [<http://what-when-how.com/water-science/bioaccumulation-of-heavy-metals-water-science/>].

Inglezakis, V.J. and Grigoropoulou, H. (2004) Effects of operating conditions on the removal of heavy metals by zeolite in fixed bed reactors. *Journal of Hazardous Materials*, **12**, pp. 37-43.

Inglezakis, V.J., Hadjiandreou, K.J., Loizidou, M.D., Grigoropoulou, H.P. (2001) Pretreatment of natural clinoptilolite in a laboratory-scale ion exchange packed bed. *Water Research*, **35** (9), pp. 2161-2166.

Inglezakis, V.J., Loizidou, M.D. and Grigoropoulou, H.P. (2001) Applicability of simplified models for the estimation of ion exchange diffusion coefficients in zeolites. *Journal of Colloid and Interface Science*, **234**, pp.434-441.

Inglezakis, V.J., Loizidou, M.D. and Grigoropoulou, H.P. (2002) Equilibrium and kinetic ion exchange studies of Pb²⁺, Cr³⁺, Fe³⁺ and Cu²⁺ on natural clinoptilolite. *Water Research*, **36**, pp.2784-2792.

Inglezakis, V.J., Loizidou, M.D. and Grigoropoulou, H.P. (2003) Ion exchange of Pb^{2+} , Cu^{2+} , Fe^{3+} and Cr^{3+} on natural clinoptilolite: selectivity determination and influence of acidity on metal uptake. *Journal of Colloid and Interface Science*, **261**, pp.49-54.

Inglezakis, V.J., Loizidou, M.M. and Grigoropoulou, H.P. (2004) Ion exchange studies on natural and modified zeolites and the concept of exchange site accessibility. *Journal of Colloid and Interface Science*, **275**(2), pp. 570 – 576.

Inglezakis, V.J., Stylianou, M.A., Gkantou, D. and Loizidou, M.D. (2007) Removal of Pb (II) from aqueous solutions by using clinoptilolite and bentonite as adsorbents. *Desalination*, **210**(3), pp. 248 - 256.

Inglezakis, V.J., Zorpas, A.A., Loizidou, M.D., Grigoropoulou, H.P. (2003) Simultaneous removal of metals Cu^{2+} , Fe^{3+} and Cr^{3+} with anions SO_4^{2-} and HPO_4^{2-} using clinoptilolite. *Microporous and Mesoporous Materials*, **61**, pp. 167-171.

Jamil, S. T., Gad-Allah, T. A., Ibrahim, H. S. and Saleh, T.S. (2011) Adsorption and isothermal models of atrazine by zeolite prepared from Egyptian Kaolin. *Solid State Sciences*, **13**, pp.198-203.

Jamil, S. T., Ibrahim, H.S., Abd E.I. and El-Wakeel, T. (2010) Application of zeolite prepared from Egyptian kaolin for removal of heavy metals: I. Optimum conditions. *Desalination*, **258**, pp.34–40.

Kakali, G., Perraki, T., Tsivilis, S., Badogiannis, E. (2001) Thermal treatment of kaolin: the effect of mineralogy on the pozzolanic activity. *Applied Clay Science*, **20**, pp.73-80.

Karmen, M., Nataša Z. L., Mario, Š., Anamarija, F.(2013) Natural Zeolites in Water Treatment – How Effective is Their Use.< www.intechopen.com/.../water-treatment/natural-zeolites-in-water-treatment-how-effective>, Chapter 5, pp89-95

Kesraoui, O.S., Cheeseman, C. R. and Perry, R. (1994) Natural zeolite utilisation in pollution control: A review of applications to metals' effluents. *Journal of Chemical Technology & Biotechnolog*, **59**(2), pp. 121-126.

Khulbe K.C., Mann R.S., Tezel F.H., Triebe R.W., Erdem-Senatalar A., Sirkecioglu A. (1994) Characterization of clinoptilolite by interaction of H₂S, CO and SO₂ by the e.s.r. technique. *Zeolites*, **14**(6), pp.481 – 485.

Klimkiewicz, R. and Drag, E.B. (2004) Catalytic activity of carbonaceous deposits in zeolite from halloysite in alcohol conversions. *Journal of Physics and Chemistry of Solids*, **65**, pp.459–464.

Kocaoba, S., Orhan, Y. and Akyuz, T. (2007) Kinetics and equilibrium studies of heavy metal ions removal by use of natural zeolite. *Desalination*, **214**, pp.1-10.

Korkuna, O., Leboda, R., Skubiszewska-Ziemia, J., Vrublevska, T., Gunko, V.M. and Ryczkowski, J. (2006) Structural and physicochemical properties of natural zeolites: clinoptilolite and mordenite. *Microporous and Mesoporous Materials*, **87**, pp. 243.

Kovo, A.S. and Holmes S.M. (2010) Effect of aging on the synthesis of kaolin-based zeolite Y from ahoko Nageria using a novel metakaolnization technique. *Journal of dispersion Science.Technology*, **31**, pp. 442-448.

Koyama K., Takeuchi Y.(1977) Clinoptilolite: the distribution of potassium atoms and its role in thermal stability, *Z. Kristallogr.* **145**,pp. 216.

Kristof, J., Mink, J., Horvath, E. and Gabor, M. (1993) Intercalation study of clay minerals by Fourier transform infrared spectrometry. *Vibrational Spectroscop*, **5**, pp. 61-67.

Kulprathlpanja, S. (2010) Zeolites in industrial separation and catalysis. *Focus on Catalysts*, **2010**(7), pp. 8.

Kumar, J.V. and Hayashi, S. (2009) Modification on natural clinoptilolite zeolite for its NH₄⁺ retention capacity. *Journal of Hazardous Materials*. **169**(1-3), pp. 29-35.

Lambert, J.F., Minman, W.S. and Fripiat, J.J. (1989) Revisiting kaolinite dehydroxylation: A silicon-29 and aluminum-27 MAS NMR study. *Journal of the American Chemical Societ*, **111**, pp.3517-3522.

Langella, A., Pansini, M. Cappelletti, P., de Gennaro, B., de Gennaro, M. and Colella, C. (2000) NH_4^+ , Cu^{2+} , Zn^{2+} , Cd^{2+} and Pb^{2+} exchange for Na^+ in sedimentary clinoptilolite, North Sardinia, Italy. *Microporous and Mesoporous Material*, **37**, pp. 337-343.

Li, G. (2005) FT-IR studies of zeolite materials: characterization and environmental applications." PhD diss., University of Iowa.<<http://ir.uiowa.edu/etd/96>>.

Liu, Q., Spears, D.A. and Liu, Q. (2001) MAS NMR study of surface-modified calcined kaolin. *Applied Clay Science*, **19**, pp.89-94.

Lussier, R. (1991) A novel clay-based catalytic material-preparation and properties. *Journal of Catalysis*, **129**(1), pp. 225-237.

Macingova, E. and Luptakova A. (2012) Recovery of Metals from Acid Mine Drainage. Institute of Geotechnics, Slovak Academy of Sciences. *chemical engineering transport*, **28**, pp. 043- 53.

Mackenzie, R.C. (1971) Differential Thermal Analysis 1. *Analytica Chimica Acta*, **53**(1), pp.221.

Madani, A., Aznar, A., Sanz, J. and Serratosa, J.M. (1989) ^{29}Si and ^{27}Al NMR study of zeolite formation from alkali-leached kaolinites. Influence of thermal preactivation. *Journal of physical chemistry*, **94**, pp. 760-765.

Malliou, E., Loizidou, M. and Spyrellis, N. (1994) Uptake of lead and cadmium by clinoptilolite. *Science of the Total Environment*, **149**, pp.139 – 144.

Mantell, C.L. (1951) *Adsorption*, McGraw – Hill Inc.: New York and London.

Margeta, K., Logar, N.Z., Šiljeg, M. and Farkaš, A.(2013) Natural Zeolites in Water Treatment – How Effective is Their Use, Chapter 5 [online][accessed on 08 November 2016] available at: <<http://www.intechopen.com/books/water-treatment/natural-zeolites-in-water-treatment-how-effective-is-their-use>>.

Masters, G.M. (1998) *Introduction to Environmental Engineering and Science*. 2nd ed, Prentice – Hall International Inc.:U.S.A.

Meier, W.M. (1968) Zeolite structures. In: Molecular Sieves, *Journal of Society of Chemical Industry*, London, pp.10-27.

Meier, W.M., Olson, D.H. and Baerlocher, Ch. (1996) *Atlas of zeolite structure types*. 4th ed. Elsevier: London.

Mier, M.V., Callejas, R.L., Gehr, R., Cisneros, B.E.J. and Alvarez P.J.J. (2001) Heavy metal removal with Mexican clinoptilolite: multi – component ionic exchange. *Water Research*, **35**(2), pp.373 – 378.

Millennium Development Goals (2000) Global Water Supply and Sanitation Assessment Report 2000, WHO, Geneva, Switzerland [On line] [Accessed 5th November 2016]. available at< http://www.who.int/water_sanitation_health/monitoring/jmp2000.pdf>.

Milton (1968) Molecular Sieves. *Journal of the Society of Chemical Industry*, **68**, pp. 199–203.

Misaelides, M (2011) Application of natural zeolites in environmental remediation: A short review. *Microporous and Mesoporous Materials*, **144**, pp. 15–18.

Misaelides, P., Godelitsas, A., Charistos, V. and Ioannou, D. (1994) Heavy metal uptake by zeoliferous rocks from Metaxades, Thrace, Greece: an exploratory study. *Journal of Colloid and Interface Science*, **183**(1), pp. 159 – 166.

Moreno, N., Querol, X. and Ayora, C. (2001) Utilization of zeolites synthesised from coal fly ash for the purification of acid mine waters. *Environmental Science and Technology*, **35**, pp. 3526-3534.

Mortier, W.J. (1982) *Structure Commission of the International Zeolite Association, Compilation of extra framework sites in zeolites*. Scientific Ltd: Butterworth.

Motsi, T., Rowson, N.A. and Simmons, M.J.H. (2009) Adsorption of heavy metals from acid mine drainage by natural zeolite. *International Journal of Mineral Processing*, **92**, pp.42–48.

Mulligan, C. N., Yong, R. N., Gibbs, B. F. (2001) Heavy metal removal from sediments by biosurfactants. *Journal of Hazardous Materials*, **85**, pp.111–125.

Mumpton, F.A. (1999) Use of natural zeolites in agriculture and industry. *Proceedings to the national Academy of Sciences in the U.S.A.*, **96**(7), pp. 3463 – 3470.

Murray, H. H. (2007) Applied Clay Mineralogy, Occurrences, Processing And Application Of Kaolins, Bentonites, Palygorskite-Sepiolite, And Common Clays. 1st ed. Oxford: Elsevier's Science & Technology.

Myroslav, S., Boguslaw, B., Artur, T. P. and Jacek, N. (2006) Study of the Selection Mechanism of Heavy Metal (Pb^{2+} , Cu^{2+} , Ni^{2+} and Cd^{2+}) adsorption on clinoptilolite. *Journal of Colloid and Interface Science*. **304**, pp. 21-28.

Nageeb, R.M. (2013) *Adsorption Technique for the Removal of Organic Pollutants from Water and Wastewater*, Chapter 7.

Nesse W.D. (2000) *Introduction of mineralogy*. Oxford University Press: Oxford.

Newsam, J.M. (1986) Zeolite Cage Structure, *American Association for the Advancement of Science*, **231**(4742), pp. 1093 – 1099.

Olad, A. and Naseri, B. (2010) Preparation, characterization and anticorrosive properties of a novel polyaniline/clinoptilolite nanocomposite. *Progress in Organic Coatings*, **67**, pp. 233 - 238.

Ören, A.H. and Kaya, A. (2006) Factors affecting adsorption characteristics of Zn^{2+} on two natural zeolites. *Journal of Hazardous Materials*, **13**, pp. 59–65.

Ouki S.K., Cheeseman C. and Perry R. (1994) Natural zeolite utilisation in pollution control: a review of applications to metal effluents. *Journal of Chemical Technology and Biotechnology*, **59**, pp. 121 – 126.

Ouki, S.K. and Kavannagh, M. (1997) Performance of natural zeolites for the treatment of mixed metal contaminated effluents. *Waste Management & Research*, **15**, pp. 383-394.

Ouki, S.K. and Kavannagh, M. (1999) Treatment of metals contaminated wastewaters by use of natural zeolites. *Water Science and Technology*, **39**(10-11), pp. 115 – 122.

- Ozaydin, S., Kocar, G. and Hepbasli, A. (2006) Natural zeolites in energy applications, *Energy Sources Part A: Recovery Utilization and Environmental Effects*, **28**, pp. 1425-1431.
- Oztas, N.N., Karabakan, A. and Topal, O. (2008) Removal of Fe (III) ion from aqueous solution by adsorption on raw and treated clinoptilolite samples. *Journal of Microporous and Mesoporous Materials*, **111**(1 – 3), pp. 200 – 205.
- Panayotova, M. and Velikov, B. (2003) Influence of zeolite transformation in the homoionic form on the removal of some metal ions from wastewater. *Journal Science and Health*, **A38**(3), pp. 545 – 554.
- Panday K.K., Prasad, G. and Singh V.N. (1985) Copper(II) removal from aqueous solutions by fly ash. *Water Reserch*, **19**(7), pp.869–73.
- Pandey, P., Sambi, S.S., Sharma, S.K. and Singh, S. (2009) Batch Adsorption Studies for the Removal of Cu (II) Ions by ZeoliteNaX from Aqueous Stream. *Proceedings of the World Congress on Engineering and Computer Science*, **I**, San Francisco, USA
- Papageorgiou, K.S., Katsaros, K.F., Kouvelos, P.E., Nolan, W.J., LeDeit, H. and Kanellopoulos, K.N. (2006) Heavy metal sorption by calcium alginate beads from *Laminaria digitata*. *Journal of Hazardous Materials*, **B137**, pp.1765 – 1772.
- Patterson, J.W. (1987) *Metal Speciation Separation and Recovery*, Chelsea: Lewis Publishers.
- Payne, K.B. and Abdel-Fattah,T.M. (2004) Adsorption of Divalent Lead Ions by Zeolites and Activated Carbon: Effects of pH, Temperature, and Ionic Strength. *Journal of Environmental Science and Health*, **39**(9), pp.2275-91
- Payra S. and Dutta P. K. (2003) *Handbook of Zeolite Science and Technology*, Marcel Dekker :New York, pp. 1–19.
- Peng, J., Song, Y., Yuan, P., Cui, X. and Qiu, G. (2009) The remediation of heavy metals contaminated sediment. *Journal of Hazardous Materials*, **161**(2 - 3), pp. 633 – 640.
- Peric, J., Trgo, M. and Medvidovic, N.V. (2004) Removal of zinc, copper and lead by natural zeolite-a comparison of adsorption isotherms. *Water Research*, **38**, pp. 1893-1899.

Perraki, T. and Orfanoudaki, A. (2004) Mineralogical study of zeolites from Pentalofos area. *Applied Clay Science*, **25**, pp.9-6.

Petrov, I. and Michalev, T. (2012) Synthesis of Zeolite A: A Review. *НАУЧНИ ТРУДОВЕ НА РУСЕНСКИЯ УНИВЕРСИТЕТ*, 51, pp.30-35

Pohl, Walter L. (2011) *Economic geology: principles and practice*. West Sussex: Wiley-Blackwell.

Polat, E., Karaca, M., Demir, H. and Onus, N. (2004) Use of natural zeolite (clinoptilolite) in agriculture. *Journal of Fruit and Ornamental Plant Research*, **12**(1), pp. 183 – 189.

Pollard, S.J., Fowler, G.D., Sollars, C.J. and Perry, R. (1992) Low-cost adsorbents for waste and waste-water treatment—a review. *Science of the Total Environment*, **116**(1-2), pp. 31-52.

Popuri, S.R., Vijaya, Y., Boddu, V.M. and Abburi, K. (2008) Adsorptive removal copper and nickel ions from water using chitosan PVC beads. *Bioresource Technology*, **100**(1), pp. 194 – 199.

Prasad, M., Xu, H.Y. and Saxena, S. (2008) Multi-component sorption of Pb(II), Cu(II) and Zn(II) onto low-cost mineral adsorbent. *Journal of Hazardous Materials*, **154**, pp.221-229.

Querol, X., Plana, F., Alastuey, A. and Lopez-Soler A. (1997) Synthesis of Na-zeolites from fly ash. *Fuel*, **76**(8), pp. 793–799.

Ragnarsdottir, KV, Graham, CM and Allen, GC. (1996) Surface chemistry of reacted heulandite determined by SIMS and XPS. *Journal of Chemical Geology*, **131**(1 – 4), pp. 167 – 181.

Ramalho, R.S. (1997) *Introduction to wastewater treatment processes*, 2nd ed, Academic Press: Elsevier Science.

Ramos R.L., Armenta G.A., Gutierrez L.V.G., Coronado R.M.G., Barron J.M. (2004) Ammonia exchange on clinoptilolite from mineral deposits located in Mexico. *Journal of Chemical Technology and Biotechnology*. **79**, pp.651 – 657.

- Rengaraj, S., Yeon, K., and Moon, S.H. (2001) Removal of chromium from water and wastewater by ion exchange resins. *Journal of Hazardous Materials*, **87**(1- 3), pp. 273 – 287.
- Ribero, F.R, Rodrigues,A.E., Rollmann, L.D. and Naccache, C. (1984) *Zeolite:Science and Technology*. Lancaster: Martinus Nijhoff.
- Richardson, J.F. and Harker, J.H. (2002) *Coulson and Richardson's chemical Engineering*, 5th ed. Butterworth-Heinemann: Oxford.
- Rios, C.A., Williams, C.D. and Maple M.J. (2007) Synthesis of zeolites and zeotypes by hydrothermal transportation of kaolinite and metakaolinite. *BISTUA*, **5** (1), pp. 15–26.
- Rivera, A., Rodriguez-Fuentes, G. and Altshuler, E. (2000) Time evolution of a natural clinoptilolite in aqueous medium: conductivity and pH experiments. *Microporous and Mesoporous Materials*, **40**(1 – 3), pp. 173 – 179.
- Rondón, W., Freire, D., Benzo, Z., Sifontes A., González Y, Valero, M. and Brito J. L. (2013) Application of 3A Zeolite Prepared from Venezuelan Kaolin for Removal of Pb (II) from Wastewater and Its Determination by Flame Atomic Absorption Spectrometry. *American Journal of Analytical Chemistry*, **4**, pp. 584-593.
- Ruiz, R., Blanco, C., Pesquera, C., Gonzalez, F., Benito, I. and Lopez, J.L. (1997) Zeolitization of a bentonite and its application to the removal of ammonium ion from waste water. *Applied Clay Science*, **12**, pp.73-83.
- Ruthven, D.M. (1984) *Principles of adsorption and adsorption processes*. A Wiley – Interscience Publication, John Wiley and Sons Inc: New York.
- Saija, L.M., Ottana, R. and Zipelli C. (1983) Zeolitization of pumice in ash-sodium salt solutions. *Materials Chemistry and Physics*, **8**, pp. 207–216.
- Saikia, N.J., Bharali, D.J., Sengupta, P., Bordoloi, D., Goswamee, R.L., Saikia, P.C. and Bothakur, P.C. (2003) Characterization, beneficiation and utilization of a kaolinite clay from Assam, India. *Applied Clay Science*, **24**, pp. 93–103.

Salam, O. E. A., Reiad, N. A. and ElShafei, M. M. (2011) A study of the removal characteristics of heavy metals from wastewater by low-cost adsorbents. *Journal of Advanced Research*, **2**, pp.297-303.

Salem, A. and Akbari S. R. (2011) Removal of lead from solution by combination of natural zeolite–kaolin–bentonite as a new low-cost adsorbent. *Chemical Engineering Journal*, **174**, pp.619– 628.

Sand, L.B. and Mumpton, F.A. (1978) *Natural Zeolites Occurrence Properties and Use*. Pergamon Press Ltd: New York.

Sarioglu M. (2005) Removal of ammonium from municipal wastewater using natural Turkish (Dogantepe) zeolite. *Separation and Purification Technology*, **41**, pp.1- 11.

Schroeder, E.D. (1977) *Water and Wastewater Treatment*. McGraw – Hill, Inc: New York.

Schroeder, Paul (2003) *Kaolin*[New Georgia Encyclopedia].[Accessed 10 July 2016]. Available at <<http://www.georgiaencyclopedia.org/nge/Article.jsp?id=h-1178>>.

Semmens, M. and Martin, W. (1988) The influence of pretreatment on capacity and selectivity of clinoptilolite for metal ions. *Water Research*, **22**, pp. 537 – 542.

Semmens M.J., Seyfarth M., L.B. Sand, F.A. Mumpton F.A (1978) *Natural Zeolites. Occurrence, Properties and Use*, Pergamon Press, New York.

Shahwan T., Akar D., Eroglu A.E. (2005) Physicochemical characterization of the retardation of aqueous Cs⁺ ions by natural kaolinite and clinoptilolite minerals. *Journal of Colloid and Interface Science*, **285**(1), pp.9 – 17.

Sheta, A.S., Falatah, A.M., Al-Sewailem, M.S., Khaled, E.M. and Salam, A.S.H., (2003) Sorption characteristics of zinc and iron by natural zeolite and bentonite. *Microporous Mesoporous Material*, **61**, pp.127–136.

Sinha, P.K., Paniker, P.K. and Amalraj, R.V. (1995) Treatment of radioactive liquid waste containing caesium by indigenously available synthetic zeolites: A comparative study. *Waste Management*, **15**, pp.149-157.

Šiška, J. (2005) Extraction of heavy metals and ammonium from waters by unsaturated fatty acids and their soaps. *Hydrometallurgy*, **76**, pp.155-172.

Somorjai, G.A. (1993) *Introduction to Surface Chemistry and Catalysis*, John Wiley & Sons, Inc.: New York.

Sprynskyy, M., Boguslaw B., Terzyk, A.P. and Namiesnik, J. (2006) Study of the selection mechanism of heavy metal (Pb^{2+} , Cu^{2+} , Ni^{2+} and Cd^{2+}) adsorption on clinoptilolite. *Journal of Colloid and Interface Science*, **304**, pp.21-28.

Sprynskyy, M., Golembiewski, R., Trykowski, G. and Buszewski, B. (2010) Heterogeneity and hierarchy of clinoptilolite porosity. *Journal of Physics and Chemistry of Solids*, **71**, pp.1269.

Stefanović Š., Zabukovec L., Margeta K., Tušar, N., Arčon I., Maver K., Kovač, J. and Kaučič V. (2007) Structural investigation of Zn^{2+} sorption on clinoptilolite tuff from the Vranjska Banja deposit in Serbia. *Microporous and Mesoporous Materials*. **105**(3), pp.251-259.

Szoztak, R. (1998) *Molecular Sieves: Principles of Synthesis and Identification*. 2nd ed. Blackie Academic and Professional: London.

Tanaka, H., Yamasaki, N., Muratani, M. and Hino, R. (2003) Structure and formation process of (K, Na)-clinoptilolite. *Materials Research Bulletin*, **38**, PP.713.

Tatsuo, O. and Nagae M., (2003) Quick activation of optimized zeolites with microwave heating and utilization of zeolite for re-useable desiccant. *Journal of Porous Materials*, **10**, pp.139-143.

Tchobanoglous G. and Burton F.L. (1991) *Wastewater Engineering: Treatment, Disposal, Reuse*. 3rd ed. Signapore: McGraw-Hill International Editions.

Tien, C. (1994) *Adsorption calculations and modelling*. Butterworth – Heinemann: New York.

Trgo, M. and Peric, J. (2003) Interaction of the zeolitic tuff with Zn-containing simulated pollutant solutions. *Journal of Colloid and Interface Science*, **260**, pp.166–175.

Tsitsishvili G.V., Andronikashvili T.G., Kirov G.N., Filizova L.D. (1992) *Natural Zeolites*. Ellis Horwood Limited: Great Britain.

Turner, M.D., Laurence, R.L., Conner, W.C. (2000) Microwave radiation's influence on sorption and competitive sorption of zeolites. *AIChE Journal*, **46** (4), pp. 758 – 768.

Ugal, J.R., Hassan, K.H. and Ali, I.H. (2010) Preparation of type 4A zeolite from Iraqi kaolin: Characterization and properties measurements. *Journal of the Association of Arab Universities for Basic and Applied Sciences*, **9**, pp. 2–5.

Um W., Papelis C. (2004) Metal ion sorption and desorption on zeolitized tuffs from Nevada test site. *Environmental Science and Technology*, **38**, pp.496 – 502.

United Nations Framework Convention on Climate Change (2007) updated.[online].[accessed 10 August 2016] Available at: <http://unfccc.int/kyoto_protocol/items/2830>.

U.S. Geological Survey(2011) Mineral Commodity Summaries, January 2011.
Valcke, E., Engels, B. and Cremers, A. (1997) The use of zeolites as amendments in radiocaesium- and radiostrontium-contaminated soils: A soil-chemical approach. Part II: Sr-Ca exchange in clinoptilolite, mordenite and zeolite A, *Zeolites*, **18**, pp. 212-217.

Van der Marel, H.W. and Beutelspacher, H. (1976) *Atlas of Infrared Spectroscopy of Clay Minerals and Their Admixtures*, 1st ed. Elsevier: Amsterdam.

Watanabe Y., Yamada H., Kokusen H., Tanaka J., Moriyoshi Y., Komatsu Y. (2003) Ion exchange behavior of natural zeolites in distilled water, hydrochloric acid, and ammonium chloride solution. *Separation Science and Technology*, **38**(7), pp.1519 – 1532.

Walek, T.T., Saito, F. and Zhang, Q. (2008) The effect of low solid/liquid ratio on hydrothermal synthesis of zeolites from fly ash. *Fuel*, **87**, pp. 3194–3199.

Wan Ngah, W.S. and Hanafiah, M. (2008) Removal of heavy metal ions from wastewater by chemically modified plant wastes as adsorbents: a review. *Bioresour Technol* **99**, pp.3935–3948.

Wang, C.F., Li, J.S., Wang, L.J. and Sun, X.Y. (2008) Influence of NaOH concentrations on synthesis of pure-form zeolite A from fly ash using two-stage method. *Journal of Hazardous Materials*, **155**, pp. 58–64.

Wang, S.B, Ang, H.M. and Tadé, M.O. (2008) Novel applications of red mud as coagulant, adsorbent and catalyst for environmentally benign processes. *Chemosphere*, **72**, pp. 1621-1635.

Wang, S.B. and Wu, H.W. (2006) Environmental-benign utilisation of fly ash as low-cost adsorbents. *Journal of Hazardous Materials*, **136**, pp. 482-501.

Wilson, M.J. (1994) *Clay Mineralogy: Spectroscopic and Chemical Determinative Methods*. Chapman and Hall: New York, 1994.

Wingenfelder, U., Hansen, C., Furrer, G. and Schulin R. (2005) Removal of heavy metals from mine waters by natural zeolites. *Environmental Science and Technology*, **35**, pp. 4606-4613.

World Bank Group (2016) Introduction to Wastewater Treatment Processes [online].[Accessed 5 November 2016]. Available at: <<http://water.worldbank.org/shw-resource-guide/infrastructure/menu-technical-options/wastewater-treatment>>.

Yang, R.T. (2004) Adsorbents: Fundamentals and Application. *Journal of Hazardous Materials*.**109**, pp. 227–229.

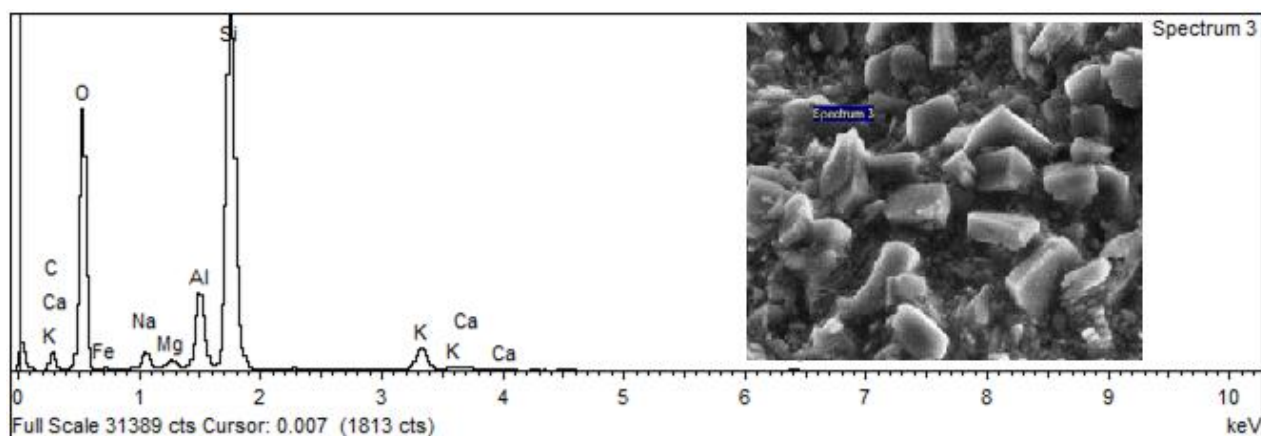
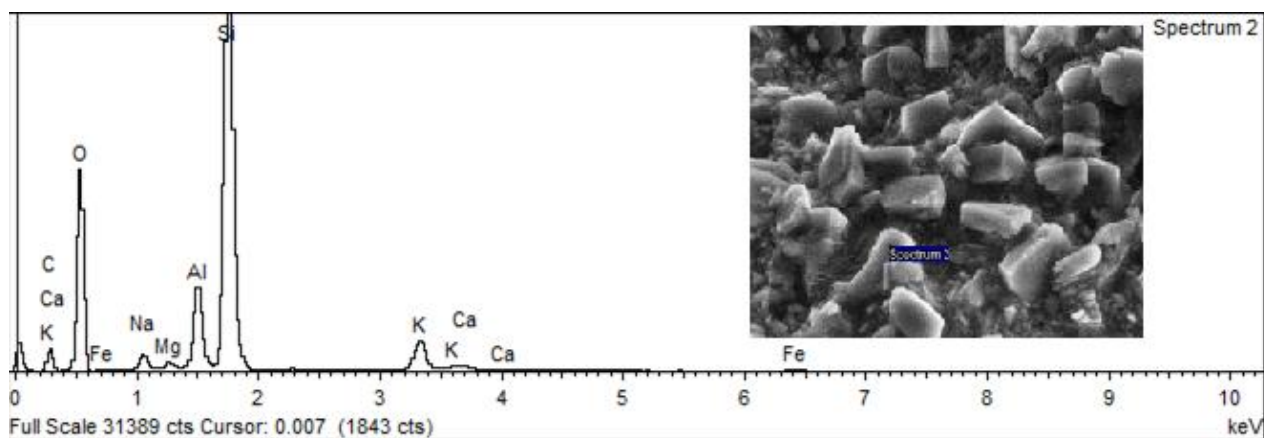
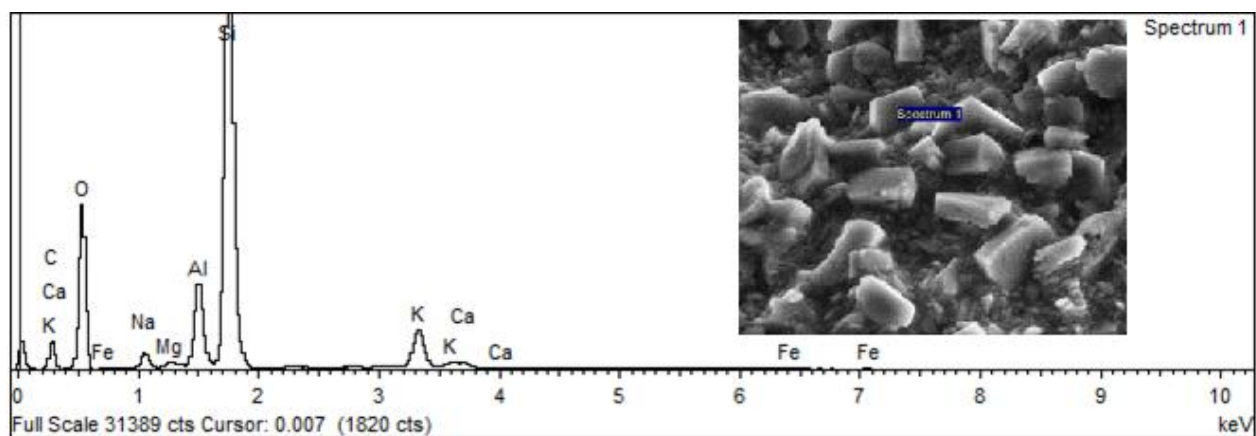
Yu, J.J., Shukla, S.S., Dorris, K.L., Shukla, A. and Margrave, J.L. (2003) Adsorption of chromium from aqueous solutions by maple sawdust. *Journal of Hazardous Materials*, **B100**(1),pp.53-63.

APPENDIX

APPENDIX A

The localisation of four analysed sites designated by numbers and a typical EDS curve are showing below:

1. Natural zeolite spectra:



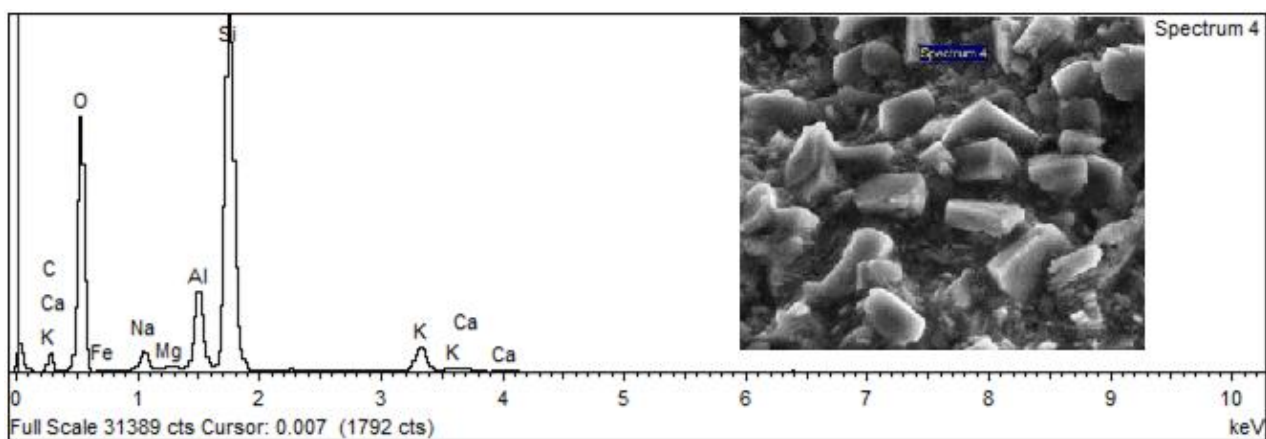
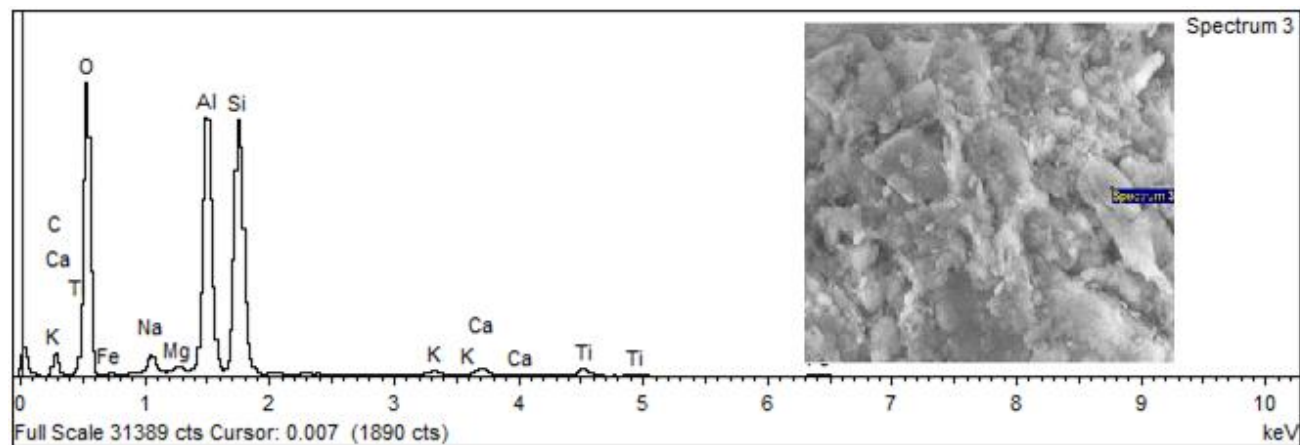
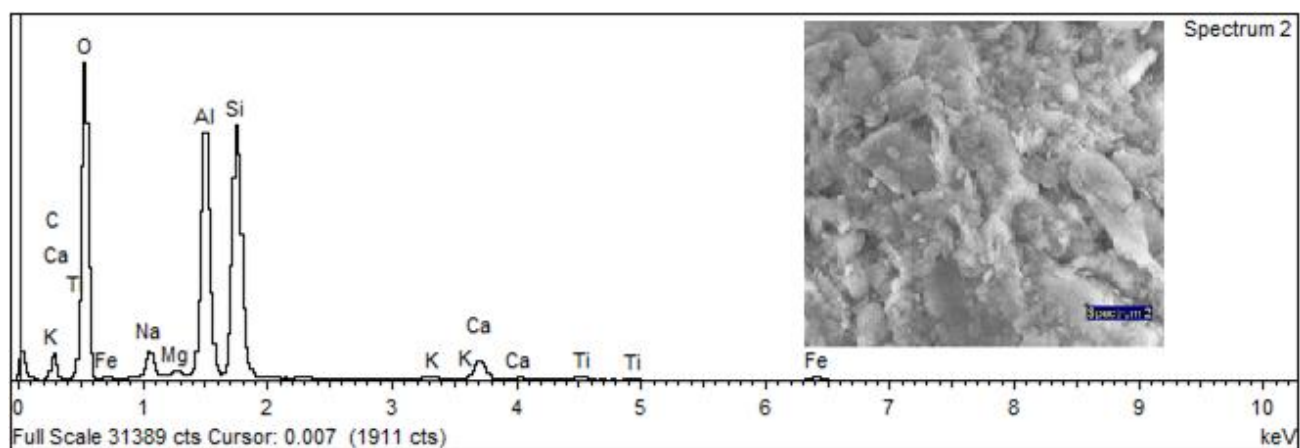
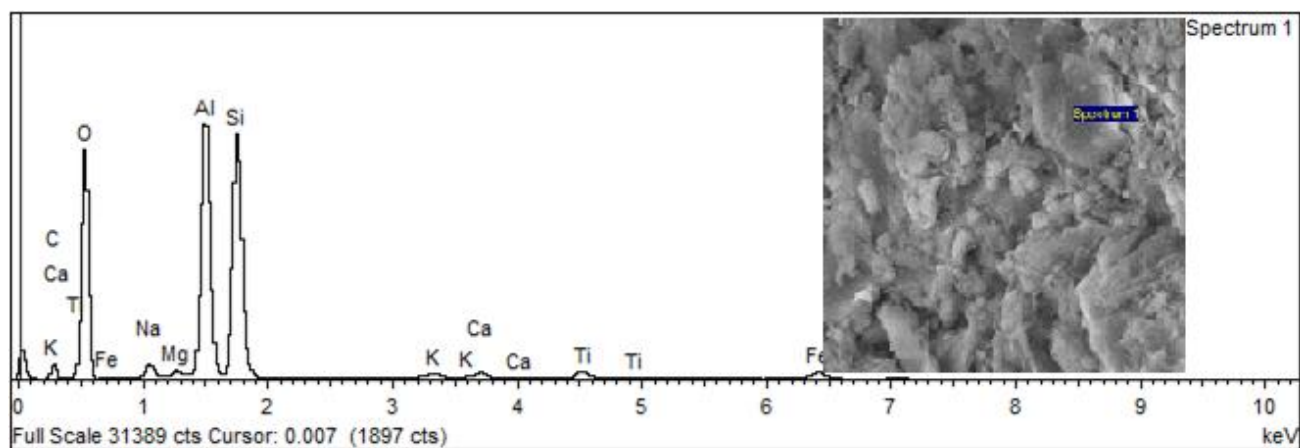


Figure A.1: EDS analysis showing the elemental composition and the scanning method for natural zeolite spectrum 1, 2, 3 and 4.

Table A.1: EDS analysis showing the elemental composition and the scanning method for “as received” natural zeolite.

Element	Na ₂ O %	MgO %	Al ₂ O ₃ %	SiO ₂ %	K ₂ O %	CaO %	TiO ₂ %	Fe ₂ O ₃ %
Spectrum 1	1.18	0.27	3.92	22.14	3.13	0.36	0.064	0.37
Spectrum 2	1.25	0.33	4.01	22.13	2.47	0.32	0.065	0.44
Spectrum 3	1.31	0.38	3.78	20.05	1.9	0.31	0.063	0.33
Spectrum 4	1.57	0.16	4.02	20.54	2.04	0.24	0.062	0.23
Average	1.33	0.29	3.93	21.22	2.39	0.31	0.06	0.34
Std.deviation	0.17	0.09	0.11	1.08	0.55	0.05	0.00	0.09

2. Kaolinite spectra:



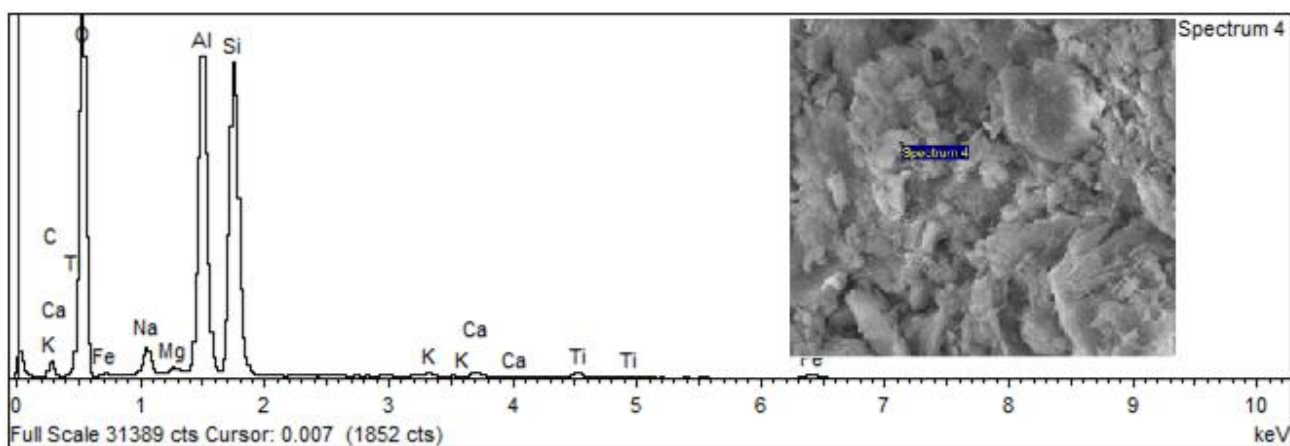


Figure A.2: EDS analysis showing the elemental composition and the scanning method for kaolinite spectrum 1,2,3 and 4.

Table A.2: EDS analysis showing the elemental composition and the scanning method for “as received” kaolinite

Element	Na ₂ O %	MgO %	Al ₂ O ₃ %	SiO ₂ %	K ₂ O %	CaO %	TiO ₂ %	Fe ₂ O ₃ %
Spectrum 1	1.31	0.32	14.91	17.21	0.39	0.52	1.07	1.92
Spectrum 2	1.95	0.21	11.74	13.82	0.13	1.56	0.42	0.77
Spectrum 3	1.45	0.23	12.77	14.93	0.23	0.66	0.84	0.65
Spectrum 4	1.86	0.18	14.54	16.95	0.14	0.3	0.5	0.84
average	1.64	0.23	13.49	15.72	0.22	0.76	0.70	1.04
Std. deviation	0.26	0.05	1.29	1.41	0.10	0.47	0.26	0.50

APPENDIX B

X-Ray Fluorescence (XRF) result of six analysed samples designated by numbers and a typical table are shown below:

Table B.1: Chemical composition (wt.%) of the natural zeolite performed.

Element	Na₂O %	MgO %	Al₂O₃ %	SiO₂ %	K₂O %	CaO %	TiO₂ %	Fe₂O₃ %
Sample 1	3.67	0.862	4.572	38.46	2.174	0.991	0.0641	0.765
Sample 2	4.7	0.897	4.59	38.6	2.19	0.978	0.0651	0.7264
Sample 3	4.12	0.898	4.616	38.97	2.126	1.023	0.0636	0.7382
Sample 4	4	0.863	4.312	34.96	2.118	0.878	0.0626	0.7677
Sample 5	3.61	0.859	4.505	38.13	2.091	0.94	0.0639	0.7275
Sample 6	4.61	0.947	4.566	38.67	2.039	0.927	0.0644	0.723
Average	4.12	0.89	4.53	37.97	2.12	0.96	0.06	0.74
Std.deviation	0.46	0.03	0.11	1.50	0.06	0.05	0.0008	0.02

APPENDIX C

The XRD spectra of natural zeolite modified and unmodified kaolinite clays.

1. Natural Zeolite:

Anchor Scan Parameters

Dataset Name:	Natural Zeolite (Clinoptilolite).
File name:	C:\XRD Data\AMS_Sample1.xrdml
Sample Identification:	Sample1
Comment:	Configuration=Reflection-transmission spinner, Owner=User-1, Creation date=6/28/2012 10:39:29 AM
	Goniometer=Theta/Theta; Minimum step size 2Theta:0.0001; Minimum step size Omega:0.0001
	Sample stage=Reflection-transmission spinner; Minimum step size Phi:0.1
	Diffractometer system=EMPYREAN
	Measurement program=C:\PANalytical\Data Collector\Programs\powder 15mm PDS.xrdmp, Identifier={0B3B2317-9C50-4321-8234-537F3D3E9F38}
	Batch program=C:\PANalytical\Data Collector\Programs\changer batch 4.xrdmp, Identifier={6080F58B-96FE-494C-BDA3-33B4A6E5B20E}
Measurement Date / Time:	9/9/2014 12:03:21 PM
Operator:	Univ Wolverhampton
Raw Data Origin:	XRD measurement (*.XRDML)
Scan Axis:	Gonio
Start Position [°2Th.]:	5.0064
End Position [°2Th.]:	79.9904
Step Size [°2Th.]:	0.0130
Scan Step Time [s]:	8.6700
Scan Type:	Continuous
PSD Mode:	Scanning
PSD Length [°2Th.]:	3.35
Offset [°2Th.]:	0.0000
Divergence Slit Type:	Fixed
Divergence Slit Size [°]:	0.2500
Specimen Length [mm]:	10.00
Measurement Temperature [°C]:	25.00
Anode Material:	Cu
K-Alpha1 [Å]:	1.54060
K-Alpha2 [Å]:	1.54443
K-Beta [Å]:	1.39225
K-A2 / K-A1 Ratio:	0.50000
Generator Settings:	40 mA, 40 kV
Diffractometer Type:	0000000001126545
Diffractometer Number:	0
Goniometer Radius [mm]:	240.00
Dist. Focus-Diverg. Slit [mm]:	100.00
Incident Beam Monochromator:	No
Spinning:	Yes

Scan List

Vis.	Dataset Name	Start pos. [°2Th.]	End pos. [°2Th.]	Step [°2Th.]	Meas.Date/Time
*	AMS_Sample1	5.0064	79.9904	0.0130	9/9/2014 12:03:21 PM
*	Determine ..	5.0064	79.9904	0.0130	9/9/2014 12:03:21 PM

Pattern List

Visible	Ref.Code	Score	Compound Name	Displ.[°2Th]	Scale Fac.	Chem. Formula
*	98-009-7840	66	Clinoptilolite (Na..	0.013	1.024	H18.08 Al6 Na8 O81..

Peak List

Pos.[°2Th.]	Height [cts]	FWHMLeft[°2Th.]	d-spacing [Å]	Rel. Int. [%]
5.359(3)	136(8)	0.012(7)	16.47679	9.78
5.372(3)	68(8)	0.012(7)	16.47679	4.89
7.92(5)	98(4)	3.6(2)	11.15675	7.01
7.94(5)	49(4)	3.6(2)	11.15675	3.51
9.8086(8)	1394(17)	0.177(3)	9.01023	100.00
9.8330(8)	697(17)	0.177(3)	9.01023	50.00
11.112(1)	710(15)	0.153(3)	7.95631	50.94
11.139(1)	355(15)	0.153(3)	7.95631	25.47
13.004(3)	255(12)	0.231(7)	6.80247	18.31
13.036(3)	128(12)	0.231(7)	6.80247	9.15
13.295(3)	130(14)	0.08(1)	6.65400	9.32
13.329(3)	65(14)	0.08(1)	6.65400	4.66
14.876(3)	134(6)	0.115(3)	5.95033	9.62
14.913(3)	67(6)	0.115(3)	5.95033	4.81
16.881(2)	167(10)	0.142(7)	5.24794	11.96
16.923(2)	83(10)	0.142(7)	5.24794	5.98
17.266(1)	381(9)	0.148(4)	5.13180	27.29
17.309(1)	190(9)	0.148(4)	5.13180	13.65
19.042(2)	255(7)	0.152(5)	4.65705	18.26
19.089(2)	127(7)	0.152(5)	4.65705	9.13
20.372(3)	110(8)	0.11(1)	4.35589	7.87
20.423(3)	55(8)	0.11(1)	4.35589	3.93
22.294(7)	871(50)	0.20(1)	3.98438	62.47
22.350(7)	435(50)	0.20(1)	3.98438	31.23
22.429(1)	646(83)	0.122(3)	3.96072	46.30
22.486(1)	323(83)	0.122(3)	3.96072	23.15
22.719(2)	503(8)	0.209(4)	3.91091	36.09
22.776(2)	252(8)	0.209(4)	3.91091	18.05
23.109(4)	86(6)	0.075(7)	3.84574	6.16
23.167(4)	43(6)	0.075(7)	3.84574	3.08
23.969(4)	116(12)	0.12(1)	3.70969	8.29
24.029(4)	58(12)	0.12(1)	3.70969	4.14
25.021(1)	253(8)	0.134(5)	3.55601	18.12
25.084(1)	126(8)	0.134(5)	3.55601	9.06
25.699(7)	71(6)	0.19(2)	3.46370	5.11
25.764(7)	36(6)	0.19(2)	3.46370	2.56
26.004(1)	582(13)	0.139(3)	3.42377	41.75
26.070(1)	291(13)	0.139(3)	3.42377	20.87
26.273(2)	259(12)	0.137(7)	3.38930	18.55
26.340(2)	129(12)	0.137(7)	3.38930	9.28
26.598(2)	163(10)	0.088(6)	3.34860	11.70
26.666(2)	82(10)	0.088(6)	3.34860	5.85
26.785(2)	208(8)	0.128(7)	3.32565	14.89
26.853(2)	104(8)	0.128(7)	3.32565	7.45
27.695(4)	63(5)	0.071(5)	3.21841	4.54
27.766(4)	32(5)	0.071(5)	3.21841	2.27
28.128(1)	485(11)	0.152(3)	3.16983	34.80
28.200(1)	243(11)	0.152(3)	3.16983	17.40
28.563(2)	201(7)	0.190(7)	3.12261	14.40
28.635(2)	100(7)	0.190(7)	3.12261	7.20

Graphics

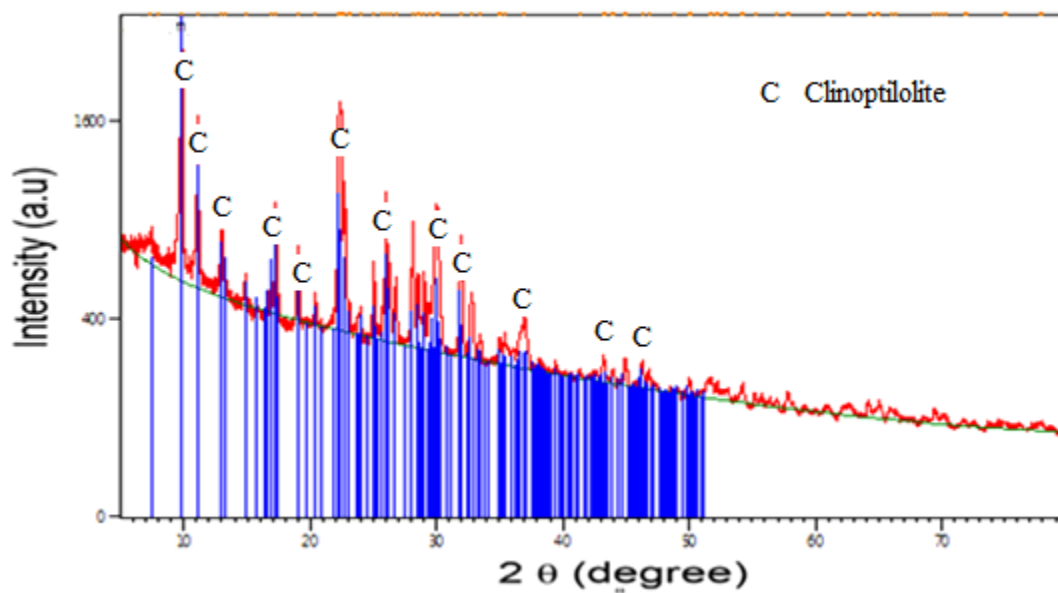


Figure C.1: XRD analysis showing the mineralogical analysis of Clinoptilolite (Natural Zeolite).

2. Synthetic zeolite A (Alkaline fusion prior to hydrothermal synthesis):

Anchor Scan Parameters

Dataset Name: zeolite A (Alkaline fusion prior to hydrothermal synthesis).
 File name: C:\XRD Data\Ali_Classic.xrdml
 Sample Identification: Alkaline fusion
 Comment: Configuration=Reflection-transmission spinner, Owner=User-1, Creation date=6/28/2012 10:39:29 AM
 Goniometer=Theta/Theta; Minimum step size 2Theta:0.0001; Minimum step size Omega:0.0001
 Sample stage=Reflection-transmission spinner; Minimum step size Phi:0.1
 Diffractometer system=EMPYREAN
 Measurement program=C:\PANalytical\Data Collector\Programs\powder 15mm PDS.xrdmp, Identifier={0B3B2317-9C50-4321-8234-537F3D3E9F38}
 Batch program=C:\PANalytical\Data Collector\Programs\Changer full main.xrdmp, Identifier={4FDD0C44-F627-4613-AA67-3A3AE6CF93A8}
 2/9/2016 4:05:05 PM
 Measurement Date / Time:
 Operator: Univ Wolverhampton
 Raw Data Origin: XRD measurement (*.XRDML)
 Scan Axis: Gonio
 Start Position [°2Th.]: 5.0064
 End Position [°2Th.]: 79.9904
 Step Size [°2Th.]: 0.0130
 Scan Step Time [s]: 8.6700
 Scan Type: Continuous
 PSD Mode: Scanning
 PSD Length [°2Th.]: 3.35
 Offset [°2Th.]: 0.0000
 Divergence Slit Type: Fixed
 Divergence Slit Size [°]: 0.2500
 Specimen Length [mm]: 10.00
 Measurement Temperature [°C]: 25.00
 Anode Material: Cu
 K-Alpha1 [Å]: 1.54060
 K-Alpha2 [Å]: 1.54443
 K-Beta [Å]: 1.39225
 K-A2 / K-A1 Ratio: 0.50000
 Generator Settings: 40 mA, 40 kV
 Diffractometer Type: 0000000001126545
 Diffractometer Number: 0
 Goniometer Radius [mm]: 240.00
 Dist. Focus-Diverg. Slit [mm]: 100.00
 Incident Beam Monochromator: No
 Spinning: Yes

scan List

Vis.	Dataset Name	Start pos. [°2Th.]	End pos. [°2Th.]	Step [°2Th.]	Meas.Date/Time
*	Ali_3A	5.0064	79.9904	0.0130	10/21/2015 11:38:0..
*	Determine ..	5.0064	79.9904	0.0130	10/21/2015 11:38:0..

Pattern List

Visible	Ref.Code	Score	Compound Name	Displ.[°2Th]	Scale Fac.	Chem. Formula
*	00-039-0222	79	Sodium Aluminum Si..	-0.058	0.797	Na96 Al96 Si96 O38..
*	98-000-4387	72	Zeolite A	-0.074	0.796	H40 Al12 K12 O68 S..

Peak List

Pos.[°2Th.]	Height [cts]	FWHMLeft[°2Th.]	d-spacing [Å]	Rel. Int. [%]
7.1313(5)	2885(40)	0.095(1)	12.38587	100.00
7.1490(5)	1442(40)	0.095(1)	12.38587	50.00
10.1053(6)	1650(26)	0.103(2)	8.74629	57.21
10.1305(6)	825(26)	0.103(2)	8.74629	28.60
12.3981(8)	886(22)	0.095(3)	7.13354	30.70
12.4290(8)	443(22)	0.095(3)	7.13354	15.35
13.78(6)	32(3)	2.0(1)	6.41940	1.11
13.82(6)	16(3)	2.0(1)	6.41940	0.56
16.038(1)	455(14)	0.101(4)	5.52182	15.78
16.078(1)	228(14)	0.101(4)	5.52182	7.89
17.585(8)	40(5)	0.19(1)	5.03929	1.39
17.629(8)	20(5)	0.19(1)	5.03929	0.70
20.347(4)	60(8)	0.09(1)	4.36101	2.07
20.399(4)	30(8)	0.09(1)	4.36101	1.03
21.43(2)	107(11)	0.30(2)	4.14215	3.70
21.49(2)	53(11)	0.30(2)	4.14216	1.85
21.5940(5)	871(17)	0.108(2)	4.11200	30.19
21.6483(5)	435(17)	0.108(2)	4.11200	15.09
22.777(4)	70(6)	0.12(1)	3.90101	2.44
22.834(4)	35(6)	0.12(1)	3.90101	1.22
23.9021(3)	1592(13)	0.120(1)	3.71988	55.20
23.9624(3)	796(13)	0.120(1)	3.71988	27.60
24.994(8)	31(7)	0.09(3)	3.55980	1.07
25.057(8)	15(7)	0.09(3)	3.55980	0.53
26.0266(6)	649(11)	0.107(2)	3.42085	22.51
26.0924(6)	325(11)	0.107(2)	3.42085	11.26
27.0265(4)	1281(15)	0.112(1)	3.29652	44.42
27.0949(4)	641(15)	0.112(1)	3.29652	22.21
28.935(3)	101(6)	0.17(1)	3.08332	3.51
29.008(3)	51(6)	0.17(1)	3.08332	1.75
29.8477(3)	1900(15)	0.117(1)	2.99105	65.87
29.9236(3)	950(15)	0.117(1)	2.99105	32.93
30.7371(8)	433(9)	0.109(4)	2.90650	15.00
30.8153(8)	216(9)	0.109(4)	2.90650	7.50
32.4456(5)	794(10)	0.117(2)	2.75724	27.52
32.5285(5)	397(10)	0.117(2)	2.75724	13.76
33.274(1)	209(7)	0.124(7)	2.69048	7.25
33.359(1)	105(7)	0.124(7)	2.69048	3.62
34.0775(5)	912(11)	0.118(2)	2.62884	31.61
34.1648(5)	456(11)	0.118(2)	2.62884	15.80
35.6492(9)	347(7)	0.117(3)	2.51646	12.04
35.7408(9)	174(7)	0.117(3)	2.51646	6.02
36.403(4)	57(4)	0.14(2)	2.46609	1.96
36.496(4)	28(4)	0.14(2)	2.46609	0.98
37.161(8)	28(3)	0.22(4)	2.41747	0.96
37.257(8)	14(3)	0.22(4)	2.41747	0.48
37.893(2)	94(5)	0.13(1)	2.37245	3.26
37.991(2)	47(5)	0.13(1)	2.37245	1.63
40.034(2)	107(4)	0.120(6)	2.25039	3.71
40.137(2)	53(4)	0.120(6)	2.25039	1.85

Graphics

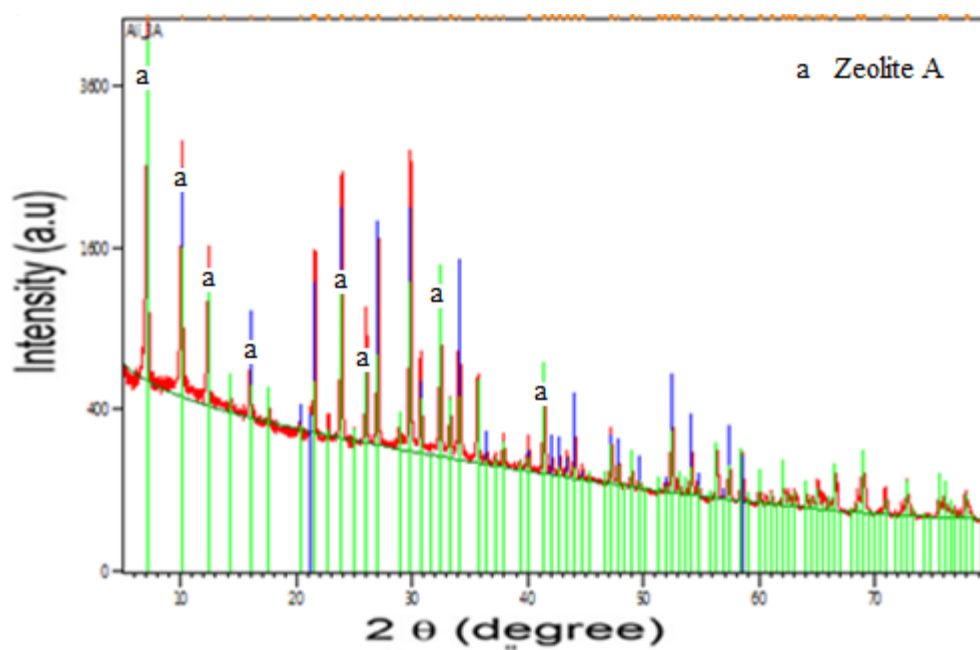


Figure C.2: XRD analysis showing the mineralogical analysis of zeolite A (alkaline fusion prior to hydrothermal synthesis).

3. Synthetic zeolite A (Conventional hydrothermal synthesis):

Anchor Scan Parameters

Dataset Name: zeolite A (conventional hydrothermal synthesis).
 File name: C:\XRD Data\AS_3M.xrdml
 Sample Identification: 3M
 Comment: Configuration=Reflection-transmission spinner, Owner=User-1, Creation date=6/28/2012 10:39:29 AM
 Goniometer=Theta/Theta; Minimum step size 2Theta:0.0001; Minimum step size Omega:0.0001
 Sample stage=Reflection-transmission spinner; Minimum step size Phi:0.1
 Diffractometer system=EMPYREAN
 Measurement program=C:\PANalytical\Data Collector\Programs\powder 15mm PDS.xrdmp, Identifier={0B3B2317-9C50-4321-8234-537F3D3E9F38}
 Batch program=C:\PANalytical\Data Collector\Programs\changer batch 4.xrdmp, Identifier={5A7AA560-2DE8-4809-8C93-4F872ADD5147}
 Measurement Date / Time: 2/29/2016 9:23:29 AM
 Operator: Univ Wolverhampton
 Raw Data Origin: XRD measurement (*.XRDML)
 Scan Axis: Gonio
 Start Position [°2Th.]: 5.0064
 End Position [°2Th.]: 79.9904
 Step Size [°2Th.]: 0.0130
 Scan Step Time [s]: 8.6700
 Scan Type: Continuous
 PSD Mode: Scanning
 PSD Length [°2Th.]: 3.35
 Offset [°2Th.]: 0.0000
 Divergence Slit Type: Fixed
 Divergence Slit Size [°]: 0.2500
 Specimen Length [mm]: 10.00
 Measurement Temperature [°C]: 25.00
 Anode Material: Cu
 K-Alpha1 [Å]: 1.54060
 K-Alpha2 [Å]: 1.54443
 K-Beta [Å]: 1.39225
 K-A2 / K-A1 Ratio: 0.50000
 Generator Settings: 40 mA, 40 kV
 Diffractometer Type: 0000000001126545
 Diffractometer Number: 0
 Goniometer Radius [mm]: 240.00
 Dist. Focus-Diverg. Slit [mm]: 100.00
 Incident Beam Monochromator: No
 Spinning: Yes

Scan List

Vis.	Dataset Name	Start pos. [°2Th.]	End pos. [°2Th.]	Step [°2Th.]	Meas.Date/Time
*	zeolite A	5.0064	79.9904	0.0130	2/29/2016 9:23:29 AM
*	Determine ..	5.0064	79.9904	0.0130	2/29/2016 9:23:29 AM

Pattern List

Visible	Ref.Code	Score	Compound Name	Displ.[°2Th]	Scale Fac.	Chem. Formula
*	98-001-6491	83	Zeolite A (C ₂ H ₄ -l..	-0.064	0.952	C ₁₂ H ₁₂ Al ₁₂ Na ₁₂ ..
*	96-810-0405	62	zeolite A..	-0.078	0.380	Na _{8.00} Si _{6.00} Al ₆ ...

Peak List

Pos.[°2Th.]	Height [cts]	FWHMLeft[°2Th.]	d-spacing [Å]	Rel. Int. [%]
7.1336(6)	2221(35)	0.102(2)	12.38171	100.00
7.1514(6)	1110(35)	0.102(2)	12.38171	50.00
10.1200(6)	1392(23)	0.110(2)	8.73364	62.67
10.1452(6)	696(23)	0.110(2)	8.73364	31.34
12.4161(9)	747(18)	0.111(3)	7.12321	33.64
12.4471(9)	374(18)	0.111(3)	7.12321	16.82
13.9526(8)	803(14)	0.141(3)	6.34207	36.17
13.9874(8)	402(14)	0.141(3)	6.34207	18.09
16.071(1)	387(9)	0.128(3)	5.51059	17.42
16.111(1)	193(9)	0.128(3)	5.51059	8.71
21.6424(7)	745(12)	0.121(2)	4.10291	33.54
21.6968(7)	372(12)	0.121(2)	4.10291	16.77
23.9659(5)	1148(7)	0.1239(2)	3.71013	51.70
24.0263(5)	574(7)	0.1239(2)	3.71013	25.85
24.3432(8)	744(8)	0.189(3)	3.65347	33.51
24.4046(8)	372(8)	0.189(3)	3.65347	16.75
26.090(1)	263(8)	0.136(6)	3.41264	11.86
26.156(1)	132(8)	0.136(6)	3.41264	5.93
26.5681(8)	598(14)	0.099(3)	3.35235	26.91
26.6353(8)	299(14)	0.099(3)	3.35235	13.46
27.1017(6)	900(12)	0.124(2)	3.28755	40.52
27.1703(6)	450(12)	0.124(2)	3.28755	20.26
29.9337(4)	1105(12)	0.128(2)	2.98265	49.75
30.0098(4)	552(12)	0.128(2)	2.98265	24.87
30.824(2)	161(6)	0.141(8)	2.89847	7.23
30.903(2)	80(6)	0.141(8)	2.89847	3.61
31.627(2)	210(3)	0.291(6)	2.82675	9.46
31.707(2)	105(3)	0.291(6)	2.82675	4.73
32.541(2)	210(7)	0.140(7)	2.74934	9.44
32.624(2)	105(7)	0.140(7)	2.74934	4.72
34.1799(6)	657(9)	0.138(3)	2.62120	29.59
34.2675(6)	329(9)	0.138(3)	2.62120	14.80
34.719(1)	320(5)	0.257(6)	2.58174	14.41
34.808(1)	160(5)	0.257(6)	2.58174	7.20
41.532(2)	116(5)	0.137(9)	2.17261	5.23
41.640(2)	58(5)	0.137(9)	2.17261	2.61
42.872(1)	226(4)	0.250(8)	2.10776	10.16
42.983(1)	113(4)	0.250(8)	2.10776	5.08
44.179(2)	133(4)	0.160(8)	2.04837	6.00
44.295(2)	67(4)	0.160(8)	2.04837	3.00
49.905(8)	28(1)	0.41(3)	1.82594	1.24
50.037(8)	14(1)	0.41(3)	1.82594	0.62
52.624(1)	162(4)	0.156(5)	1.73782	7.31
52.764(1)	81(4)	0.156(5)	1.73782	3.65
54.315(2)	89(3)	0.129(4)	1.68763	4.03
54.461(2)	45(3)	0.129(4)	1.68763	2.01
58.516(4)	52(1)	0.41(1)	1.57607	2.32
58.676(4)	26(1)	0.41(1)	1.57607	1.16

Graphics

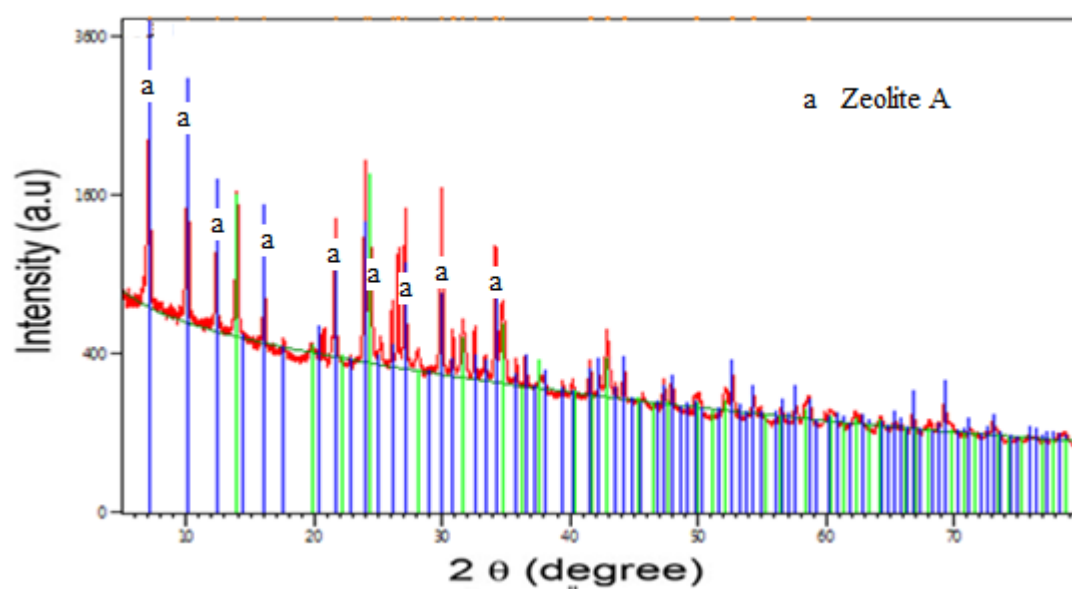


Figure C.3: XRD analysis showing the mineralogical analysis of zeolite A (conventional hydrothermal synthesis).

4. Natural kaolinite:

Anchor Scan Parameters

Dataset Name: Kaolinite
 File name: C:\XRD Data\AS received kaolinite
 Sample Identification: Kaolinite
 Comment: Configuration=Reflection-transmission spinner, Owner=User-1, Creation date=6/28/2012 10:39:29 AM
 Goniometer=Theta/Theta; Minimum step size 2Theta:0.0001; Minimum step size Omega:0.0001
 Sample stage=Reflection-transmission spinner; Minimum step size Phi:0.1
 Diffractometer system=EMPYREAN
 Measurement program=C:\PANalytical\Data Collector\Programs\powder 15mm PDS.xrdmp, Identifier={0B3B2317-9C50-4321-8234-537F3D3E9F38}
 Batch program=C:\PANalytical\Data Collector\Programs\changer batch 4.xrdmp, Identifier={6E32CB8E-5A72-40E0-B0B3-44A67F3B40F8}
 Measurement Date / Time: 6/28/2016 9:07:12 AM
 Operator: Univ Wolverhampton
 Raw Data Origin: XRD measurement (*.XRDML)
 Scan Axis: Gonio
 Start Position [°2Th.]: 5.0064
 End Position [°2Th.]: 79.9904
 Step Size [°2Th.]: 0.0130
 Scan Step Time [s]: 8.6700
 Scan Type: Continuous
 PSD Mode: Scanning
 PSD Length [°2Th.]: 3.35
 Offset [°2Th.]: 0.0000
 Divergence Slit Type: Automatic
 Irradiated Length [mm]: 15.00
 Specimen Length [mm]: 10.00
 Measurement Temperature [°C]: 25.00
 Anode Material: Cu
 K-Alpha1 [Å]: 1.54060
 K-Alpha2 [Å]: 1.54443
 K-Beta [Å]: 1.39225
 K-A2 / K-A1 Ratio: 0.50000
 Generator Settings: 40 mA, 40 kV
 Diffractometer Type: 0000000001126545
 Diffractometer Number: 0
 Goniometer Radius [mm]: 240.00
 Dist. Focus-Diverg. Slit [mm]: 100.00
 Incident Beam Monochromator: No
 Spinning: Yes

Scan List

Vis.	Dataset Name	Start pos. [°2Th.]	End pos. [°2Th.]	Step [°2Th.]	Meas.Date/Time
*	kaolinite	5.0064	79.9904	0.0130	6/28/2016 9:07:12 AM
*	Determine ..	5.0064	79.9904	0.0130	6/28/2016 9:07:12 AM

Peak List

Pos.[°2Th.]	Height [cts]	FWHMLeft[°2Th.]	d-spacing [Å]	Rel. Int. [%]
5.7234	64.36	0.5117	15.44189	1.28
12.2225	1992.90	0.0895	7.24159	39.64
13.4897	45.72	0.0768	6.56407	0.91
18.8101	25.11	0.2558	4.71773	0.50
19.8053	1133.15	0.0768	4.48284	22.54
20.2744	897.30	0.0384	4.38018	17.85
20.7834	1196.12	0.0384	4.27404	23.79
21.1541	578.14	0.0768	4.19997	11.50
21.3344	489.43	0.2047	4.16489	9.73
21.8510	177.30	0.0640	4.06757	3.53
22.9899	190.25	0.1023	3.86859	3.78
24.8270	2818.70	0.0512	3.58633	56.06
25.2360	913.45	0.0895	3.52913	18.17
25.9897	172.14	0.0384	3.42847	3.42
26.5486	5027.80	0.0780	3.35477	100.00
26.6254	2352.29	0.0312	3.35358	46.79
29.3521	366.49	0.0780	3.04041	7.29
30.0845	39.09	0.0780	2.96804	0.78
30.8015	9.88	0.3120	2.90056	0.20
31.4324	38.25	0.2184	2.84377	0.76
32.1007	56.19	0.4992	2.78608	1.12
33.2444	56.45	0.1872	2.69279	1.12
34.8852	1109.37	0.0780	2.56980	22.06
35.4444	643.38	0.9984	2.53053	12.80
35.8755	929.46	0.0780	2.50110	18.49
36.4546	299.46	0.0936	2.46269	5.96
37.6898	558.03	0.1248	2.38477	11.10
38.4520	1392.38	0.0780	2.33924	27.69
39.0961	630.68	0.1560	2.30217	12.54
39.3543	731.16	0.0936	2.28766	14.54
40.2218	289.72	0.0624	2.24029	5.76
40.3461	225.65	0.0468	2.23923	4.49
41.0776	155.12	0.4368	2.19557	3.09
42.3629	274.41	0.1248	2.13189	5.46
43.1163	88.94	0.1872	2.09636	1.77
45.4282	382.56	0.2496	1.99491	7.61
45.7043	499.13	0.0936	1.98350	9.93
47.9509	186.31	0.1560	1.89568	3.71
48.4284	77.48	0.3120	1.87809	1.54
49.1850	60.21	0.3744	1.85096	1.20
50.0514	775.65	0.0624	1.82093	15.43
50.1786	344.98	0.0780	1.82113	6.86
50.9144	213.03	0.5616	1.79207	4.24
54.2616	306.17	0.0312	1.68916	6.09
54.3897	227.67	0.1092	1.68549	4.53
54.7627	511.07	0.0936	1.67489	10.16
54.9374	572.49	0.1248	1.66997	11.39
55.2902	518.82	0.2496	1.66015	10.32
56.8173	192.44	0.0468	1.61910	3.83
58.1347	46.05	0.3744	1.58551	0.92

Graphics

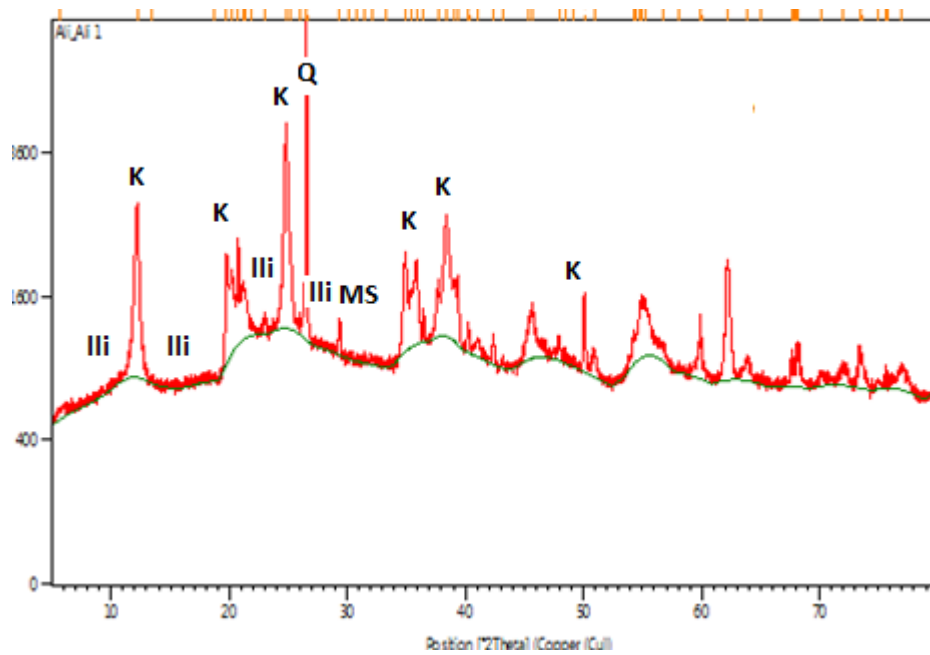


Figure C.4: Shows the XRD pattern of kaolinite. Kaolinite (K); illite(Ili); muscovite(Ms); quartz(Q).